



STATENS GEOTEKNISKA INSTITUT
SWEDISH GEOTECHNICAL INSTITUTE

Calculating long-term
settlement in soft clays
– with special focus on the
Gothenburg region

MATS OLSSON

Report 74

LINKÖPING 2010

Report Swedish Geotechnical Institute
SE-581 93 Linköping

Order Information service, SGI
Tel: +46 13 20 18 04
Fax: +46 13 20 19 09
E-mail: info@swedgeo.se
Internet: www.swedgeo.se

ISSN 0348-0755

ISRN SGI-R--10/74--SE

THESIS FOR THE DEGREE OF LICENTIATE OF ENGINEERING

Calculating long-term settlement in soft clays
– with special focus on the Gothenburg region

MATS OLSSON



Department of Civil and Environmental Engineering
Division of GeoEngineering
CHALMERS UNIVERSITY OF TECHNOLOGY
Göteborg, Sweden 2010

Calculating long-term settlement in soft clays
- with special focus on the Gothenburg region
MATS OLSSON

© MATS OLSSON, 2010

ISSN 1652-9146
Lic 2010:3

Department of Civil and Environmental Engineering
Division of GeoEngineering
Chalmers University of Technology
SE-412 96 Göteborg
Sweden
Telephone + 46 (0)31 772 10 00
www.chalmers.se

Chalmers reproservice
Göteborg, Sweden 2010

Calculating long-term settlement in soft clays

- with special focus on the Gothenburg region

MATS OLSSON

Department of Civil and Environmental Engineering

Division of GeoEngineering

Chalmers University of Technology

ABSTRACT

Long-term settlement in clay constitutes an engineering challenge in road design and construction in areas with deep deposits of soft clay. Soil improvement and construction of building foundations or embankments can be quite complicated and expensive in such areas. Construction costs need to be balanced against high maintenance costs. In order to do this optimally, there is a need to predict long-term settlement with a high degree of accuracy.

Two different test sites were chosen for back-calculation, a test embankment at Nödinge and a groundwater lowering at Kaserntorget. There was also one hypothetical test site.

In this thesis a short description is presented of the fundamental behaviour of soft clays with regard to compressibility as well as a short explanation of the theory for the three different models that has been used within this thesis – Embankco, GS Settlement and the Soft Soil Creep model.

Soil parameter determination for long-term settlement analysis is discussed together with some of the inherent complications. For the IL oedometer test the study shows that if the time for the load stage of interest is not sufficiently long the evaluated creep parameter could be misleading. Back-calculation of CRS oedometer test, using the Soft Soil Creep model, is performed for this model and a procedure is suggested.

The outcome of the analysis shows that all three models produce similar results for the hypothetical case. For the two test sites in question, both GS Settlement and the Soft Soil Creep model were capable of predicting the measured settlement with acceptable accuracy. The Embankco program was only used for the hypothetical case.

Keywords: Soft clay, creep, test sites, long-term settlement.

ACKNOWLEDGMENTS

The work presented in this thesis was conducted at the Division of GeoEngineering at Chalmers University of Technology, under the supervision of Professor Claes Alén. Financial contributors were the Swedish Road Administration, SGI and Chalmers University of Technology, who are greatly acknowledged for their support.

I wish to thank my supervisor Professor Claes Alén for initiating this project and for his great interest and guidance during this project. I also wish to thank Professor Göran Sällfors for all his support and interesting discussions during the project.

Special thanks to my co-supervisor and colleague Per-Evert Bengtsson at SGI for his critical examination, support and guidance throughout the project. I would also like to thank my employer, SGI, for giving me the opportunity to dedicate the last three years to this project.

I would like to thank Tyrens in Gothenburg for providing me with valuable data.

I would also like to express my appreciation to all my colleagues and friends for their support and encouragement and to Anna-Karin for her love, patience and support.

Göteborg, April 2010
Mats Olsson

TABLE OF CONTENTS

ABSTRACT	iii
ACKNOWLEDGMENTS	v
TABLE OF CONTENTS.....	vii
LIST OF NOTATIONS	xi
1. INTRODUCTION.....	1
<i>1.1 Background</i>	<i>1</i>
<i>1.2 Research objectives.....</i>	<i>1</i>
<i>1.3 Scope of Work</i>	<i>2</i>
<i>1.4 Limitations</i>	<i>2</i>
2. FUNDAMENTAL BEHAVIOUR OF SOFT CLAYS WITH REGARD TO COMPRESSIBILITY.....	5
<i>2.1 Introduction.....</i>	<i>5</i>
<i>2.2 Natural state of soft clays</i>	<i>5</i>
2.2.1 Influence of ground water changes.....	6
<i>2.3 Yielding of soft clays</i>	<i>7</i>
2.3.1 Strain rate effects.....	8
2.3.2 Temperature effects	11
<i>2.4 Consolidation of soft clays</i>	<i>12</i>
2.4.1 Theory of consolidation.....	14
2.4.2 Delayed consolidation	15
<i>2.5 Models for consolidation</i>	<i>17</i>
2.5.1 General	17
2.5.2 Taylors model.....	17
2.5.3 The Isotache model	17
2.5.4 The Bjerrum model	18
2.5.5 The time resistance concept	19
<i>2.6 Overconsolidated conditions</i>	<i>20</i>
3. PROGRAMS FOR CALCULATING TIME-DEPENDENT BEHAVIOUR	23
<i>3.1 Embankco</i>	<i>23</i>

3.1.1	Soil model	23
3.1.2	Calculation method	24
3.2	<i>GS Settlement</i>	25
3.2.1	Soil model	25
3.2.2	Calculation method	28
3.3	<i>Soft Soil Creep model</i>	30
3.3.1	Soil model	30
3.4	<i>Relationships between model parameters</i>	35
4.	DETERMINATION OF SOIL PARAMETERS	37
4.1	<i>Introduction</i>	37
4.2	<i>Determination of soil parameters for settlement analysis</i>	37
4.2.1	Evaluation of the creep parameter from laboratory tests.....	38
4.2.2	Creep parameters at the preconsolidation stress – empirical	39
4.2.3	The Chalmers model	40
4.2.4	Modelling laboratory tests.....	44
4.3	<i>Discussion</i>	48
5.	TEST SITES	51
5.1	<i>Hypothetical test site</i>	51
5.1.1	Ground conditions	52
5.2	<i>The Nödinge test embankment</i>	54
5.2.1	Ground conditions	54
5.2.2	Test embankment	57
5.2.3	Measurements.....	58
5.3	<i>Kaserntorget - Groundwater lowering</i>	61
5.3.1	Ground conditions	61
5.3.2	Measurements.....	64
6.	CALCULATIONS AND COMPARISONS.....	67
6.1	<i>Hypothetical test site</i>	67
6.1.1	Input parameters	67
6.1.2	Results and comparison between programs	70
6.1.3	Discussion	72
6.2	<i>Nödinge test embankment</i>	73
6.2.1	Input parameters	73
6.2.2	Results and comparison with measurements.....	81
6.2.3	Discussion	84
6.3	<i>Kaserntorget</i>	86
6.3.1	Input parameters	86
6.3.2	Groundwater level over time.....	92

6.3.3	Results and comparison with measurements.....	92
6.3.4	Discussion	97
7.	DISCUSSION	101
7.1	<i>Introduction.....</i>	<i>101</i>
7.2	<i>Soil parameters</i>	<i>102</i>
7.3	<i>Modelling</i>	<i>104</i>
7.4	<i>Conclusions.....</i>	<i>106</i>
7.4.1	Recommendations	107
7.4.2	Concluding remarks	107
8.	FURTHER RESEARCH.....	109
8.1	<i>Laboratory testing.....</i>	<i>109</i>
8.2	<i>Field test and monitoring.....</i>	<i>109</i>
8.3	<i>Numerical modelling.....</i>	<i>109</i>
8.4	<i>Constitutive modelling</i>	<i>110</i>
	REFERENCES	111

LIST OF NOTATIONS

Roman letters

e	Void ratio
e_0	Initial void ratio
k	Hydraulic conductivity
K_0^{nc}	Lateral earth pressure ratio in the NC-region
K_0	Lateral earth pressure ratio
M	Critical state line
M_0	Constant constrained modulus below the effective vertical preconsolidation pressure, Swedish method
M_L	Constant constrained modulus between the stresses σ'_c and σ'_L , Swedish method
M'	Modulus number
p	Mean stress $(\sigma_1 + \sigma_2 + \sigma_3)/3$
p'	Mean effective stress $(\sigma'_1 + \sigma'_2 + \sigma'_3)/3$
q	Deviatoric stress $(\sigma_1 - \sigma_3)$
r, r_s	Creep number or Time resistance number
R	Time resistance
s'	The average value σ'_{vert} and σ'_{hors} $(\sigma'_v + \sigma'_h)/2$
t	The difference between σ'_{vert} and σ'_{hors} $(\sigma'_v - \sigma'_h)/2$
t_r	Reference time
u	Pore pressure
w_L	Liquid limit
w_N	Natural water content
z	depth

Greek letters

α_s	Creep parameter according to Swedish praxis
γ	Unit weight of the soil
γ_w	Unit weight of water
$\Delta \varepsilon_{cr}$	Creep strain during one time step
Δu	Excess pore pressure
Δu_{cr}	Excess pore pressure due to creep
ε	Strain
ε_z	Strain in the z-direction
ε_v	Volumetric strain
ε^c	Creep strain
κ^*	Modified swelling index (SSC swelling index)

λ^*	Modified compression index (SSC compression index)
μ^*	Modified creep index (SSC creep index)
ν	Poisson's ratio
ν_{ur}	Poisson's ratio for unloading/reloading
σ'_0	In situ effective stress
σ'_1	Major principal effective stress
σ'_2	Intermediate principal effective stress
σ'_3	Minor principal effective stress
σ_1	Major principal total stress
σ_2	Intermediate principal total stress
σ_3	Minor principal total stress
σ'_{hors}	Horizontal effective stress
σ'_{vert}	Vertical effective stress
σ'_c	Preconsolidation stress
σ'_{vc}	Vertical preconsolidation stress
ϕ'	Effective frictional angle

Abbreviations

CRS	Constant Rate of Strain
IL	Incremental Loading
LCC	Lime Cement Column
NC	Normal Consolidated
OC	Overconsolidated
OCR	Over Consolidation Ratio
POP	Over consolidation formulated as $POP = \sigma'_c - \sigma'_0$
SGI	Swedish Geotechnical Institute
SSC	Soft Soil Creep model in Plaxis

1. INTRODUCTION

This chapter provides the background to this thesis and defines the main research objectives and presents the scope of work. The limitations that are imposed are also described.

1.1 Background

Long-term settlements in clay constitute an engineering challenge in road design and construction in areas with deep deposits of soft clay. Soil improvement or the construction of building foundations or embankments can be quite complicated and expensive in such areas. Construction costs need to be balanced against high maintenance costs. In order to do this optimally, there is a need to predict long-term settlement with a high degree of accuracy.

However, predicting long-term settlement is not an easy task. Today there are numerous different numerical tools to help the engineer to predict the long-term settlement. Even though the numerical tools have become more refined and involve more detailed soil behaviour the engineer needs to balance this, when using them, against the quality of the soil properties that have been determined.

It is of interest to investigate whether, with programs normally used, it is possible to predict the long-term settlement in deep deposits of soft clays. This is of particular interest in cases where the calculated final stress is close to the evaluated preconsolidation stress.

1.2 Research objectives

The overall objective of this thesis was to predict long-term settlement from real and realistic conditions and, if possible, put forward some recommendations.

This thesis therefore focuses on how to calculate long-term settlement in soft clays and discusses ways of interpreting or evaluating some of the most important parameters to be used.

The specific objectives of the thesis are as follows:

- Using a conceptual model that could capture the settlement behaviour so that prediction of long-term settlement is possible under real and realistic conditions.

- Discuss and highlight some difficulties concerning determination of soil parameters from laboratory tests.
- Discuss benefits and limitations of the models used.
- Give some recommendations when using numerical tools for predicting long-term settlement.

1.3 Scope of Work

At the beginning of the thesis there is a brief summary of earlier research studies on the behaviour of soft clays with focus on compressibility.

The research project is based on field investigations and was conducted before this project started. An inventory was therefore made to find appropriate test sites. Two different test sites were chosen for back-calculation, the Nödunge test embankment and the groundwater lowering at Kaserntorget. There was also one hypothetical test site, which was constructed to show how the programs used in the thesis correspond to each other with realistic input. The test sites are described in Chapter 5.

The specific objectives of the thesis are thus fulfilled if the following tasks are performed

- Using numerical tools, available for the industry, to calculate long-term settlement under real and realistic conditions.
- Compare measured and calculated values.
- Give some recommendations when using numerical tools for predicting long-term settlement.

Some laboratory tests were also conducted to further investigate different compressibility parameters for soft clays.

1.4 Limitations

Prediction of long-term settlement in soft clays is a very complex research field. It is impossible to account for all aspects of the problem. The following are some of the most important limitations on this thesis

- The focus is on vertical settlement
- Programs handling one- and two-dimensional situations are used.

- The thesis focuses mainly on soft clays that have an OCR of less than 1.5.
- The focus is also on clays in the region around Gothenburg. However, the methodology could be used for other places with soft clays.

2. FUNDAMENTAL BEHAVIOUR OF SOFT CLAYS WITH REGARD TO COMPRESSIBILITY

This chapter introduces the basic behaviour of soft clays with a special focus on compressibility with regard to consolidation and creep settlement when subjected to a surcharge load and/or lowering of the groundwater. The focus is also on normally to slightly overconsolidated ($OCR < 1.5$) clays, typical of the Gothenburg region.

2.1 Introduction

The compressibility behaviour of soft soils has been studied for the past hundred years. The literature contains a substantial number of research papers on both compressibility and the consolidation process and how to model it with or without creep effects.

The pioneering work on stress-strain behaviour during one-dimensional consolidation was done by Terzaghi (1923). He published a theory for one-dimensional consolidation and today it is regarded as the classic consolidation theory, described further in Chapter 2.4.1.

Since then numerous researchers from various parts of the world have examined the problem of the behaviour of soft clays or soft soils, including Bjerrum (1967), Sällfors (1975), Mesri & Godlewski (1977), Leroueil et al. (1985), Larsson (1986), Boudali et al. (1994) and Claesson (2003) to name but a few.

2.2 Natural state of soft clays

The soft clays discussed here are recent glacial and post-glacial Scandinavian deposits, formed within the last 10,000 years under water. The resulting ground surface today is typically flat and featureless, except when dissected by rivers or other erosional channels. In most cases, no material has been eroded from the surface except from areas with such channels. Consequently, in a geological sense the bulk of the material can be regarded as normally consolidated although in its natural state, this soil will in fact usually exhibit the characteristics of slightly overconsolidated clay.

A number of factors may give rise to some degree of overconsolidation in the soil, the most important ones being:

- Changes in the static groundwater level

- Secondary or delayed consolidation (creep)

Strong overconsolidation effects may be introduced in the thin surface crust by weathering or desiccation due to evaporation or extraction of moisture by plant roots, although these influences are mostly limited to just a few metres or so in thickness. Salts in the pore fluid may also cause a form of apparent overconsolidation through the creation of bonds between particles.

2.2.1 Influence of ground water changes

A simple cycle of events producing overconsolidation in a clay deposit has been described by Parry (1970) and is shown in Figure 2.1. During deposition under water, the soil at point P in Figure 2.1a will follow curve 1 in Figure 2.1b. After some time the water will be drawn down to the top surface of the soil, although this drawdown does not produce any change in effective stress at point P. However, the physiographic or climatic factors producing this drawdown may result in the water table being drawn down below the surface of the soil to a depth of z_m . Providing static groundwater conditions are reached with the level at z_m , the soil at point P will follow curve 2 in Figure 2.1b, and the vertical effective stress will attain a maximum value of σ'_{vm} . If the groundwater level rises to z_0 , the soil will follow curve 3, and the vertical effective stress at point P becomes σ'_{v0} . The overconsolidation ratio (OCR) is then:

$$OCR = \frac{\sigma'_{vm}}{\sigma'_{v0}} \quad (2.1)$$

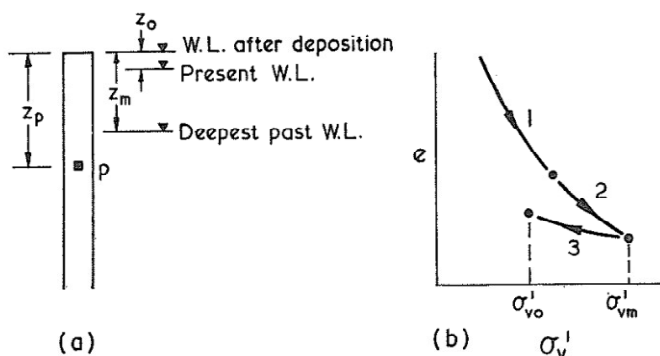


Figure 2.1 Overconsolidation caused by groundwater movements by Parry (1970).

Real soil will have a much more complex history than this, although the important points are the maximum past water table depth z_m and the existing water table depth z_0 .

2.3 Yielding of soft clays

Yield stresses are the combination of principal effective stresses at which the deformations of a soil change from being elastic to elastic-plastic, Wood (1990). One of the most important parameters for estimating the deformation characteristics of a clay deposit is the preconsolidation pressure. This is defined as the apparent maximum effective stress to which the soil has been subjected. This pressure is normally evaluated from where the clay yields in an oedometer test. Unfortunately, the stress path in the oedometer could be quite different from the stress path in the field. Figure 2.2 contains a simplified description of how the stress path is thought to occur in the field when the soil is being loaded and Figure 2.3 shows a more likely stress path for the soil in the oedometer case.

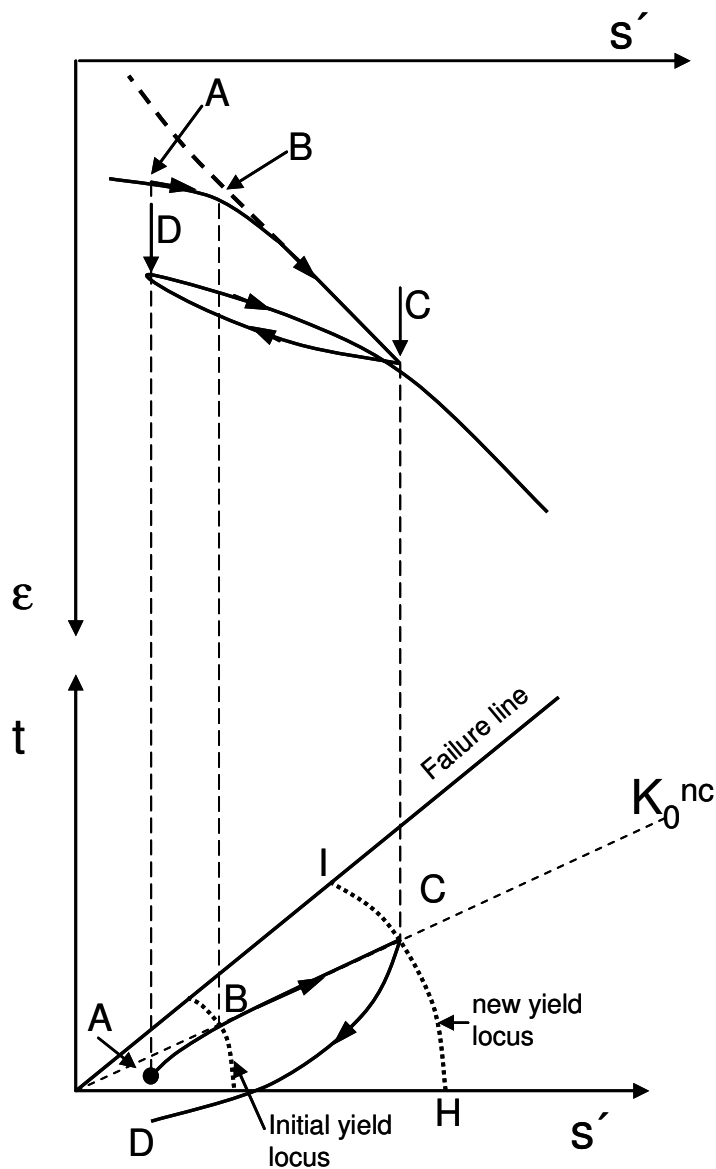


Figure 2.2 Consolidation curves, stress paths and yield locus.

(1975), Leroueil et al. (1985), Claesson (2003) to name but a few. A general observation is that the higher the strain rate the higher the effective stress for a certain strain. This is shown in Figure 2.4, where two CRS – oedometer tests have been conducted on a sample of soft clay taken at a depth of 16 m from Nödinge, just north of Gothenburg. The CRS oedometer tests are performed with two different strain rates, 0.7 %/hr and 0.07 %/hr.

In Sweden, the normal strain rate for CRS oedometer tests is 0.0024 mm/min with a sample height of 20 mm. This rate corresponds to about 0.7 %/hr, and the strain rate was suggested by Sällfors (1975). Sällfors also showed a methodology on how to evaluate the preconsolidation stress from the CRS oedometer test, see Figure 2.5. The stress-strain axis is set at a fixed ratio in a linear plot, normally a 10/1 ratio for the stress (kPa)/strain (%). This was concluded after a series of field tests where pore pressure and settlement were measured. This implies that using the Sällfors method of evaluating the preconsolidation stress gives a more appropriate value for the preconsolidation stress compared to the preconsolidation stress evaluated in the field tests.

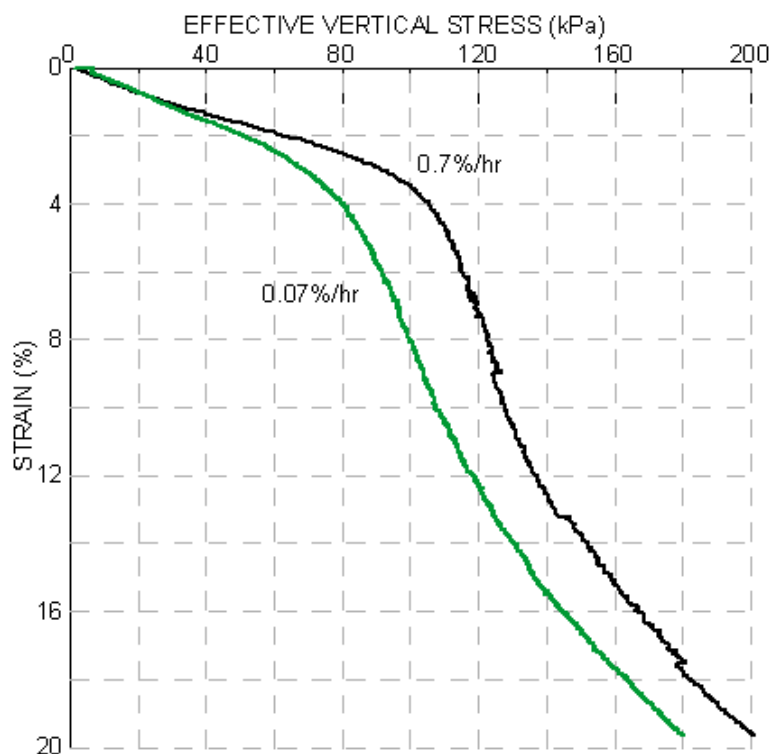


Figure 2.4 CRS oedometer tests, sample height 20 mm, with different strain rates, Nödinge depth 16 m.

If the strain rates in the laboratory tests are compared with the strain rates in the field they are much higher in the laboratory. Compression curves

from the laboratory test normally correspond, to a strain rate of about 10^{-8} s^{-1} , see Figure 2.6, or higher.

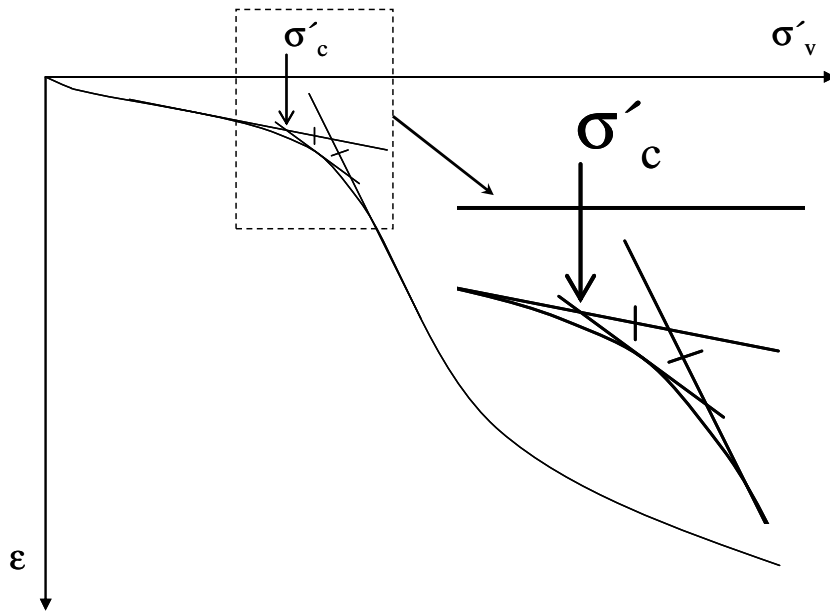


Figure 2.5 Principle for evaluating the preconsolidation stress according to Sällfors (1975).

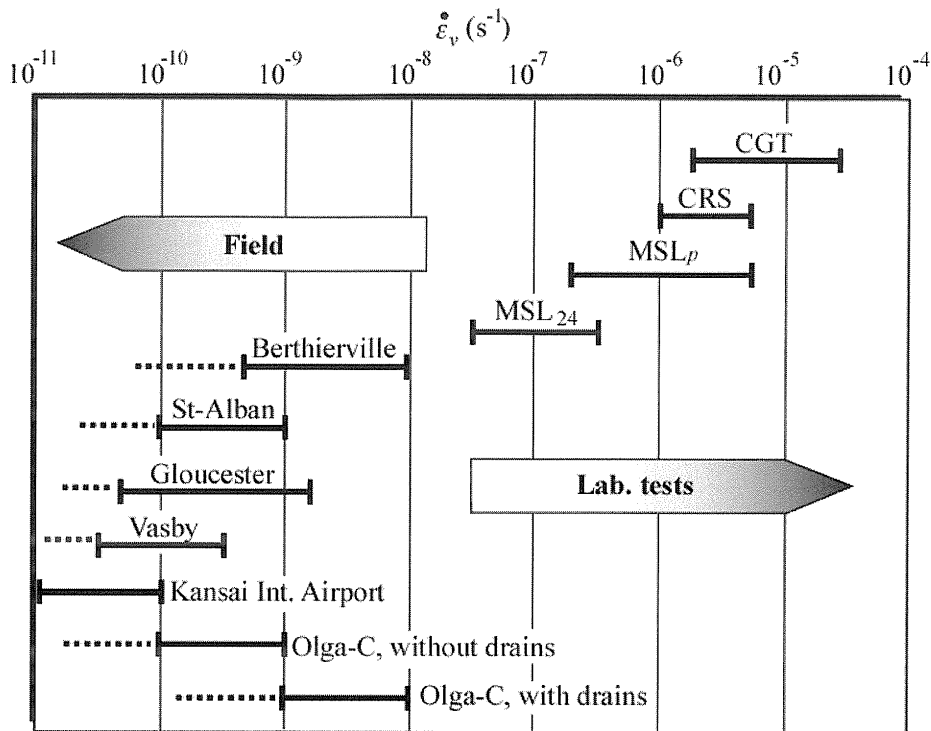


Figure 2.6 Ranges of strain rates encountered in laboratory tests and in situ, Leroueil (2006).

2.3.2 Temperature effects

Strain rate effects are clearly not the only factor influencing the preconsolidation stress. The effects of temperature has been studied by several researchers, including Campanella & Mitchell (1968), Tidfors (1987), Tidfors & Sällfors (1989), Eriksson (1989), Boudali et al. (1994), Marques et al. (2004). Tidfors (1987) made a laboratory study of the temperature effects on deformation properties of soft clay. The study concluded, as did many researchers before and after, that the evaluated preconsolidation stress is decreasing with increasing temperature and vice versa, see Figure 2.7.

It was also stated by Tidfors (1987) that the evaluated preconsolidation stress from the laboratory tests decreased by about 6-10% when conducted at room temperature ($\sim 20^\circ\text{C}$) compared to a normal temperature of $+8^\circ\text{C}$ for high-plastic clays. This is a difference of about $10\text{-}15^\circ\text{C}$ compared to the temperature in the field.

In most cases this is only of interest when conducting laboratory tests and done at a temperature that is different from the in-situ case. However, most of the time the temperature in the clay deposits is very constant and normally temperature effects in Scandinavian soft clays can be ignored in the field cases.

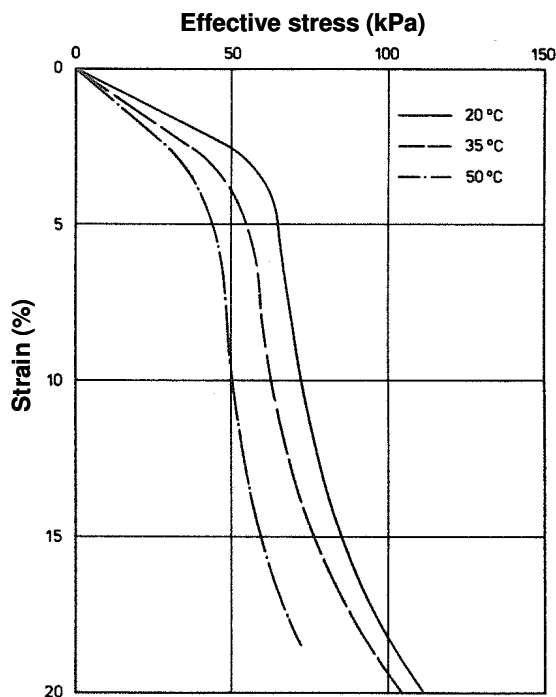


Figure 2.7 Stress-strain curves from CRS oedometer tests at different temperatures for samples taken at a depth of 7 m at Bäckebol, Tidfors (1987).

2.4 Consolidation of soft clays

From the response of soils under one-dimensional conditions it is apparent that when the effective stress increases, the soil compresses. When a load is applied to a saturated soil specimen this compression does not occur immediately. This behaviour is a consequence of the soil constituents, the skeletal material and the pore water being almost incompressible compared to the soil structure. Consequently, deformation can only take place by water being squeezed out of the voids. This can only occur at a finite rate and initially, when the soil is loaded, it ideally undergoes no volume change.

Under one-dimensional conditions this implies that initially at load application there can ideally be no vertical strain and thus no change in vertical effective stress. For one-dimensional conditions we have

$$\varepsilon_z = \varepsilon_v = \frac{\Delta e}{1+e} \quad (2.2)$$

where ε_z = vertical strain
 ε_v = volumetric strain
 e = void ratio

Hence, if the volumetric strain is zero then the change in the void ratio is zero.

When the load is first applied the total stress increases but, as shown above for one-dimensional conditions, there can be no instantaneous change in vertical effective stress, implying that the pore-pressure must increase by exactly the same amount as the increase in total stress.

Subsequently, there will be flow from regions of higher excess pore pressure to regions of lower excess pore-pressure, the excess pore pressures will dissipate, the effective stress will change and the soil will deform (consolidate) with time.

When a clay sample is suddenly loaded in the oedometer test, its decrease in void ratio/compression with time is typically as shown in Figure 2.8. The consolidation process is traditionally divided into a primary and a secondary consolidation/compression phase. During the primary consolidation phase, settlement is controlled by the dissipation of excess pore pressures and Darcy's law. During secondary consolidation, the rate

of settlement is controlled by soil viscosity, Leroueil (2006). However, settlement requires a hydraulic gradient, i.e. excess pore pressure exists at that stage. Secondary consolidation or creep is characterised by the slope of the consolidation/compression curve. The secondary compression index is normally presented as

$$C_{\alpha\varepsilon} = \frac{\Delta\varepsilon}{\Delta\log(t)} \quad \text{or} \quad C_{\alpha e} = \frac{\Delta e}{\Delta\log(t)}$$

and in Sweden its commonly expressed as

$$\alpha_s = \frac{\Delta\varepsilon}{\Delta\log(t)}$$

See Table 3.3 for conversion between the creep parameters above.

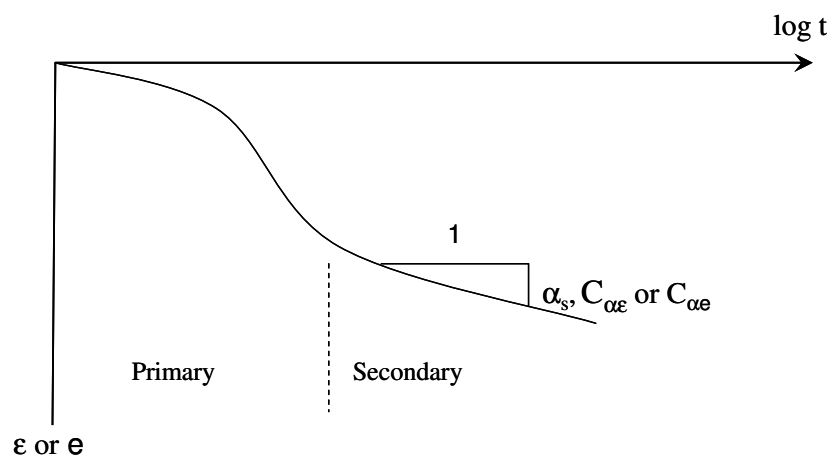


Figure 2.8 Consolidation curve.

The consolidation/compression phases described above are normally the result of the incremental oedometer test. If the results from a creep test performed in a triaxial apparatus were to be plotted in a strain-log(time) diagram with arithmetic axes, as shown in Figure 2.9, the process could be divided into three parts: (1) primary, (2) secondary and (3) tertiary creep. The first two, primary and secondary, are explained above. Tertiary creep, however, is characterised by an increasing strain rate with time and this type of failure is usually denoted as creep failure or creep rupture. For a more detailed description of the creep stages see e.g Augustesen et al. (2004).

During a creep process the strain rate normally decreases with the logarithm of time. According to Larsson (1977) the strain rate decreases

until the effective stress path reaches the effective failure line. The strain rate then becomes constant or increases and the sample fails.

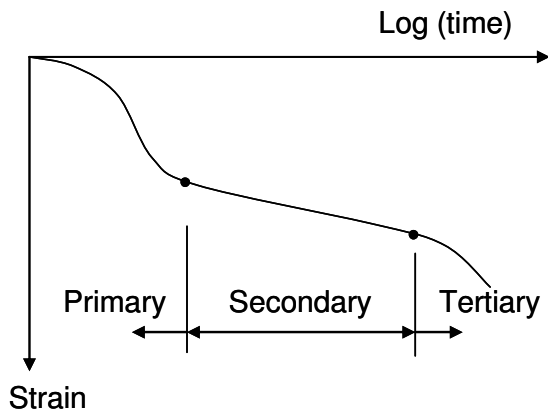


Figure 2.9 Definition of primary, secondary and tertiary compression in a strain versus log (time) plot.

2.4.1 Theory of consolidation

The classic theory of consolidation was developed by Terzaghi (1923). This is still today the foundation of one-dimensional consolidation theory. The theory is based on a number of assumptions.

- The soil is fully saturated and homogeneous.
- The water and soil particles are incompressible.
- Darcy's law applies.
- The hydraulic conductivity is constant during the consolidation process.
- The compression and pore pressure process are one-dimensional.
- The change in pore water pressure is equal to the change in effective stress.
- The strain is only dependent on the change in effective stress, i.e. creep or secondary consolidation is not considered.

The differential equation for solving the one-dimensional consolidation process can be derived from these assumptions.

$$\frac{\partial u}{\partial t} = \frac{M}{\gamma_w} \cdot \frac{\partial}{\partial z} \left(k \cdot \frac{\partial u}{\partial z} \right) \quad (2.3)$$

where u = pore pressure
 M = oedometer modulus
 t = time
 k = hydraulic conductivity
 z = depth
 γ_w = unit weight of water

If the hydraulic conductivity is assumed to be constant with depth, the equation above could be rewritten as

$$\frac{\partial u}{\partial t} = c_v \left(\frac{\partial^2 u}{\partial z^2} \right) \quad (2.4)$$

where $c_v = \frac{M \cdot k}{\gamma_w}$ coefficient of consolidation

For the analytical solution to equation (2.4) see e.g. Terzaghi (1943) or Jumikis (1967).

2.4.2 Delayed consolidation

The quasi-preconsolidation effect introduced by secondary or delayed consolidation has been discussed by a number of researchers, e.g. Suklje (1957), Leonards & Altschaeffl (1964), Bjerrum (1967) and Larsson (1986). Bjerrum (1967) showed a system of consolidation curves representing different times after load application, see Figure 2.10. In a thin laboratory specimen the primary consolidation phase is comparatively fast, completed in less than a day or so and corresponding closely to the 'instant' curve in Figure 2.11. If the applied stress is held constant for a long period of time, further consolidation takes place at constant vertical stress, σ'_0 , and the state of the sample moves vertically down from point A to B in Figure 2.10, crossing the delayed consolidation curves.

The same behaviour occurs after sedimentation in the field and the soil will reach a state as at point B, in Figure 2.10, after a period of around 3,000 years. In the laboratory this soil will show very little increase in strain until the applied stress reaches σ'_c at point C, where the curve breaks to join the 'instant' consolidation line. This breaking point indicates yield in the soil.

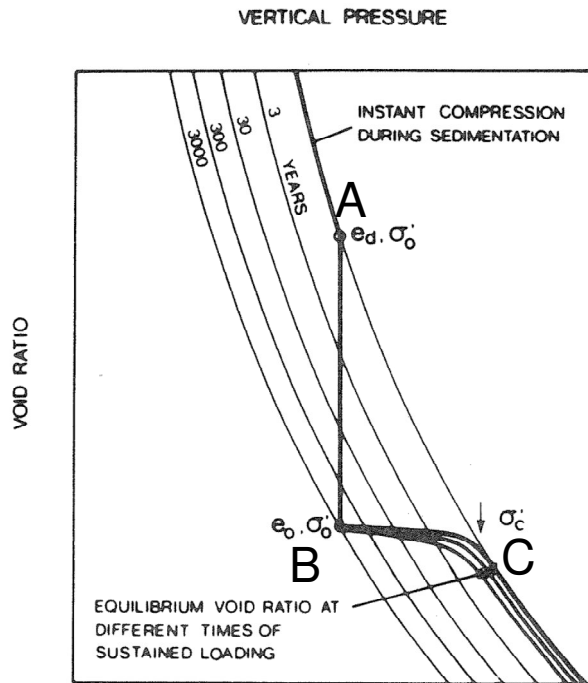


Figure 2.10 Effects of secondary compression on void ratio and preconsolidation stress, Bjerrum (1967).

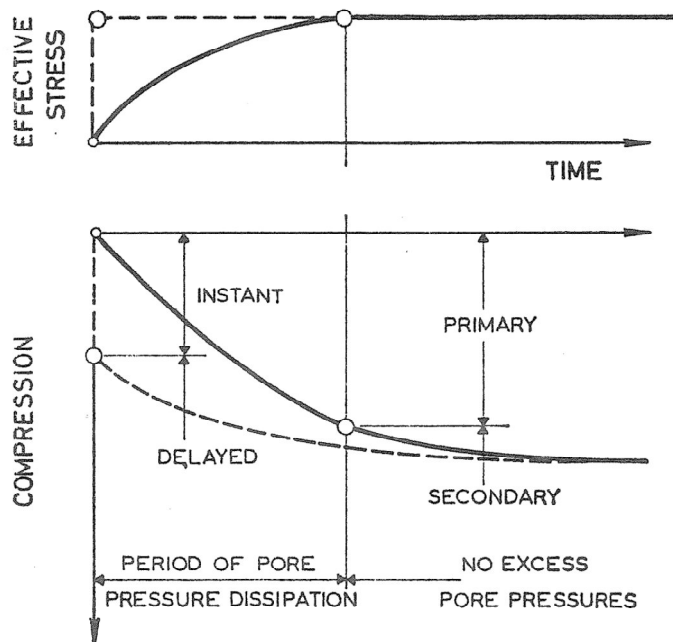


Figure 2.11 Definition of “instant” and “delayed” compression compared with “primary” and “secondary” compression, Bjerrum (1967).

2.5 Models for consolidation

2.5.1 General

The time-dependency of the effective stress-strain relationship has been given many names, such as creep, secondary consolidation, time-resistance, viscosity and many more, all of which attempt to describe the same process. Laboratory tests and field observations reported by Buisman (1936) and Taylor (1942) clearly indicate the effect of time on the compressibility of clays. Buisman found that settlements increased linearly with logarithmic of time under constant effective stress for observation of clay in the field and in the laboratory.

2.5.2 Taylors model

One of the first theories where secondary consolidation was at least partly involved in the primary consolidation was presented by Taylor & Merchant (1940) and a first model that looked at the change in the void ratio with a change in effective stress and time was outlined by Taylor (1942), see Figure 2.12.

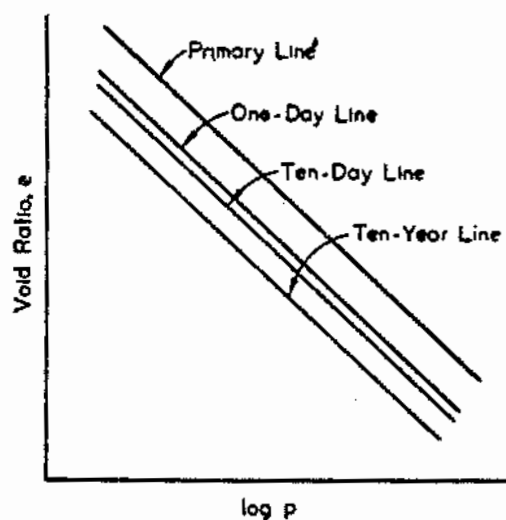


Figure 2.12 Void ratio – effective stress relationships for different times, Taylor (1942).

2.5.3 The Isotache model

Suklje (1957) presented a more generalised theory, where the rate of strain depends on the mean values of void ratio and the effective stress. This relationship was presented using a set of isotaches, see Figure 2.13.

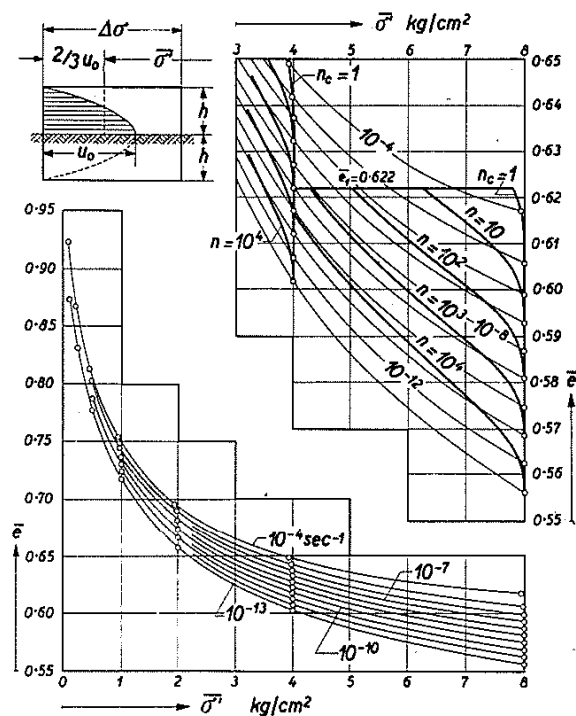


Figure 2.13 Isotaches set for a lacustrine chalk sample from Suklje (1957).

This was the first model to suggest that the behaviour of clay is governed by a unique relationship between effective stress, void ratio and rate of strain. In this model it is assumed that creep occurs during both the primary and secondary consolidation phases i.e. primary consolidation and creep effects are not two separate processes. Suklje's model also accounted for that the time-dependent strains are influenced by the layer thickness, hydraulic conductivity and drainage conditions.

2.5.4 The Bjerrum model

Bjerrum (1967) presented a unique relationship between void ratio, overburden pressure and time, see Figure 2.10. This model is similar to Suklje's model, i.e. not dividing primary consolidation and creep effects into two separate processes. This means that for any given value of the overburden pressure and void ratio these corresponds to an equivalent time of constant loading and a certain rate of delayed consolidation. This is independent of the way the clay has reached these values.

The Bjerrum model is intended to explain the apparent preconsolidation stress and over consolidation ratio of virgin clays resulting from ageing. Bjerrum also stated that the volume change that occurred could be divided into two components, see Figure 2.11, instant and delayed compression.

"Instant" compression, occurs simultaneously with the increase in effective stress and causes a reduction in the void ratio until an equilibrium value is reached at which the structure effectively supports the overburden pressure.

"Delayed" compression represents the reduction in volume at unchanged effective stresses.

Figure 2.11 shows how the compression of a clay element develops with time if its suddenly loaded with a uniformly distributed load. The dotted line shows the reaction if the soil were to behave as drained, i.e. the pore water in the voids is unable to delay the compression. Due to the viscosity of water the effective stresses will increase gradually when the excess pore pressure dissipates and consequently compression will occur along the solid line.

2.5.5 The time resistance concept

Janbu (1969) presented the time resistance concept and stated that it was a powerful and instructive tool for clarifying the stress- and time-dependent behaviour of soils under compression, swelling or recompression.

Figure 2.14 shows the results from a single load step in an oedometer test. The sample is drained at the top and pore pressure is measured at the impermeable bottom. If time were to be considered as an action and strain as a response to this action, Janbu defines time resistance as:

$$R = \frac{dt}{d\varepsilon} \quad (2.5)$$

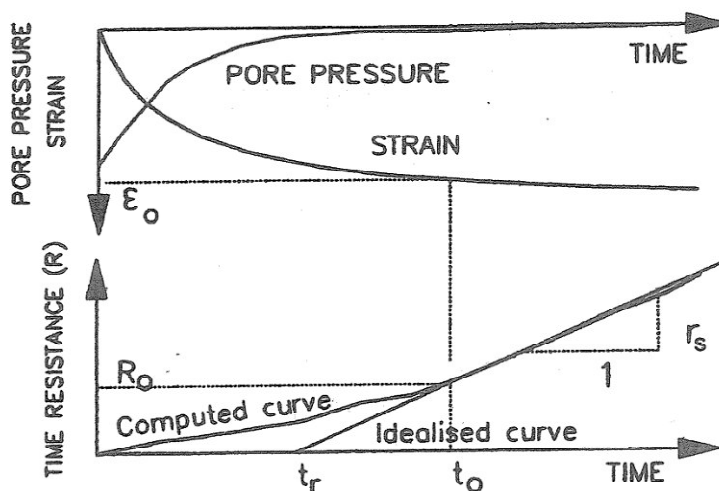


Figure 2.14 Time resistance for a load step in an oedometer Svanö et al. (1991).

From Figure 2.14 it can be seen that after a certain time t_0 the time resistance seems to increase linearly with time. We could thus write:

$$R = r_s(t - t_r) \quad (2.6)$$

where r_s is the time resistance number
and t_r is the reference time

A linear time resistance means a logarithmic creep strain with time since integration from t_0 to t gives

$$\varepsilon_c = \int_{t_0}^t \dot{\varepsilon}_c dt = \int_{t_0}^t \frac{dt}{R} = \frac{1}{r_s} \int_{t_0}^t \frac{dt}{(t - t_r)} = \frac{1}{r_s} \ln \left[\frac{t - t_r}{t_0 - t_r} \right] \quad (2.7)$$

2.6 Overconsolidated conditions

In areas where soft clay exists and no loading has occurred, more than by the soil weight it self, it is common to find overconsolidated behaviour for the clay. In Sweden the typical overconsolidation ratio (OCR), for normally consolidated clays is in the range 1.1-1.3, evaluated from an oedometer test accordingly to the Swedish standard.

Claesson (2003) extracted samples in soft clay to a depth of about 70 m in Gothenburg. The total depth of the clay layer here is about 100 m. Extensive testing was conducted and according to his findings the OCR is relative constant in relation to the depth, see Figure 2.15.

A similar study was conducted by Alte et al. (1989), Kv Guldet, and remarkable similarities with regard to the preconsolidation pressure are seen, as shown in Figure 2.15.

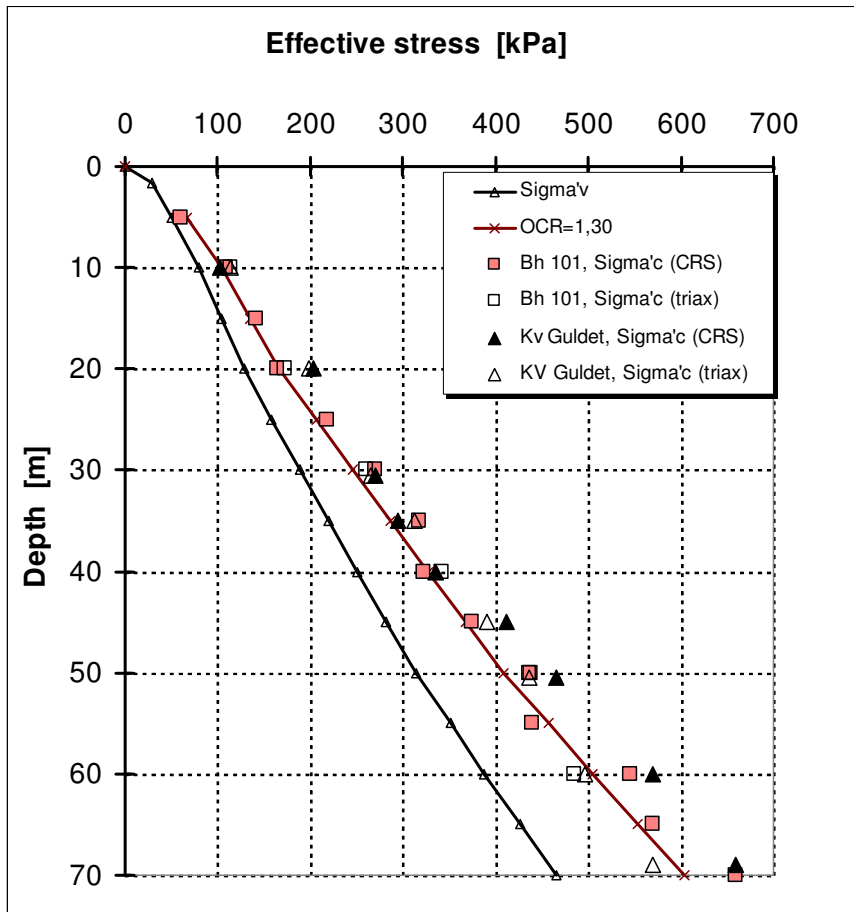


Figure 2.15 Evaluated effective stress and evaluated preconsolidation stress from CRS and triaxial tests with depth for the Lundby Strand test site and Kv Guldet Lilla Bommen, Gothenburg. Data from Claesson (2003).

The OCR effect in this profile can probably not be explained by any preloading and another effect, such as delayed compression (creep) is probably the cause.

3. PROGRAMS FOR CALCULATING TIME-DEPENDENT BEHAVIOUR

In this chapter some of the most commonly used programs for calculating settlement in soft soils in Sweden that incorporate creep are explained and discussed. Today there are, more or less, only three different programs available - Embankco, GS Settlement and the Soft Soil Creep model implemented in Plaxis - that incorporate creep settlement. These three programs will only be discussed in this chapter. The focus is on creep behaviour.

In the end of this chapter there will be a description of how different soil parameters correspond approximately to each other and a proposal for conversion between them.

3.1 Embankco

The Embankco program was developed at the beginning of 1990 as a result of co-operation between SGI and the Swedish Road Administration. The one-dimensional model that is implemented in the program is based on the theories and empirical experiences described in Larsson et al. (1997). The purpose of the program was, at that time, to develop a user-friendly computer program for the prediction of settlement, including creep, for embankments on soft soil (clay).

The Embankco computer program originates from a program called CONMULT, developed in France, Magnan et al. (1979), and further developed at Laval University of Quebec in Canada and at SGI. The program was rewritten to correspond to Swedish compression parameters, evaluated from CRS- and IL tests, and a revised creep model was implemented.

3.1.1 Soil model

The constitutive model for the effective stress vs. strain for the soil used in the calculations corresponds to the observed behaviour of the soil in tests in the field and in the laboratory, Larsson (1986). The soil parameters used for compressibility are expressed as M_0 , M_L , σ'_c , σ'_L and M' as described in e.g. Larsson (1986) or Sällfors & Andréasson (1986).

The excess pore pressure response due to a total stress changes is calculated as

$$\begin{aligned} \Delta u &= \frac{\Delta \sigma_v + \Delta \sigma_h}{2} \text{ when } \sigma'_v < \sigma'_c \\ \Delta u &= \Delta \sigma_v \quad \text{when } \sigma'_v = \sigma'_c \end{aligned} \quad (3.1)$$

The creep model implemented in the program assumes no creep if the stress ratio $\frac{\sigma'_v}{\sigma'_{vc}} < 0.8$ and a linear increase in the creep rate from this stress ratio until it reaches the maximum creep rate at the preconsolidation stress, σ'_{vc} . The program also uses a reference strain rate for whether or not creep effects are included. If the calculated strain rate is higher than this reference rate, creep effects are ignored. The reference strain rate is defined as $\alpha_s \cdot 5 \cdot 10^{-6}$ 1/s. Since creep is a time-dependent process the result of the creep effect is an increase in pore pressure corresponding to an increase in creep strain and current modulus, see Figure 3.1.

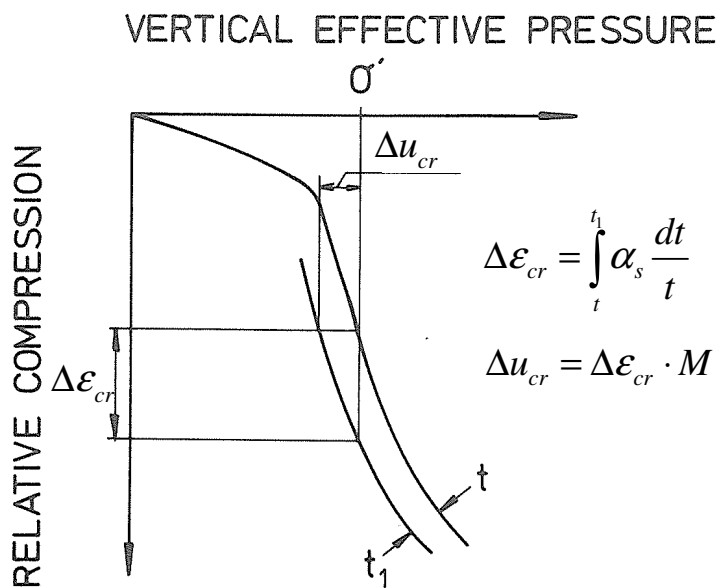


Figure 3.1 Creep effects during consolidation, Larsson (1986).

The creep effects are thus dependent on the rate at which the hydraulic conductivity and drainage conditions allow them to develop and are not only related to the time after load application, Larsson (1986).

3.1.2 Calculation method

The program uses Terzaghi's equation for one dimensional consolidation, see eq. (2.3). When creep effects are included in the equation it creates additional pore pressure, ∂u_{cr} . The consolidation equation then changes to

$$\frac{\partial u}{\partial t} = M \cdot \frac{\partial}{\partial z} \left(\frac{k}{\gamma_w} \cdot \frac{\partial u}{\partial z} \right) + \frac{\partial u_{cr}}{\partial t} \quad (3.2)$$

This equation is then solved using finite difference, explicitly, with sufficiently small time steps defined as

$$\frac{k \cdot M}{\gamma_w} \cdot \frac{\Delta t}{(\Delta z)^2} \leq 0.40 \quad (3.3)$$

Where	k	=	hydraulic conductivity
	M	=	oedometer modulus
	γ_w	=	unit weight of water
	Δz	=	soil thickness of one element
	Δt	=	time step

For each time step, the rate of strain is calculated for each layer and is compared to the reference strain rate. The pore pressure is then changed due to the creep contribution. This pore pressure increase due to creep can never be greater than the consolidated pore pressure, according to the first part of eq. (3.2), for the time step in question.

3.2 GS Settlement

The GS Settlement program is one of several programs in the Geosuite toolbox. It is intended for the calculation of time-dependent settlement under loads and boundary conditions that can vary as a function of time. The program is based on the general finite element program GEOnac (GEOtechnical nonlinear analysis code). GEOnac was developed at SINTEF 1990. The aim of the GEOnac program is to calculate stresses and deformations in geomaterials, Jostad (1993).

3.2.1 Soil model

The one-dimensional model used in GS Settlement was first developed by Svanö (1986). This model couples primary and secondary consolidation and uses the stress modulus and time resistance concept by Janbu (1970).

Figure 3.2 describes a typical response for one load step in an oedometer. At a certain time, t_c , strain is developed at a constant effective stress and

this process is defined as pure creep. The process could be described using the time resistance, R , as

$$R = dt / d\varepsilon = 1 / \dot{\varepsilon}$$

After a time, t_c , the time resistance is assumed to increase linearly with time. This implies that after t_c the strain could be expressed as

$$\varepsilon = \varepsilon_c + \frac{1}{r} \cdot \ln\left(\frac{t-t_r}{t_c-t_r}\right) \quad (3.4)$$

Where r is the time resistance number and ε_c is the reference strain for the current effective stress.

if $R=r(t-t_r)$ and $R_c=r(t_c-t_r)$ then eq. (3.4) could be written as

$$\varepsilon = \varepsilon_c + \frac{1}{r} \cdot \ln\left(\frac{R}{R_c}\right) \quad (3.5)$$

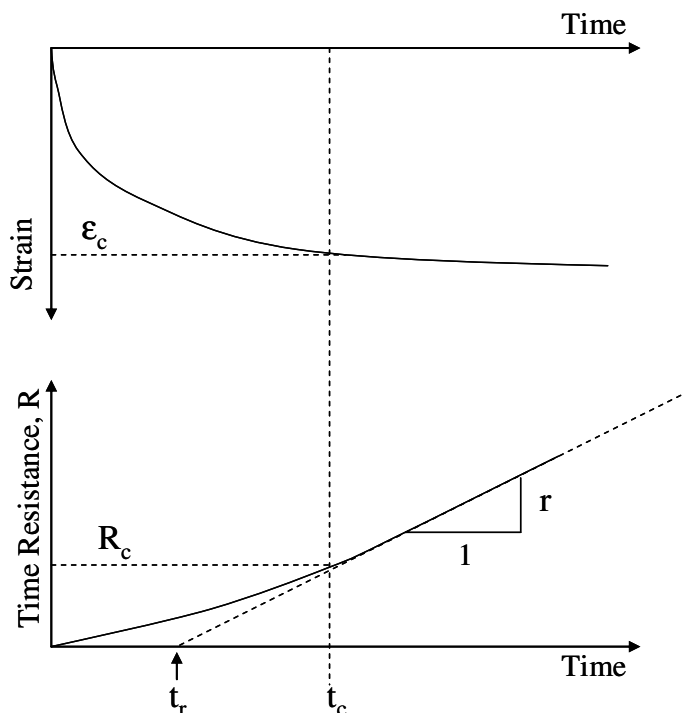


Figure 3.2 One-dimensional strain as a function of time and effective stress for one load step in an oedometer.

As can be seen in Figure 3.2, ε_c defines the strain where eq. (3.5) starts to be valid and R_c is the time resistance at ε_c for this load step. Eq. (3.5) could be inverted, see Figure 3.3

$$R = R_c \cdot e^{r(\varepsilon - \varepsilon_c)} \quad \text{for } \varepsilon \geq \varepsilon_c \quad (3.6)$$

From the equation above, a σ' - ε diagram can be established for different R values, see Figure 3.4, where r , R_c and ε_c are a function of effective stress. According to Figure 3.4, Svanö (1986) has established a general viscous stress-strain-time relationship. This is in line with the model proposed by Suklje (1978), but is extended to incorporate slight over consolidation.

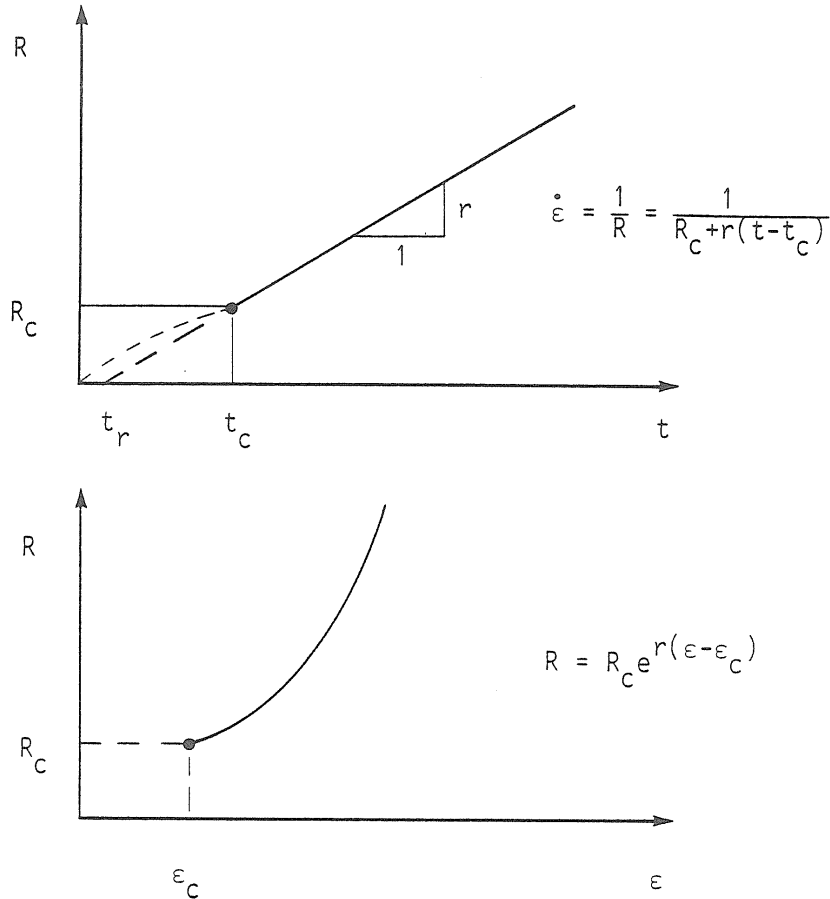


Figure 3.3 Time resistance as a function of time and time resistance as a function of strain for one load step in an oedometer ($\sigma'_v = \text{constant}$), Svanö (1986).

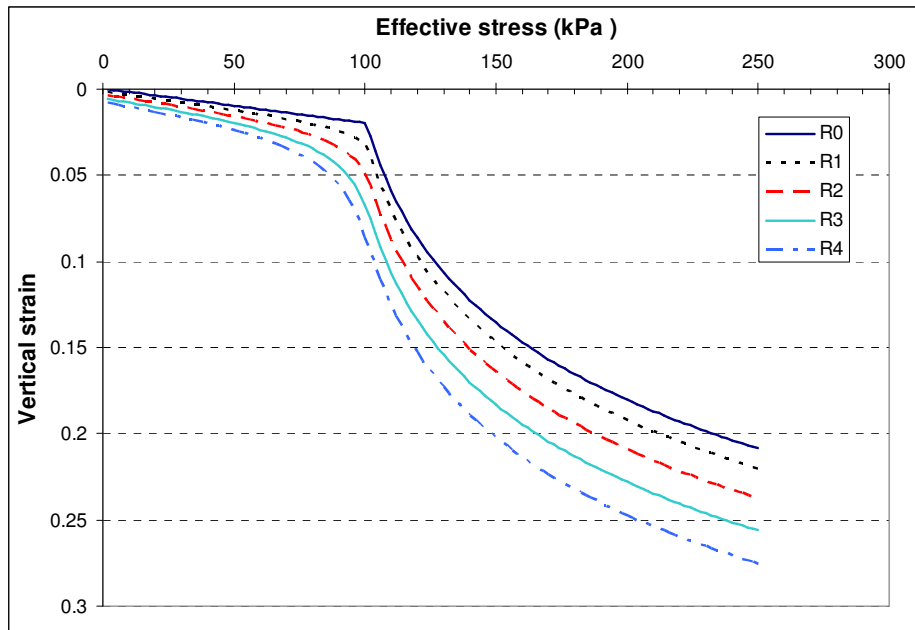


Figure 3.4 Curves with equal time resistance.

3.2.2 Calculation method

The model describes the development of strain as a creep process, Emdal & Svanö (1988). Under constant effective stress and over a time increment Δt the creep strain, $\Delta \varepsilon_{cr}$, will develop as

$$\Delta \varepsilon_{cr} = \frac{1}{r} \ln \frac{R_0 + r \Delta t}{R_0} \quad (3.7)$$

It is assumed in eq. (3.7) that the time resistance, R , is a linear function of time, i.e. $R = R_0 + r \Delta t$.

As can be seen in Figure 3.4, if an instant stress increase is made, it will move us to a lower time resistance, thus giving us a higher strain rate.

Svanö (1986) formulated that the stress increase from σ'_0 to $\sigma'_1 = \sigma'_0 + \Delta \sigma$ during a time period t_0 to $t_1 = t_0 + \Delta t$ could be idealised as

- Creep strain for σ'_0 from time t_0 to $t_0 + \Delta t / 2$
- Creep strain for σ'_1 from time $t_0 + \Delta t / 2$ to t_1

This means that in the middle of the time step the stress goes from σ'_0 to σ'_1 , see Figure 3.5. For state 'a' the creep strain is defined as

$$\Delta \epsilon_{sa} = \frac{1}{r_0} \ln \frac{R_0 + r_0 (\Delta t / 2)}{R_0} \quad (3.8)$$

For state 'b' the strain, ϵ , and time resistance, R , are updated to ϵ_1 and R_1 . R_1 , ϵ_1 and r_1 are a function of stress and are therefore given by $\sigma'_1 = \sigma'_0 + \Delta \sigma$. Creep strain in state 'b' becomes

$$\Delta \epsilon_{sb} = \frac{1}{r_1} \ln \frac{R_1 + r_1 (\Delta t / 2)}{R_1} \quad (3.9)$$

The total creep strain, and thus the total strain since all strain is defined as creep, will be

$$\Delta \epsilon_{s1} = \Delta \epsilon_{sa} + \Delta \epsilon_{sb} \quad (3.10)$$

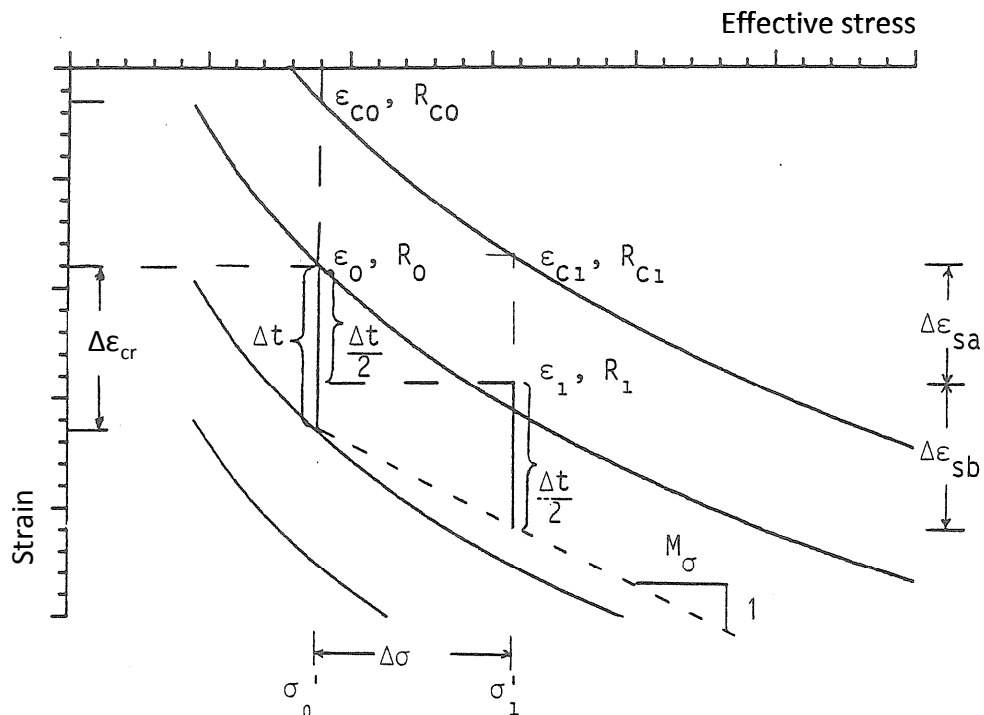


Figure 3.5 One-dimensional strain as a function of effective stress and time, Svanö (1986).

The strain that has been caused by the stress change, $\Delta \sigma$, can be defined as $\Delta \epsilon_\sigma = \Delta \epsilon_{s1} - \Delta \epsilon_c$, and the oedometer modulus can be defined as

$$M_{\sigma} = \frac{\Delta\sigma}{\Delta\varepsilon_{\sigma}} \quad (3.11)$$

$\Delta\sigma$ is unknown and iteration is made to calculate $\Delta\sigma$.

However, there have been some numerical adjustments since this model was presented by Svanö (1986) and in the present implemented model the following adjustments have been made

- The time resistance, R_c , according to eq. (3.6) is adjusted to a high value if the effective stress goes below the initial effective stress.
- For each stress increment five sub increment, i.e. $\Delta t/5$, is used instead of two as shown in Figure 3.5.
- An elastic strain is introduced for each sub increment. This elastic strain is calculated using the oedometer modulus, $M_R=M_0$, for stresses less than the preconsolidation stress and for stresses greater than the preconsolidation stress the oedometer modulus used is calculated as $M_R = M_0 \cdot \sigma'_v{}^{\max} / \sigma'_{vc}$.

3.3 Soft Soil Creep model

The Soft Soil Creep (SSC) model is a material model implemented in the Plaxis BV finite element program. This model originates from the one-dimensional creep theories presented by e.g. Buisman (1936), Suklje (1957), Bjerrum (1967) and Garlanger (1972), and has been converted to differential form to make possible an extension to a 3D-model.

Some basic characteristics of the SSC model are:

- Stress-dependent stiffness (logarithmic compression behaviour)
- Distinction between primary loading and unloading-reloading
- Secondary compression
- Memory of preconsolidation pressure
- Failure behaviour according to the Mohr-Coulomb criteria
- Modified Cam-Clay used as a reference surface (cap)

3.3.1 Soil model

The one-dimensional version of the model in SSC is based on work carried out by Stolle et al. (1997) and Vermeer et al. (1998). The total strain, see Vermeer & Neher (1999) or Brinkgreve et al. (2006) is formulated as

$$\varepsilon = \varepsilon^e + \varepsilon_{dc}^c + \varepsilon_{ac}^c = A \cdot \ln\left(\frac{\sigma'}{\sigma'_0}\right) + B \cdot \ln\left(\frac{\sigma_{pc}}{\sigma_{p0}}\right) + C \cdot \ln\left(1 + \frac{t'}{\tau_c}\right) \quad (3.12)$$

Where $t' = t - t_c$ is the effective creep time and ε is the total logarithmic strain due to an increase in effective stress from σ'_0 to σ' . The total strain is divided into elastic and a visco-plastic creep part, denoted by superscript e and c respectively. The visco-plastic part can be separated into two parts, one during consolidation and one after consolidation. This is denoted by the subscript dc and ac in Figure 3.7. The values σ_{p0} , σ_{pc} and σ_p represent the preconsolidation stress corresponding to before loading, end of consolidation state and after a time of pure creep respectively. The parameters are illustrated in Figure 3.6 and Figure 3.7. ε_{cons} in Figure 3.7 represent the strain at the end of consolidation for one load step.

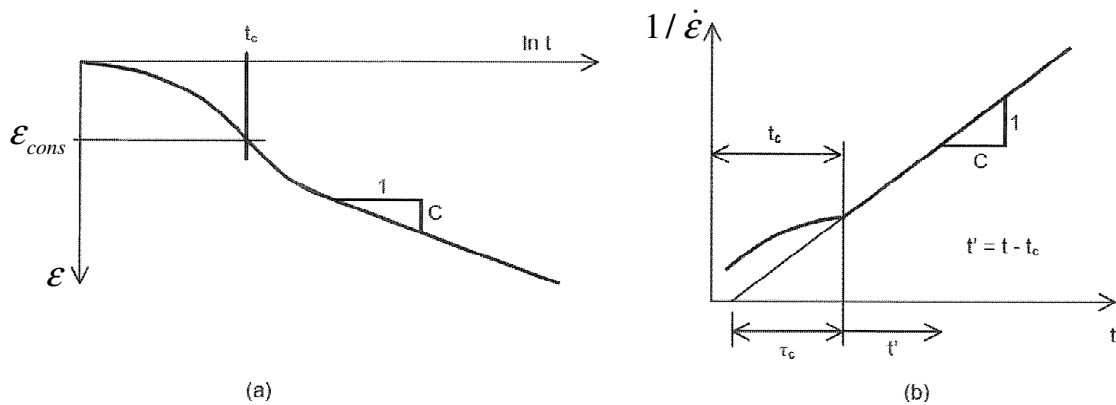


Figure 3.6 Consolidation and creep behaviour in a standard oedometer test, Brinkgreve et al. (2006).

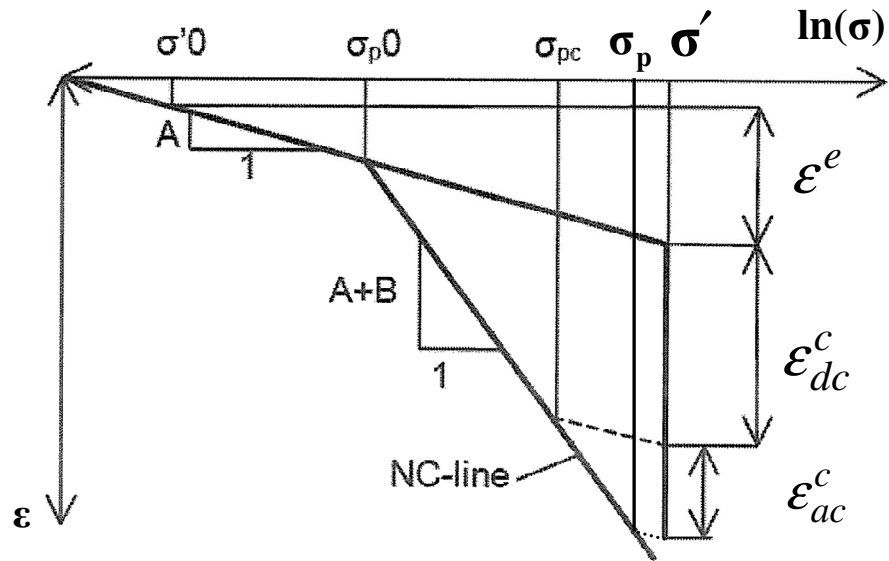


Figure 3.7 An idealised stress-strain curve from an oedometer test with a division of strain increments into an elastic and a creep component, modified from Brinkgreve et al. (2006).

In the SSC-model it is assumed that the total strain is divided into elastic and inelastic strains. In this formulation the inelastic part is assumed to be purely creep, ε^c . The SSC model also adopts the Bjerrum's idea that the preconsolidation stress depends only on the amount of creep strain that has accumulated over time. In addition to eq. (3.12) Vermeer & Neher (1999) introduce the following expression.

$$\varepsilon = \varepsilon^e + \varepsilon^c = A \cdot \ln \frac{\sigma'}{\sigma'_0} + B \cdot \ln \frac{\sigma_p}{\sigma_{p0}} \quad \rightarrow \quad \sigma_p = \sigma_{p0} \cdot \exp\left(\frac{\varepsilon^c}{B}\right) \quad (3.13)$$

As can be seen from eq. (3.13) the longer it is left to creep the larger σ_p grows. In a conventional IL test the load is maintained for a constant period of $t_c + t' = \tau$, where τ is exactly one day. For this type of IL test a so-called normal consolidation line with $\sigma_p = \sigma'$ is obtained. By combining eq. (3.12) and eq. (3.13) and assuming that $(\tau - t_c) \ll \tau$ the time dependency of the preconsolidation stress can be simplified as

$$\tau_c = \tau \cdot \left(\frac{\sigma_{pc}}{\sigma_p}\right)^{\frac{B}{C}} \quad (3.14)$$

Where τ is equal to one day, see Vermeer & Neher (1999). The differential equation can then be derived as

$$\dot{\varepsilon} = \dot{\varepsilon}^e + \dot{\varepsilon}^c = A \frac{\dot{\sigma}'}{\sigma} + \frac{C}{\tau} \left(\frac{\sigma'}{\sigma_p} \right)^{\frac{B}{C}} \quad \text{where} \quad \sigma_p = \sigma_{p0} \exp\left(\frac{\varepsilon^c}{B}\right) \quad (3.15)$$

The one-dimensional model was extended to a general three-dimensional constitutive model based on Modified Cam-Clay type ellipses, see Vermeer et al. (1998). The well-known stress invariants for pressure p' and deviatoric stress q are adopted, Brinkgreve et al. (2006). These stress invariants are used to define the size of the ellipse, see Figure 3.8, as

$$p^{eq} = p' + \frac{q^2}{M^2 p'} \quad (3.16)$$

In Figure 3.8 the soil parameter M_{CS} and M_{MC} are shown and represent the so-called 'critical state line' and the Mohr-Coulomb failure line and are defined as

$$M_{MC} = \frac{6 \cdot \sin(\varphi')}{3 - \sin(\varphi')} \quad \text{- for compression} \quad (3.17)$$

Where the φ' is the effective friction angle.

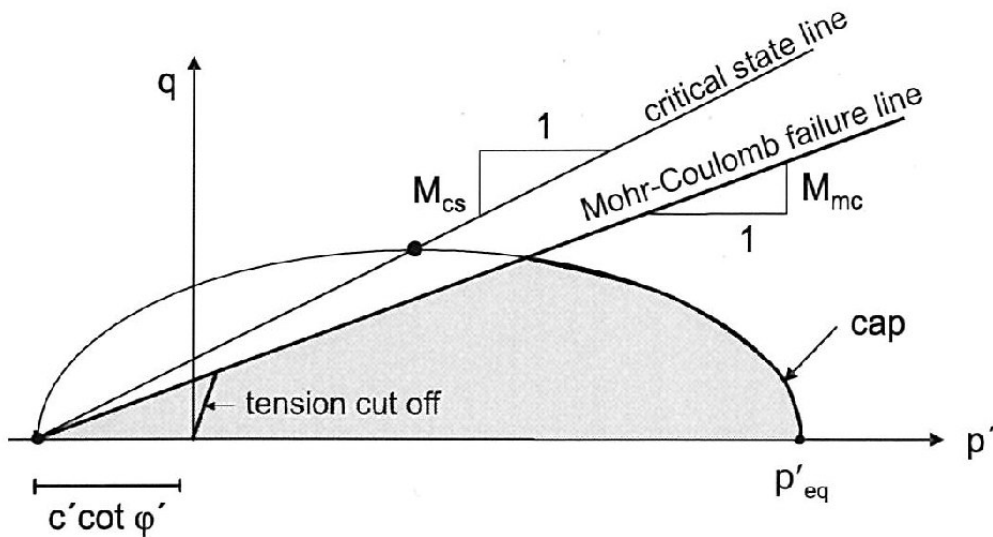


Figure 3.8 Diagram of p^{eq} ellipse in a p - q plane, Satibi (2009).

Figure 3.8 suggests that tensile stresses are possible but this could be prevented by using a tension cut-off option

In the SSC-model an important feature is adopted to simulate a relative steep NC surface. This is done by applying relatively large values for M_{CS} , see Figure 3.8, which could be different from the slope M_{MC} . The M_{CS} could be equal to M_{MC} , but quite large values for M_{CS} need to be used if a prediction of more realistic K_0^{nc} values is to be obtained. Using M_{CS} values greater than M_{MC} will lead to a relatively steep normal consolidation surface in a p-q plane.

In the SSC-model the parameters A, B and C above are changed to the material parameters κ^* , λ^* and μ^* . Conversion is made accordingly, Vermeer & Neher (1999)

$$\kappa^* \approx \frac{3 \cdot (1 - \nu_{ur})}{(1 + \nu_{ur})} \cdot A, \quad \lambda^* = B + \kappa^*, \quad \mu^* = C \quad (3.18)$$

Using the new stress invariants and parameters and omitting the elastic strain in eq. (3.15) the volumetric creep strain, ϵ_v^c , could be written as

$$\dot{\epsilon}_v^c = \frac{\mu^*}{\tau} \left(\frac{p^{eq}}{p_p^{eq}} \right)^{\frac{\lambda^* - \kappa^*}{\mu^*}}, \quad p_p^{eq} = p_{p0}^{eq} \cdot \exp\left(\frac{\Delta \epsilon_v^c}{\lambda^* - \kappa^*} \right) \quad (3.19)$$

If eq. (3.19) is integrated for a constant stress state the change in the size of the yield surface due to creep over a period of Δt is

$$\Delta \epsilon_v^c = \mu^* \cdot \ln \left(1 + \frac{\Delta t}{\tau} \left(\frac{p^{eq}}{p_{p0}^{eq}} \right)^{\frac{\lambda^* - \kappa^*}{\mu^*}} \right) \quad (3.20)$$

where τ = one day in the SSC model. This expression defines the time-dependent creep behaviour and implies that the OCR has a considerable influence on the creep rate.

3.4 Relationships between model parameters

As can be seen above, most of the theories use different names of soil parameters to describe the same behaviour. Here there will be an attempt to describe approximately the relationship between various model parameters used. The focus is on the parameters described in previous chapters.

In Table 3.1 and Table 3.2 some assumptions need to be made in order to describe the approximated relationship between the oedometer modulus, according to the Swedish praxis, and the modified index used in Plaxis. The assumptions are Poisson's ratio $\nu_{ur} = 0.2$, the ratio of $\lambda^* / \kappa^* = 5 - 10$, and the relationship according to eq. (3.18). The relationship between the Plaxis SSC creep index and the swelling- and compression index are according to Brinkgreve et al. (2006).

For the creep parameters, a straightforward relationship exists and no assumptions are necessary.

It should be mentioned that the values could be calculated from Table 3.1 and Table 3.2, although this computation is very sensitive since the choice of the average stress, σ'_v or σ'_{vc} , greatly affects the calculated values.

The values calculated from Table 3.1 and Table 3.2 should only be used to acquire an estimate of the range of the other parameters, as long as no exact correlation between them exists.

It is therefore strongly recommended that the model parameters are evaluated according to the parameters definition in the different models.

Table 3.1 Relationships between various stress-strain parameters for confined compression in the overconsolidated region.

	Oedometer modulus	Swelling index	SSC swelling index
Oedometer modulus	$M = \frac{\Delta\sigma}{\Delta\varepsilon}$	$M \approx \frac{2.3 \cdot (1 + e_0) \cdot \sigma'_v}{C_r}$	$M \approx \frac{2 \cdot \sigma'_v}{\kappa^*}$
Swelling index	$C_r \approx \frac{2.3 \cdot (1 + e_0) \cdot \sigma'_v}{M}$	$C_r = -\frac{\Delta e}{\Delta \log(\sigma'_v)}$	$C_r \approx \frac{\kappa^* \cdot 2.3 \cdot (1 + e_0)}{2}$
SSC swelling index	$\kappa^* \approx \frac{2 \cdot \sigma'_v}{M}$	$\kappa^* \approx \frac{2 \cdot C_r}{2.3 \cdot (1 + e_0)}$	$\kappa^* = \frac{\Delta\varepsilon}{\Delta \ln(p')}$

Note. σ'_v denotes a average stress in the range before the preconsolidation stress.

Table 3.2 Relationships between various stress-strain parameters for confined compression in the normal consolidated region.

	Oedometer modulus	Compression index	SSC compression index
Oedometer modulus	$M_L = \frac{\Delta\sigma}{\Delta\varepsilon}$	$M_L \approx \frac{2.3 \cdot (1+e_0) \cdot \sigma'_{vc}}{C_c}$	$M_L \approx \frac{1.1 \cdot \sigma'_{vc}}{\lambda^*}$
Compression index	$C_c \approx \frac{2.3 \cdot (1+e_0) \cdot \sigma'_{vc}}{M_L}$	$C_c = -\frac{\Delta e}{\Delta \log(\sigma'_v)}$	$C_c = \lambda^* \cdot 2.3 \cdot (1+e_0)$
SSC compression index	$\lambda^* \approx \frac{1.1 \cdot \sigma'_{vc}}{M_L}$	$\lambda^* = \frac{C_c}{2.3 \cdot (1+e_0)}$	$\lambda^* = \frac{\Delta\varepsilon}{\Delta \ln(p')}$

Note. σ'_{vc} denotes the average between the preconsolidation stress and the defined stress σ' .

Table 3.3 Relationships between various creep parameters.

	Creep parameter	Creep number	Creep index	SSC creep index
Creep parameter	$\alpha_s = \frac{\Delta\varepsilon}{\Delta \log(t)}$	$\alpha_s = \frac{2.3}{r}$	$\alpha_s = \frac{C_{ae}}{(1+e_0)}$	$\alpha_s = 2.3 \cdot \mu^*$
Creep number	$r = \frac{2.3}{\alpha_s}$	$r = \frac{dR}{dt}, R = \frac{\Delta t}{\Delta\varepsilon}$	$r = \frac{2.3 \cdot (1+e_0)}{C_{ae}}$	$r = \frac{1}{\mu^*}$
Creep index	$C_{ae} = \alpha_s \cdot (1+e_0)$	$C_{ae} = \frac{2.3 \cdot (1+e_0)}{r}$	$C_{ae} = -\frac{\Delta e}{\Delta \log(t)}$	$C_{ae} = \frac{\mu^* \cdot (1+e_0)}{0.435}$
SSC creep index	$\mu^* = \frac{\alpha_s}{2.3}$	$\mu^* = \frac{1}{r}$	$\mu^* = \frac{C_{ae}}{2.3 \cdot (1+e_0)}$	$\mu^* = \frac{\Delta\varepsilon}{\Delta \ln(t)}$

Note. $\ln(10) = 2.3 = 1/0.435$ and $r = \Delta \ln(t)/\Delta\varepsilon$.

4. DETERMINATION OF SOIL PARAMETERS

This chapter discusses how to evaluate parameters for settlement calculations from laboratory tests. The focus is on the parameters used in the computer programs described in the previous chapter.

Determination or characterisation of soil parameters is broad and contains many aspects that the engineer needs to be aware of when using them. The author makes no attempt to cover all these aspects and will therefore only address some of the parameters used in Swedish practice.

The evaluation of the “classic” parameters, from the CRS oedometer test such as M_0 , M_L , M' , σ'_c , σ'_L and r_1 or α_s will not be addressed other than in some discussions. The reader is referred to i.e. Sällfors & Andréasson (1986) or Larsson et al. (1997).

4.1 Introduction

Measuring soil properties in the laboratory is a necessary complement to numerical analysis. There is no point making a refined analysis when the material properties are not clearly identified. On the contrary, extensive laboratory testing is unnecessary if the problem is not open to analysis. The cost of laboratory testing must be recovered through greater confidence at the design stage. Together, the testing costs and increased design confidence should result in savings during construction and/or improved performance, Graham (2006).

For the Embankco program the reader is referred to Larsson (1986) and Larsson et al. (1997) for an evaluation of the different parameters used in that settlement program.

4.2 Determination of soil parameters for settlement analysis

Determination of parameters for settlement analysis is almost, always based on results from tests on thin laboratory specimens that have been extruded from the ground using a piston sampler and using a certain method. This is usually referred to as an “undisturbed” soil specimen. During extrusion and handling there is inevitable some disturbance to the soil specimen and the magnitude of disturbance resulting from sampling is difficult to measure. An indication of the disturbances to the soil could be evaluated from the test by measuring the volume change at reconsolidation and compare that with empirical values for different degree of disturbance, see Lunne et al. (1997) and Larsson et al. (2007).

A number of researchers have studied the sampling effects and how interpretation of a laboratory test should be conducted such as Ladd & Foott (1974), Sällfors (1975), La Rochelle et al. (1981), Tavenas & Leroueil (1987), Berre (1995), Hight (2001) and DeGroot (2001) to name but a few.

When determining soil parameters for settlement calculations in Sweden the CRS oedometer test is commonly used. Sällfors (1975) puts forward a method for evaluating the preconsolidation stress, which is reduced compared to the test results, due to strain rates effects, so that it corresponds to the measured field value. This implies that when using a material model that is strain-rate dependent, viscous model, the evaluated preconsolidation stress, according to Sällfors method, would probably be lower than the back-calculated preconsolidation stress from the same CRS oedometer test.

4.2.1 Evaluation of the creep parameter from laboratory tests

When evaluating the creep parameter for soft clays, the 24 hour IL oedometer test is traditionally used and with a doubling of the load for each time step. In Figure 4.1 one load step is shown from a traditionally conducted IL oedometer test for a 20 mm thick clay sample.

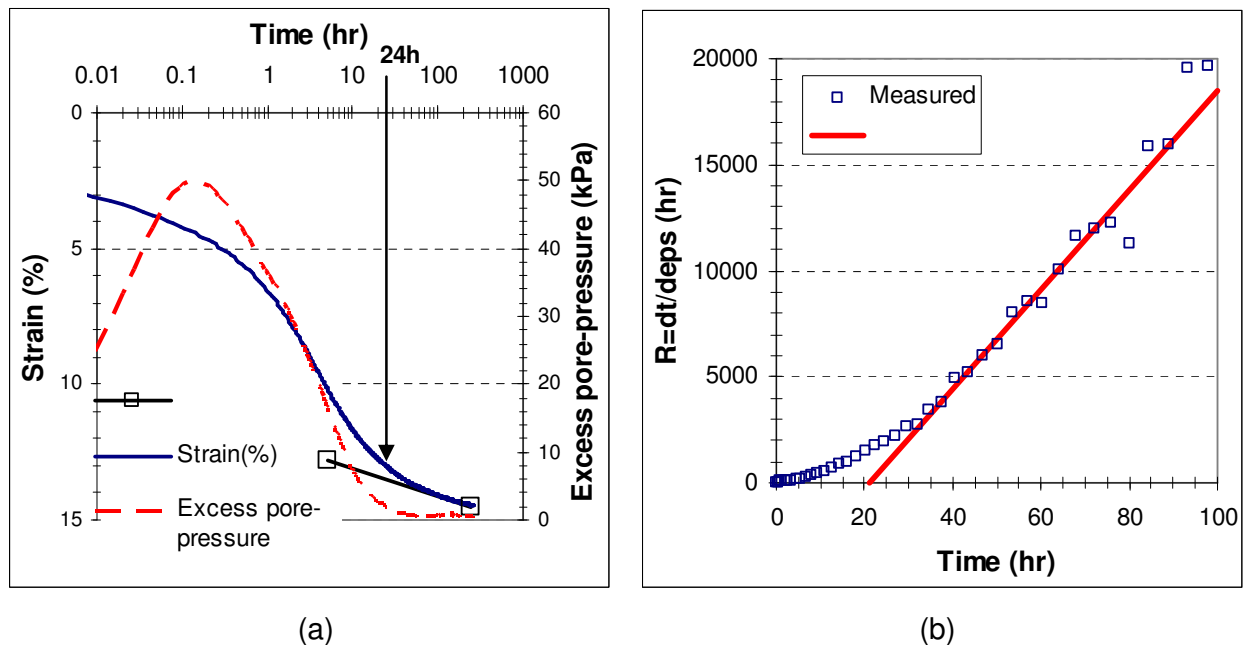


Figure 4.1 One load step in an IL oedometer test, 80-160 kPa. In (a) the log (time) – strain diagram and in (b) the time resistance, R – time diagram. Loading sequence 20, 40, 80 and 160 kPa. Evaluated preconsolidation stress was about 100 kPa. Soil sample from Surte depth 12 m.

If a comparison between the inclination after 24 hours and 100 hours in Figure 4.1 is made, it is clear that if a traditionally 24 hour procedure would be used the creep would be overestimated. This is since consolidation phase is not yet, or just, complete and the consolidation phase would contribute to a higher creep rate.

In Figure 4.1a it seems that a reasonable time period, in this case, for this load step would be between 100 to 200 hours to evaluate a proper creep parameter. But in Figure 4.1b it seems that about 48 hours would be sufficient. This is due to the plotted time scale for the two, where Figure 4.1a uses a logarithmic and Figure 4.1b a linear time scale.

The excess pore pressure in Figure 4.1a takes roughly 24 hours to dissipate, with measured excess pore-pressure less than 2 kPa. This is considerable longer time than if only the classic consolidation theory would be considered, which in that case would be a matter of minutes or perhaps hours depending on the hydraulic conductivity of the clay. This implies that the creep process is greatly influencing the consolidation phase and not only acting when consolidation is complete.

4.2.2 Creep parameters at the preconsolidation stress – empirical

Creep parameters are, more or less always, evaluated from an IL oedometer tests, see Figure 2.8. In Sweden today these tests are seldom conducted, even in cases where creep is of great importance. Normally the creep parameter is estimated empirically from the natural water content, w_N , either from Larsson et al. (1997) or according to eq. (4.1), Christensen (1995).

$$r_1 = \frac{75}{w_N^{1.5}} \quad (4.1)$$

This correlation between the natural water content and the creep parameter for clays is taken from a large number of IL oedometer tests, mainly on Swedish and Norwegian clays.

Mesri & Godlewski (1977) showed a relationship between C_α/C_c and concluded that this ratio is a constant for a given soil. Mesri & Castro (1987) stated that for the majority of inorganic soft clays the C_α/C_c ratio is

$$\frac{C_\alpha}{C_c} = 0.04 \pm 0.01 \quad (4.2)$$

If a conversion of eq. (4.2) to Swedish parameters is made according to Table 3.2 and Table 3.3 the following expression is reached

$$r_1 = \frac{M_L}{(0.04 \pm 0.01) \cdot \sigma'_{vc}} \quad (4.3)$$

4.2.3 The Chalmers model

Claesson (2003) presented a model where the creep number and oedometer curve is modified according to Figure 4.2. This model, named here as the Chalmers model, is implemented in the GS Settlement program. Five additional parameters a_0 , a_1 , b_0 , b_1 and r_0 also need be defined in addition to the classic Swedish parameters. The additional parameters are shown and defined in Figure 4.2.

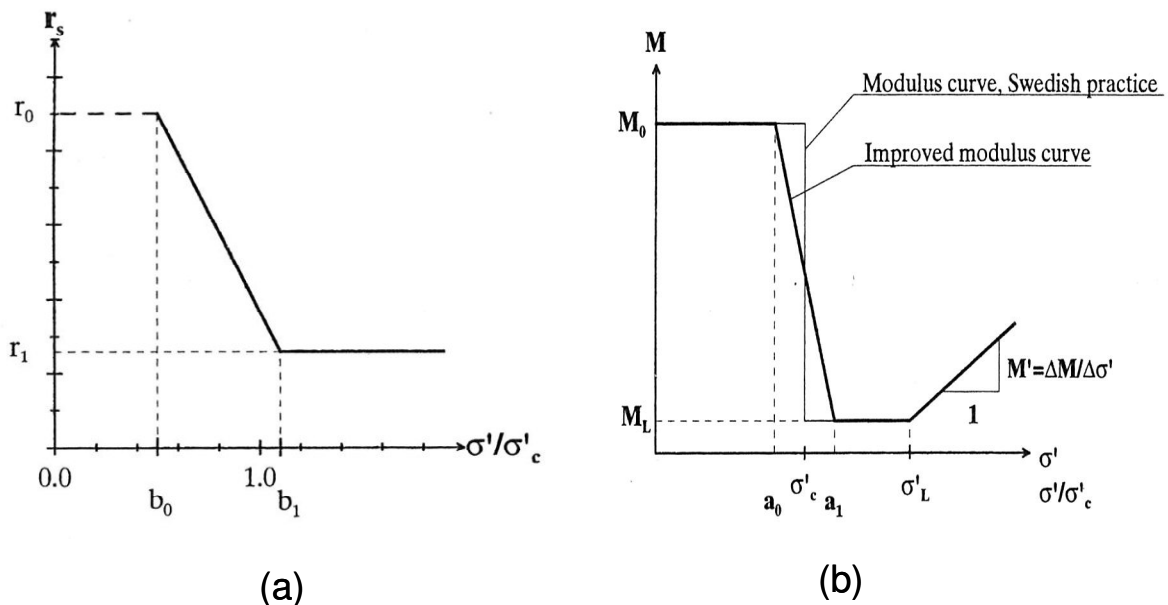


Figure 4.2 Definition of (a) the creep number model, including the factors b_0 and b_1 , and (b) the oedometer modulus curve, including the factors a_0 and a_1 as a function of the normalised effective stress, Claesson (2003).

The parameters a_0 and a_1 are according to Claesson (2003) normally set at 0.8 and 1.0 respectively. However, no actual evaluation method was put forward and in Figure 4.3 a way of evaluating these parameters is proposed. This evaluation method is based on the CRS oedometer test performed according to Swedish practice.

The evaluation method is as follows

- Evaluate σ'_c , M_0 and M_L from the stress-strain curve. (Observe that M_0 is only evaluated here for the use of finding the a_0 value)
- Draw a line parallel to the stress-strain curve so that it intersects the evaluated σ'_c . The distance “c” can then be determined.
- Plot the M_0 and M_L as horizontal lines in the modulus curve.
- Draw a line that follows the evaluated modulus between M_0 and M_L in the modulus curve.
- Move the bottom part of the line from step 4 the distance “c” horizontally towards σ'_c .
- Evaluate a_0 and a_1 as the effective stress at these point divided by the σ'_c .

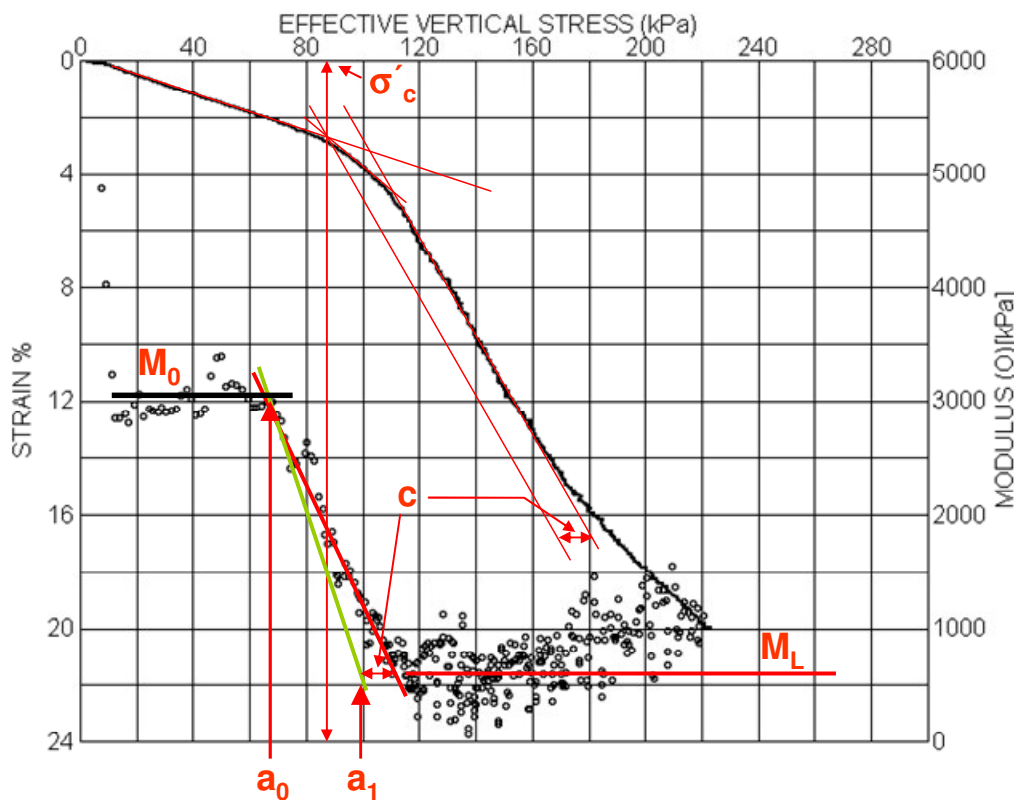


Figure 4.3 Proposed evaluation of the parameters a_0 and a_1 from a CRS oedometer test according to Swedish practice.

It should be pointed out that the parameter a is evaluated from the plotted modulus-stress curve which according to experiences produces an M_0 value that is too low, compared to the field conditions. A general practice is to multiply the evaluated M_0 from a CRS test with a factor of 3-5 to more represent the field value. This should not have any important effects

on the evaluation of the parameter a_0 , more than that the curve between M_0 and M_L will become steeper.

The assumption is that the a_0 is not strain rate dependent. In Figure 4.4 a series of evaluated oedometer curves from CRS oedometer tests with different rate of deformation, conducted by Sällfors (1975), is shown.

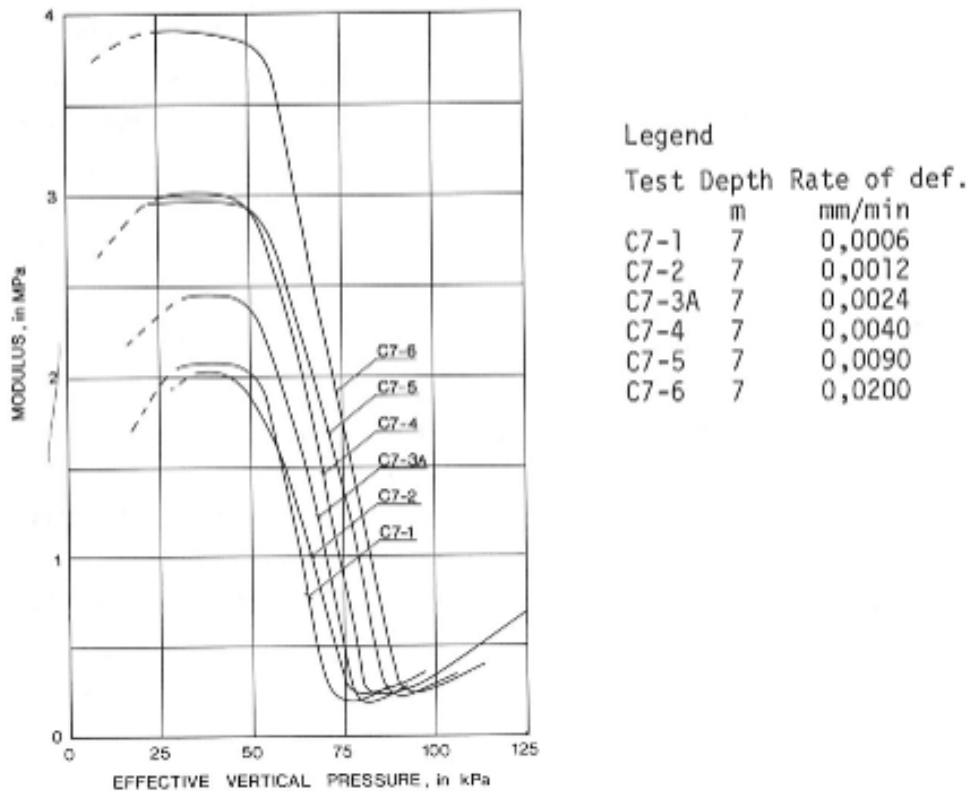


Figure 4.4 Variation in oedometer modulus due to strain rate, Sällfors (1975).

As can be seen in Figure 4.4 the assumption that a_0 is independent of strain rate is supported as the point when the M_0 falls towards M_L seems to be relatively constant for different strain rates.

The parameters r_0 and r_1 are defined in Figure 4.2 with the corresponding b_0 and b_1 values. Together these values give the creep number at the present effective stress. The parameter b_0 is for the sake of simplicity set in such a way that it corresponds to the in-situ effective stress ($\sigma'_{v0}/\sigma'_{vc}$).

Evaluation of the parameter r_0 is not straight forward. However, a method for determining this parameter was put forward by Olsson & Alén (2009). The idea behind this method is that the creep number, r , which is stress dependent, should increase towards infinity at a certain reference stress. The reference stress corresponds to the OCR the clay has reached after a very long time. Hence the creep number is given by a proposed hyperbolic

function, see eq.(4.4). The linear description of the creep number in the Chalmers model is then given such that it corresponds with the assumed r -value for the final stress level, $\sigma'_0 + \Delta\sigma$, see Figure 4.5. The reference stress is suggested at $\sigma_{ref} = \sigma'_{vc}/1.35$ in Olsson & Alén (2009).

$$r(\sigma') = \frac{\psi}{\sigma'_{vc}} \cdot (\sigma'_{vc} \cdot b_1 - \sigma_{ref}) \cdot \left[\frac{\sigma'_{vc} \cdot b_1 - \sigma'}{\sigma' - \sigma_{ref}} \right] + r_1, \quad \sigma_{ref} < \sigma' < \sigma'_{vc} \cdot b_1 \quad (4.4)$$

where $\sigma_{ref} = \frac{\sigma'_{vc}}{1.35}$ and the factor ψ is the slope of r between r_0 and r_1 for stress $\geq b_1 \cdot \sigma'_{vc}$. This factor, ψ , is based on evaluated IL oedometer tests presented by Claesson (2003) and found to normally be in the range of 2000 – 3000. The factor b_1 is normally set in the range of 1.0 – 1.1 according to Claesson (2003).

The maximum creep number r_0 then becomes

$$r_0 = \psi \cdot \frac{(\sigma'_{vc} \cdot b_1 - \sigma_{ref}) \cdot (b_1 - b_0)}{\sigma'_{v0} + \Delta\sigma - \sigma_{ref}} + r_1, \quad \sigma'_{v0} + \Delta\sigma \leq \sigma'_{vc} \cdot b_1 \quad (4.5)$$

In Figure 4.5 creep number, r , is shown as a function of the normalised effective stress according to eq. (4.4) and eq. (4.5).

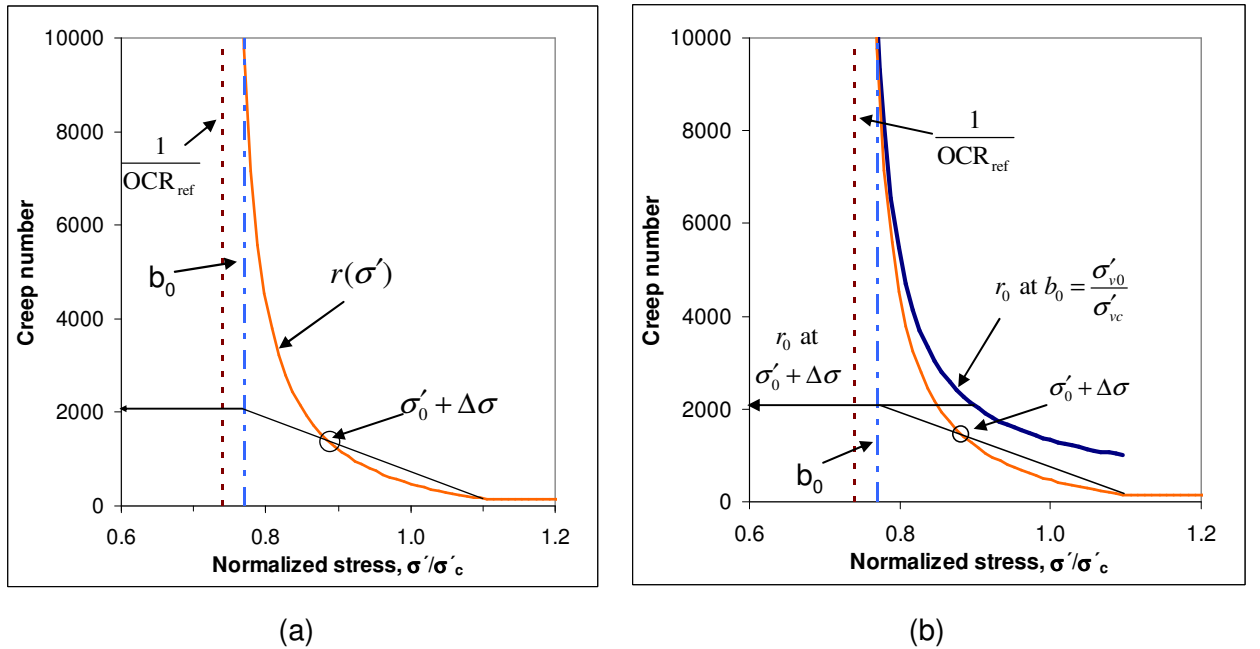


Figure 4.5 In (a) the creep number, r , and in (b) both r and r_0 as a function of normalised effective stress with $r_1=150$, $b_0=0.75$, $b_1=1.1$ and $\psi=2500$.

In Figure 4.5a the change of the creep number due to stress change is shown and an example of how to evaluate the r_0 -value at a certain final effective stress. Thus using this function for r_0 according to eq. (4.5) gives a starting creep number, r_0 , that is not only dependent on the present effective stress but also on the estimated final effective stress, i.e. after full consolidation for the applied load ($\Delta\sigma$), see Figure 4.5b.

If the evaluated creep number, r , becomes extremely high (e.g. $>10\,000$) for the final effective stress there is perhaps no need to use a creep model since the creep effects will probably be of no practical magnitude. The reason for presenting this evaluation method of the creep number, r_0 , is because the model described in Figure 4.2a probably underestimates the creep number for small applied loads, $\Delta\sigma'$. The engineer must make a critical examination of its validity.

4.2.4 Modelling laboratory tests

When using numerical programs an attempt should be made to back-calculate some of the laboratory tests that have been conducted. This is done to validate that the material model is behaving as anticipated with the selected input parameters and a calibration of the input parameters there after.

Since in Sweden the CRS oedometer test is frequently used when establishing the parameters necessary for a settlement calculation, this test will be focused on for back-calculation. Of the programs that are discussed in this thesis only the Soft Soil Creep model implemented in Plaxis software could model the CRS oedometer test.

For back-calculating a CRS oedometer test in Plaxis an axisymmetrical model as shown in Figure 4.6 is used. The boundary conditions are that the horizontal displacement is prevented at the sides of the sample and at the bottom of the sample both the vertical and the horizontal displacement are constrained.

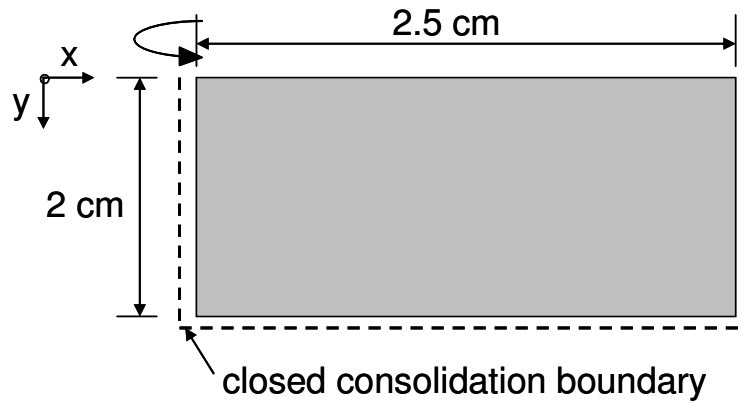


Figure 4.6 Principal sketch of an axisymmetrical model used in FE analysis to simulate a CRS oedometer test.

The procedure used in this thesis to back-calculate a CRS test is as follows

- Create the initial stress, in-situ, in the sample by applying a thin elastic soil layer on top of the 2 cm test sample, which corresponds to the overburden effective stress.
- Set the closed consolidation boundary condition according to Figure 4.6.
- Set the OCR and a proper K_0 value and calculate the stresses.
- At the first calculation phase unload the sample to a small starting vertical stresses. This is normally performed with drained condition and relatively fast.
- The sample settlement is reset back at zero and is then followed by the CRS simulation. The strain rate should correspond to the strain rate in the laboratory.

An example of a back-calculated CRS test is shown in Figure 4.7 and the input parameters used are presented in Table 4.1.

Table 4.1 Input parameters for back-calculation of CRS oedometer test.

ϕ' (deg)	c' (kPa)	κ^*	λ^*	μ^*	v_{ur}	K_0^{nc}	OCR	K_0
30°	0.1	0.018	0.27	0.0065	0.15	0.5	1.2	0.56

The K_0^{nc} value is set according to Jaky (1944), see eq. (4.6), and the K_0 value is calculated according eq. (4.7) from Schmidt (1966).

$$K_0^{nc} = 1 - \sin(\phi') \quad (4.6)$$

$$K_0 = K_0^{nc} \cdot OCR^{1.2 \cdot \sin(\phi')} \quad (4.7)$$

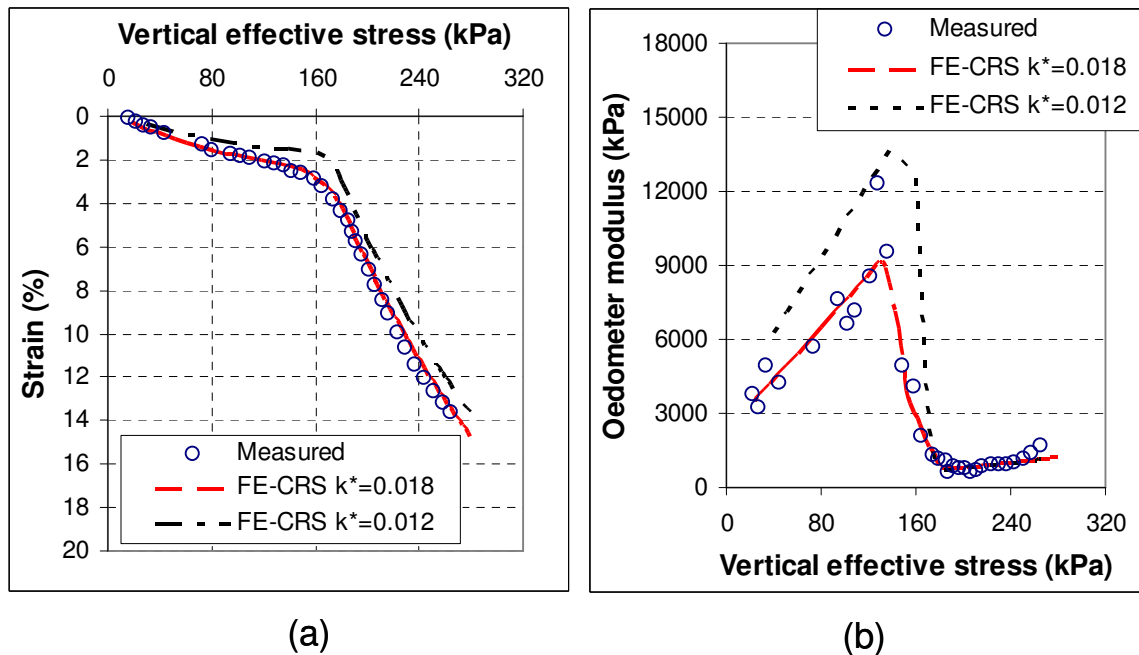


Figure 4.7 Back-calculated CRS oedometer test with two different κ^* values. In (a) the stress-strain curve is compared with the measured values and in (b) the oedometer modulus is compared. The CRS oedometer test was performed with a strain rate of 0.7%/hr.

In this back-calculation two simulations are shown. One with a direct evaluation of the oedometer modulus and one with a slightly higher oedometer modulus in the overconsolidated stress region, as seen in Figure 4.7b. This is to illustrate the effect of the κ^* value. As mentioned before, the evaluated oedometer modulus from a CRS oedometer test in the overconsolidated region is often too low compared to field conditions and a lower κ^* value would be more correct for the field condition than the one that fits the plotted CRS curve.

Kullingsjö (2007) showed the difference in a one-dimensional compression test for stress paths for a fully unloaded sample compared to an assumed stress path consolidated to in situ conditions before being compressed, see Figure 4.8.

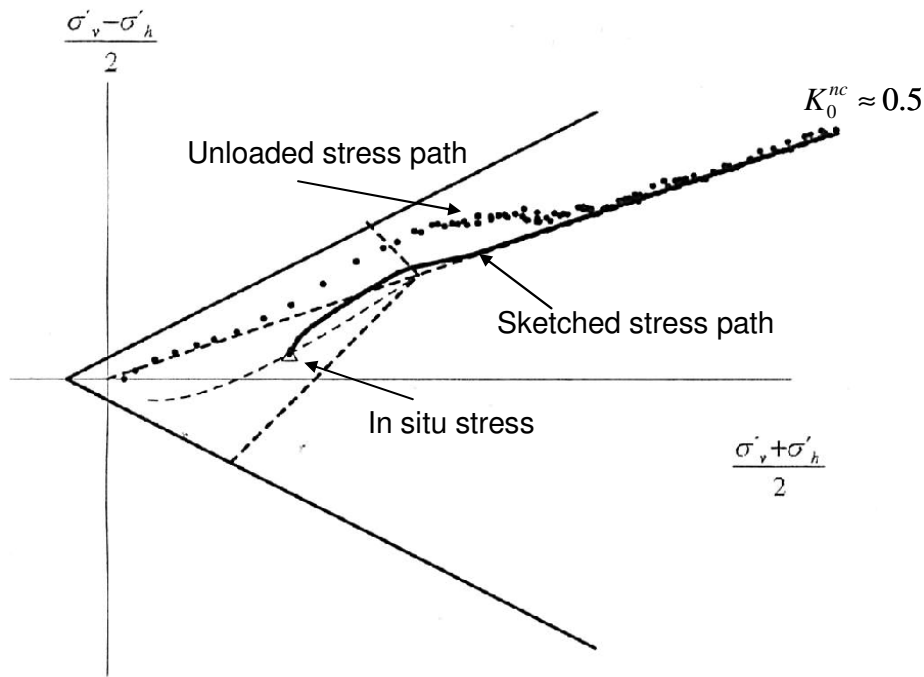


Figure 4.8 Differences between a one-dimensional compression test starting from fully unloaded conditions or consolidated to in situ stress (sketched), Kullingsjö (2007).

It becomes quite clear when the stress path for a CRS oedometer test is studied that the stress path is very different from the in situ stress path when loaded. This will affect the development of the strain during compression, and could be a contributing reason together with sample disturbance why the evaluated oedometer modulus, M_0 , is too low compared to the one in the field tests.

The evaluated oedometer modulus curve in Sweden has three different stages, where the M_0 and M_L are constant for a specified stress region, and M' where the oedometer modulus increases with effective stress, see Figure 4.2b. This formulation differs from the formulation used in the SSC model. The oedometer modulus used in the SSC model is stress-dependent for the overconsolidated (OC) and normal consolidated (NC) region, as shown in Figure 4.9.

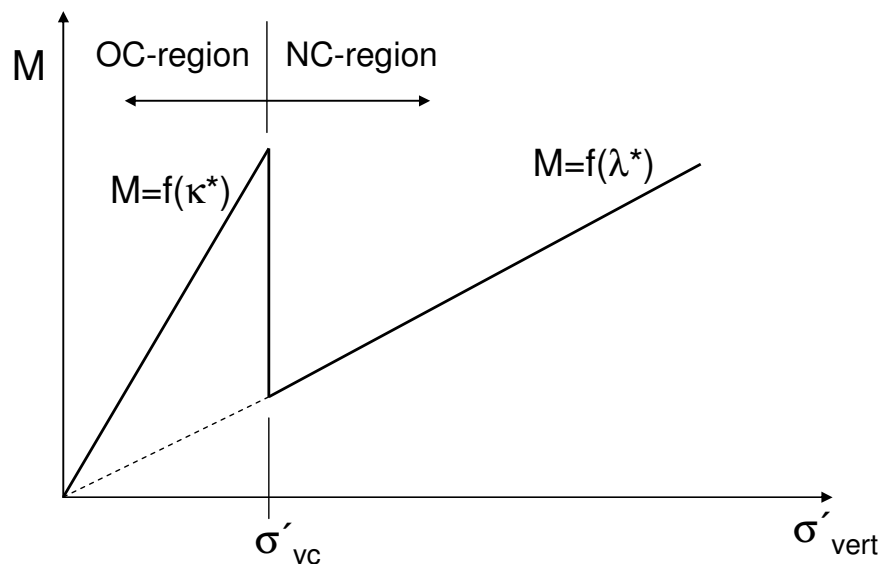


Figure 4.9 Oedometer modulus according to the SSC-model due to effective stress.

As seen in Figure 4.9 the oedometer modulus in SSC model intersects where the stress is zero, which is normally not the case for the Swedish clays, see e.g. Figure 4.3. This implies that when using this model the user must be aware of the final effective stress of interest. In most cases the final effective stress is close to the preconsolidation stress and consequently the λ^* value should often correspond to the M_L according to the Swedish evaluation method.

4.3 Discussion

As mentioned earlier, the CRS oedometer test is the most commonly used laboratory test conducted in Sweden to establish compressibility parameters for settlement analysis. It was also mentioned that the IL test are seldom conducted today, even when creep is of great importance, and that instead an empirical relation to the natural water content was used. However, in the authors opinion the IL test should be conducted if creep is of interest, at least to verify that the assumptions, i.e. that the relation to the natural water content is satisfactory.

As could be seen in Figure 4.1 the difficulties of determining the creep parameter from a traditionally IL oedometer test after 24 hours are shown for one load step. This implies that considerations have to taken for how long the time period should be for each step in IL oedometer test, to proper evaluate the creep parameter. However, evaluation with the time resistance concept seems less sensitive for underestimating the creep parameter. Considerations should also be taken regarding how the test procedure should be conducted.

When using the Chalmers model in the GS program the determination of the creep parameter, r_0 , is sometimes of great interest. This parameter is difficult to determine and a proposed method is suggested. This method is based on the findings of both Larsson et al. (1997) and Claesson (2003) regarding creep, i.e. how it behaves around the preconsolidation stress. Using values greater than 3,000 – 5,000 for the creep parameter, r_0 , should be used with care and the user should always study and critically examine the effects of using high values of r_0 . If an IL oedometer tests have been conducted a back-calculation could be done and a calibration of the creep parameters is possible.

When conducting a laboratory test on a clay sample for investigating the soil properties in the overconsolidated region or at small strains care should be taken. Researcher such as Jardine et al. (1985) and Burland (1989) found that the stiffness was considerably greater in the field than in the laboratory for small strains and that conventional laboratory tests can lead to an underestimation of the soil stiffness. This is probably an effect of disturbance and how the sample is reconsolidated in the laboratory.

This implies that the oedometer modulus, M_0 , in overconsolidated region is very difficult, if not impossible, to determine with conventional laboratory test, such as CRS oedometer tests. A better evaluation of the oedometer modulus, M_0 , could probably be reached if unload and reload cycles are conducted.

Modelling laboratory test is one way of calibrating the material model and checking that it is behaving as intended. A procedure was proposed to back-calculate a CRS oedometer test and some results were plotted together with measurements from a CRS oedometer test. This procedure is only possible with the SCC model in the Plaxis software of the three programs. If an IL test has been conducted the same type of back-calculation could be done, although, instead of applying a defined strain rate the stress increments from the laboratory and with the following consolidation time in each stress increment should be applied. Such a procedure could be simulated both in the Plaxis and the GS Settlement software.

5. TEST SITES

This chapter will describe three different test sites where one will be a hypothetical test site and the other two actual field cases.

The hypothetical test site is presented here to show the differences between the calculated results from the programs and how the results correspond to each other

The other two test sites are:

A case with a test embankment that was constructed on floating lime cement columns (LCCs) and monitored for about seven years.

A groundwater lowering in the bottom aquifer in the central part of Gothenburg, which has been monitored for about 40 years.

5.1 Hypothetical test site

The hypothetical case is created to illustrate in simple terms how the different programs work.

The hypothetical case illustrates a road embankment with a height of 1.5 m and a total width of 26 m, see Figure 5.1.

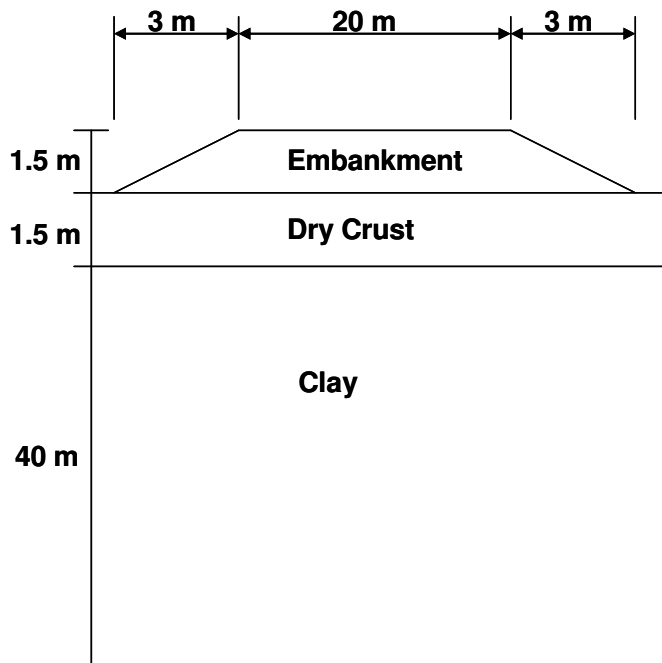


Figure 5.1 Geometry of the embankment and soil profile.

5.1.1 Ground conditions

This hypothetical case comprises a 40 m thick soil layer with soft clay and with an horizontal overlaying dry crust of 1.5 m. Underneath the clay layer there is a non-cohesive material that has a considerably higher hydraulic conductivity than the clay layer.

The unit weight is set to vary between 15 and 17 kN/m³, see Figure 5.2a. The undrained shear strength is about 10 kPa at the top of the clay layer and increases by about 1.6 kPa/m, see Figure 5.2b. The undrained shear strength is calculated from the liquid limit and the preconsolidation stress is according to Swedish empirical relation, see Larsson et al. (2007).

The water content and liquid limit are presented in Figure 5.3a. As can be seen, the water content is about 85 % in the top of the clay layer, decreasing to about 50 % at a depth of 40 m. The liquid limit is slightly less. The OCR is assumed to be equal 1.3 in the clay layer as shown in Figure 5.3b.

The ground water table is in the top of the clay layer and the pore pressure is hydrostatic. The hydraulic conductivity is in the range $1 \cdot 10^{-10}$ m/s, the lower values in relation to depth.

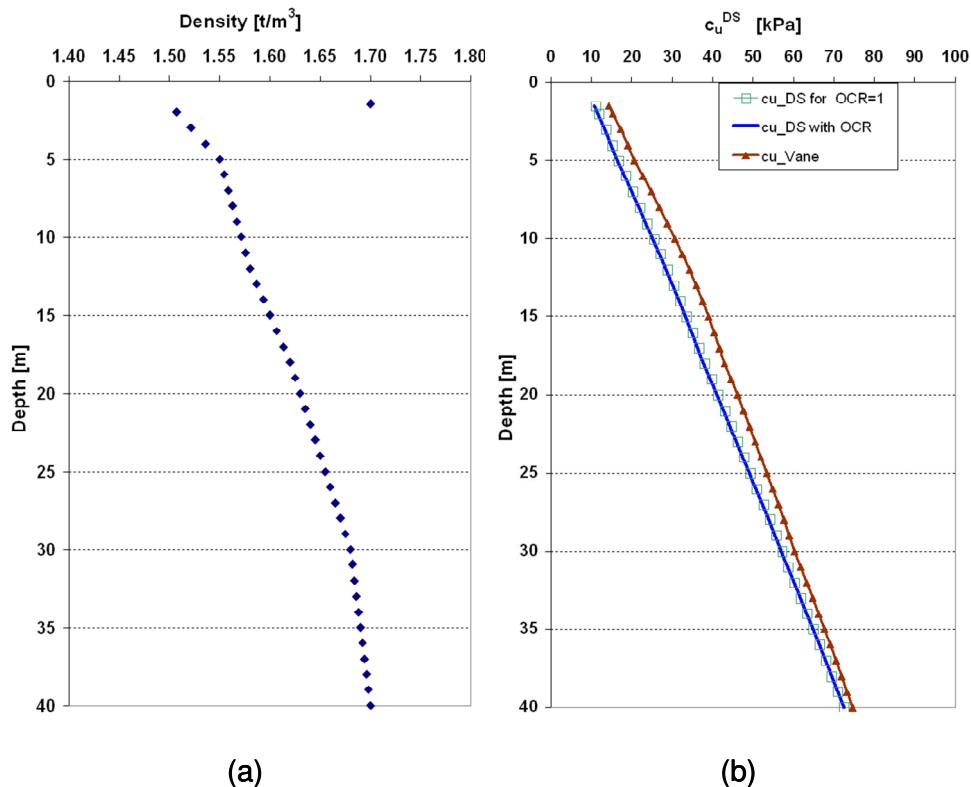


Figure 5.2 (a) Density towards depth and (b) shear strength in relation to depth.

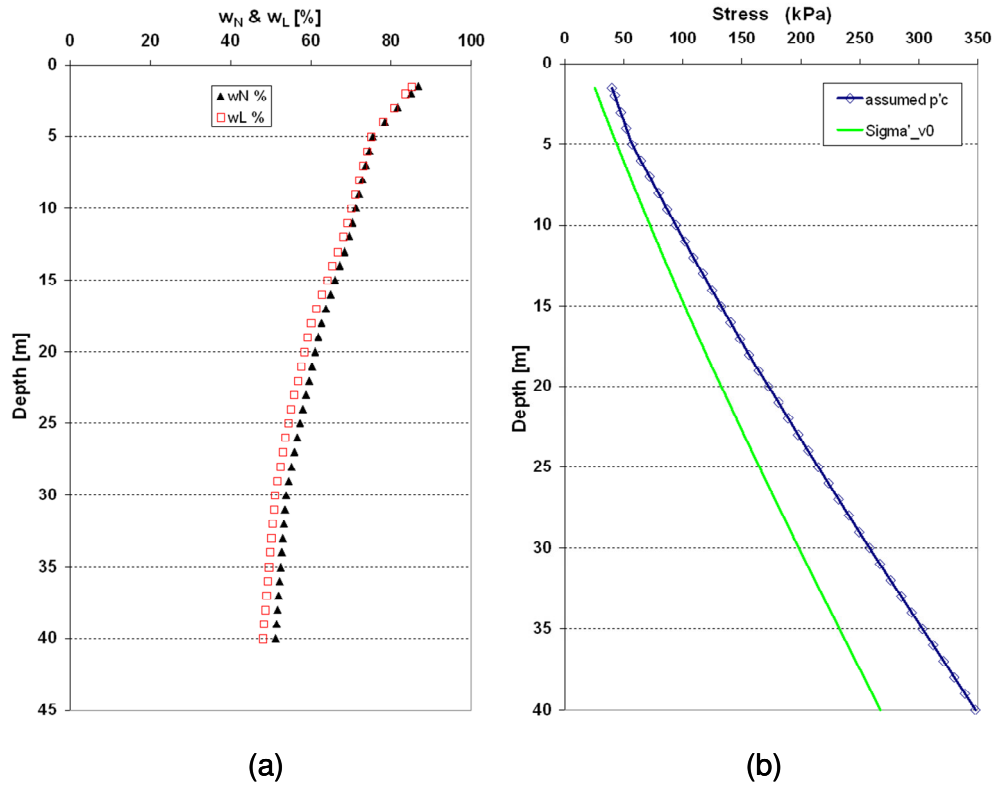


Figure 5.3 (a) water content(\blacktriangle) and liquid limit(\square)in relation to depth and (b) assumed preconsolidation stress.

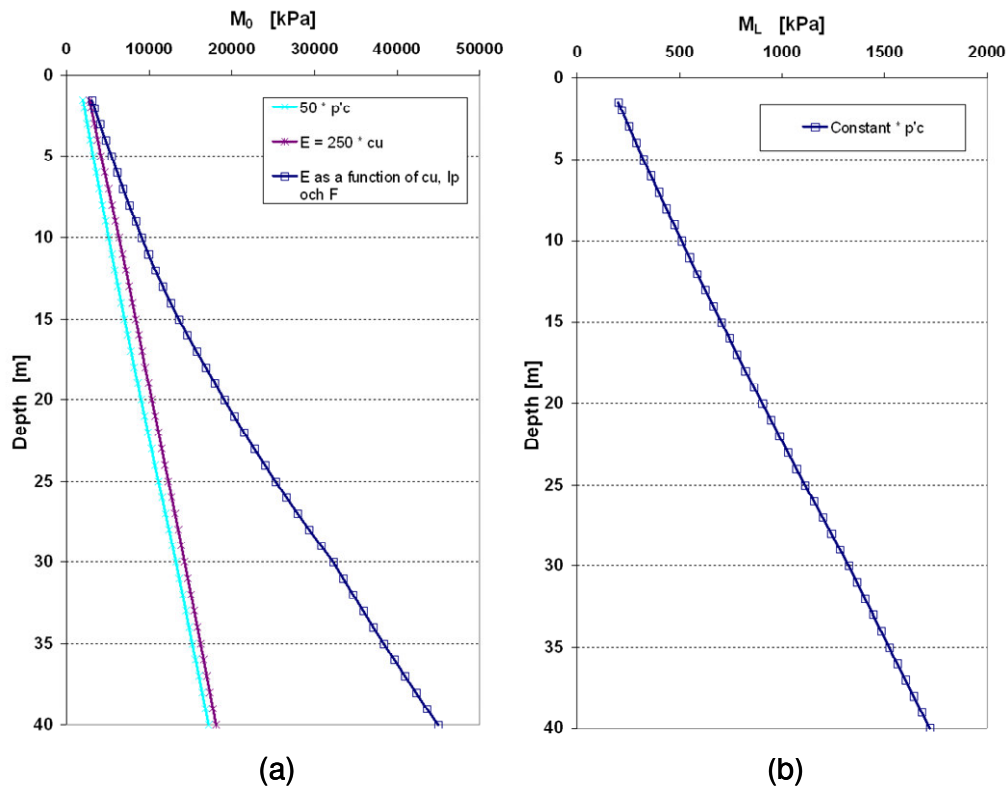


Figure 5.4 Oedometer modulus in relation to depth (a) in the overconsolidated stress region and (b) in the normal consolidated stress region.

The oedometer modulus, M_0 , as shown in Figure 5.4a is calculated in three different ways as: $50 \cdot \sigma'_c$, $250 \cdot c_u$ and as a function of c_u , I_p and $F = 2$, described in Larsson et al. (2007).

The oedometer modulus, M_L , in the normally consolidated stress region is assumed to be $M_L = 5 \cdot \sigma'_c$ as shown in Figure 5.4b. This is within the range typical of the soft clays in the Gothenburg region.

5.2 The Nödinge test embankment

The Nödinge test embankment is located about 25 km north of Gothenburg. The test embankment was constructed to study the effects of floating lime cement columns (LCCs) not reaching firm bottom and, the effects of settlement reduction and stability conditions. This was performed due to a major infrastructure project between Gothenburg and Trollhättan in western Sweden. The infrastructure project consists of 80 km of new motorway and high-speed railway. A large part of the new motorway and railway will be constructed on soft, high-plastic clay along the Göta River valley.

The Nödinge test embankment was one of three full-scale test embankments constructed during the project's feasibility studies. Information about the test embankments can be found in Alén et al. (2005), Baker et al. (2005) and Olsson et al. (2008).

The test embankments were considered necessary due to a lack of reliable methods for estimating consolidation settlement of embankments founded on floating lime-cement columns. The embankments were constructed in 2001 and were heavily instrumented in order to study the settlement of the embankments.

5.2.1 Ground conditions

The ground consists of mainly of deep deposits of soft, high-plastic clays deposited in marine conditions some 5,000 – 10,000 years ago. The clay layers are usually slightly overconsolidated. Below the clay layers there are generally a few metres of non-cohesive material. The clay is glacial and post-glacial clay.

The unit weight varies between 14.5 and 16.5 kN/m³, see Figure 5.5a. The undrained shear strength is about 10 kPa down to a depth of about 5 m and then with an increase of about 1 kPa/m, see Figure 5.5b.

The water content is about 100% at the top, decreasing to around 60% at a depth of about 30 m and then increasing to about 80%. The liquid limit is of the same order but slightly less in the upper 5 to 10 m as can be seen in Figure 5.6a. The OCR in the area is about 1.1-1.3 as can be seen in Figure 5.6b, with a slightly higher OCR in the top 5 m.

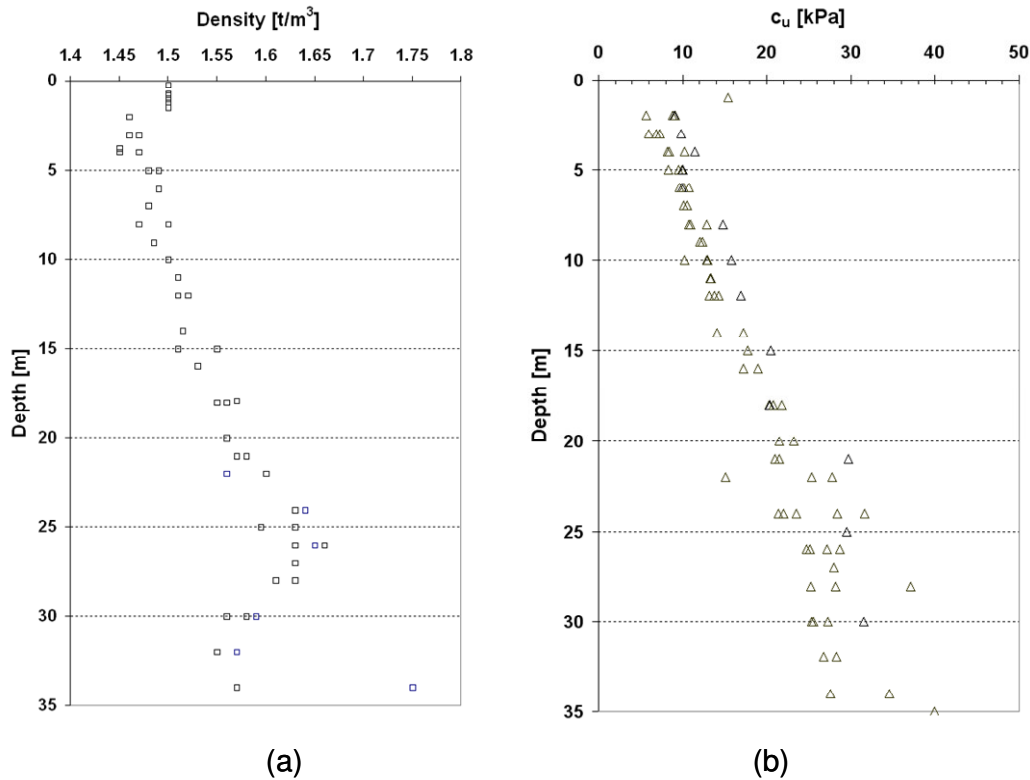


Figure 5.5 (a) Density in relation to depth and (b) shear strength in relation to depth at the Nödinge test embankment evaluated from field vane tests, CPT and fall cone tests.

The ground water table is about 0.5 m below the ground surface and the pore pressure profile is more or less hydrostatic. The hydraulic conductivity is in the range $5\text{-}10 \cdot 10^{-10}$ m/s.

The evaluated oedometer modulus, M_0 , from the CRS tests for the overconsolidated stress region starts at around 1.5 MPa at the ground surface and increases to about 10 MPa at a depth of 30 m, see Figure 5.7a. From experience the oedometer modulus, M_0 , evaluated from CRS tests in this stress region is far too low.

For the normally consolidated stress range the oedometer modulus, M_L , starts at about 150 kPa at the ground surface and increases to about 750 kPa at a depth of 30 m, see Figure 5.7b.

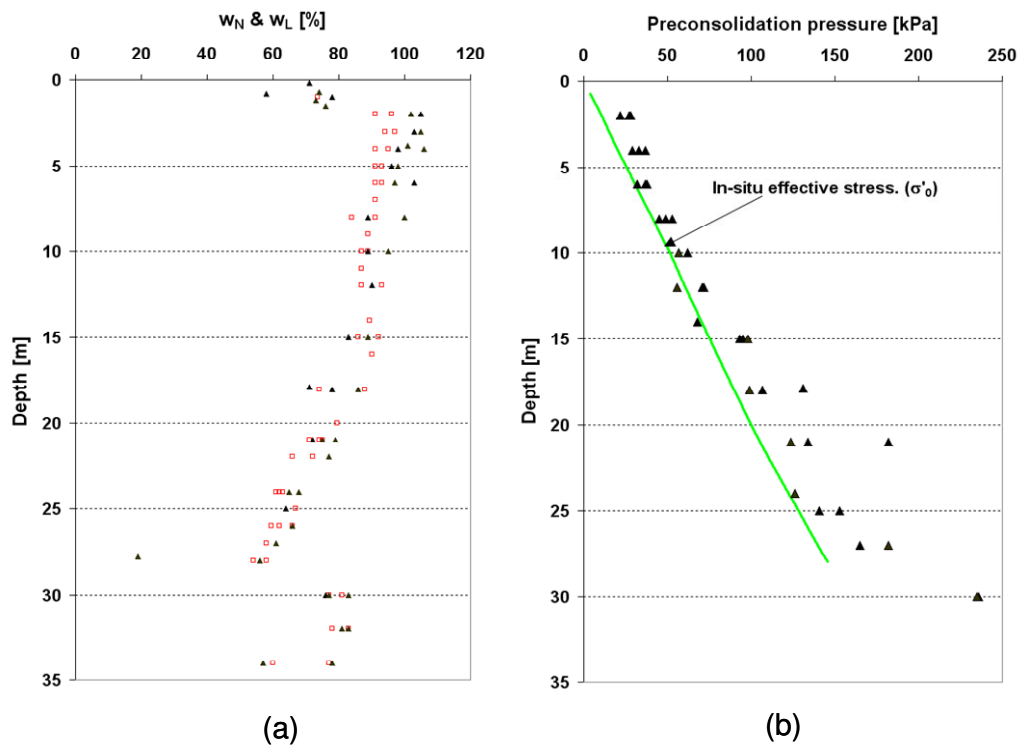


Figure 5.6 (a) water content (\blacktriangle) and liquid limit (\square) in relation to depth and (b) evaluated preconsolidation stress from CRS oedometer test performed according to the Swedish practice.

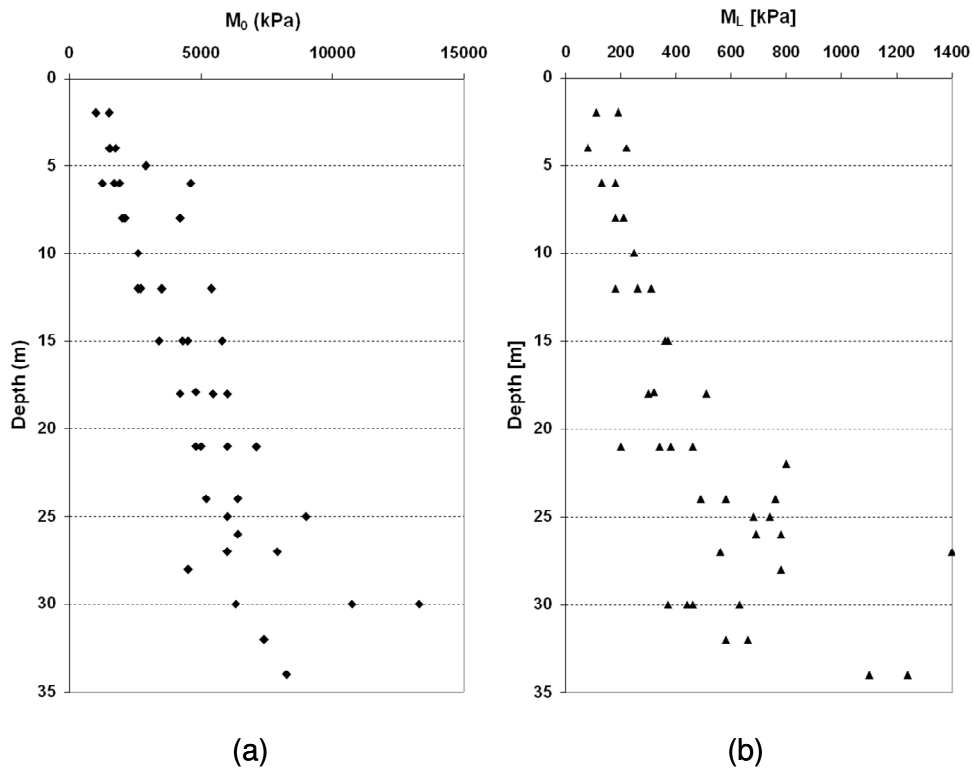


Figure 5.7 Oedometer modulus in relation to depth (a) in the overconsolidated stress region and (b) in the normal consolidated stress region.

5.2.2 Test embankment

The test embankment had a length at the crest of 25 m and a width of 13 m. At Nödinge the LCCs were installed in May 2001, about seven months before the first load increment was applied. A total of 153 columns were installed in a quadratic pattern with every other column being 12 m long and the rest 20 m long. The LCCs were constructed using the dry mix method and the binder consisted of 50% lime and 50% cement with a binder content of 90 kg/m³ of soil. The columns had a diameter of 0.6 m, see Figure 5.8.

There were two load increments for the embankment, each approximately 25 kPa. The first load increment was chosen so that no critical stresses would be exceeded in the columns. This load increment was allowed to act for a year and a half. It was approximately 25 kPa and was about 1.5 m high.

For the second load increment the opposite was the case; it was planned that the critical stresses in the columns would be exceeded, at least in the upper part of the columns. The total height of the embankment was about 2.8 m. However, the load increment was restricted so as not to risk the overall stability of the embankment, Alén et al. (2006).

Observations of the behaviour of the test embankment were performed over a period of about six years. The test embankment was removed in November 2007 due to a conflict with ongoing construction for the railway.

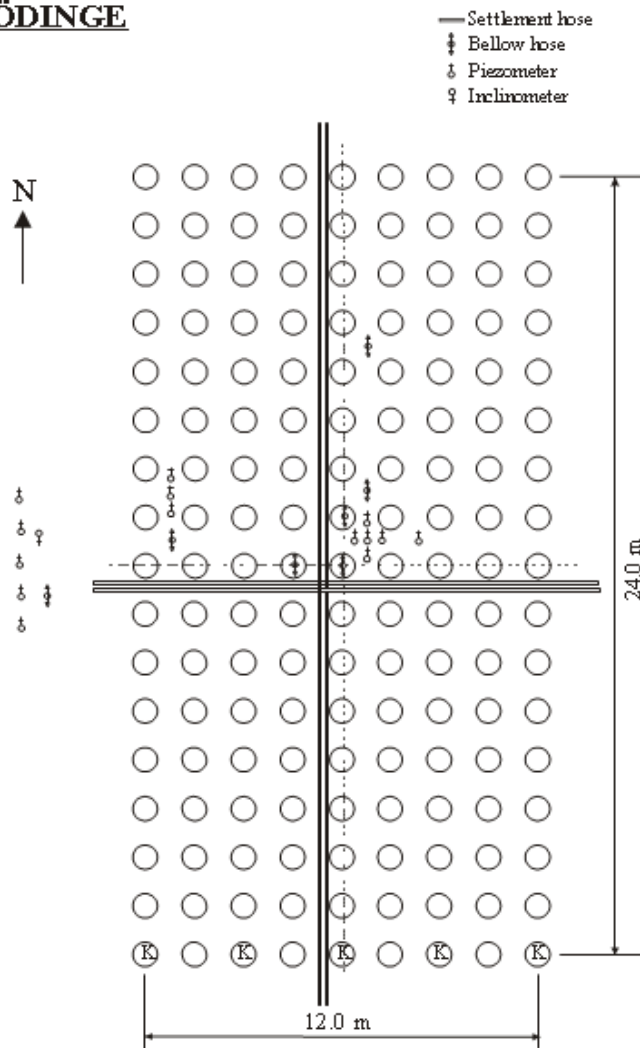
NÖDINGE

Figure 5.8 Installation pattern for lime-cement columns and the positioning of gauges, Alén et al. (2006).

5.2.3 Measurements

As can be seen in Figure 5.8 there were four different measurement devices installed in the soil underneath and just outside the test embankment. For further information about the measurement devices see Alén et al. (2006).

The results presented in Figure 5.9 to Figure 5.13 are only a selection of the measurements from the Nödinge test embankment.

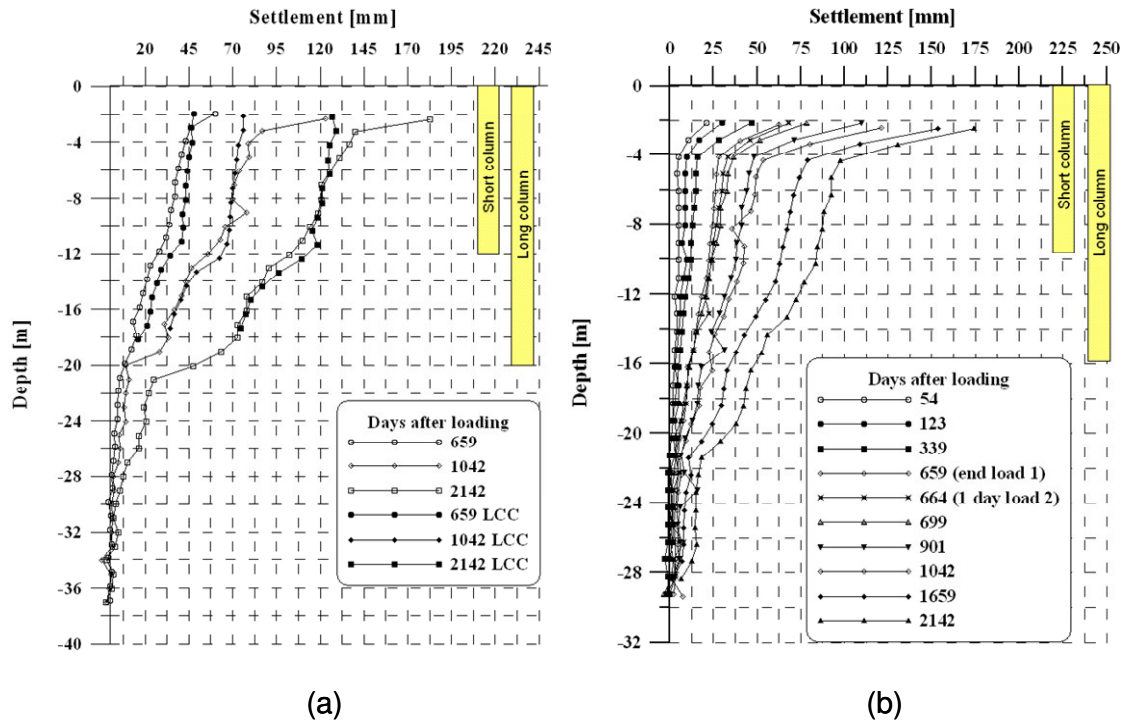


Figure 5.9 Measurements from the bellow hose (a) in the centre of the embankment, both in the clay between the LCC and in the 20 m long LCC and (b) at the western part of the embankment in the clay between the LCC.

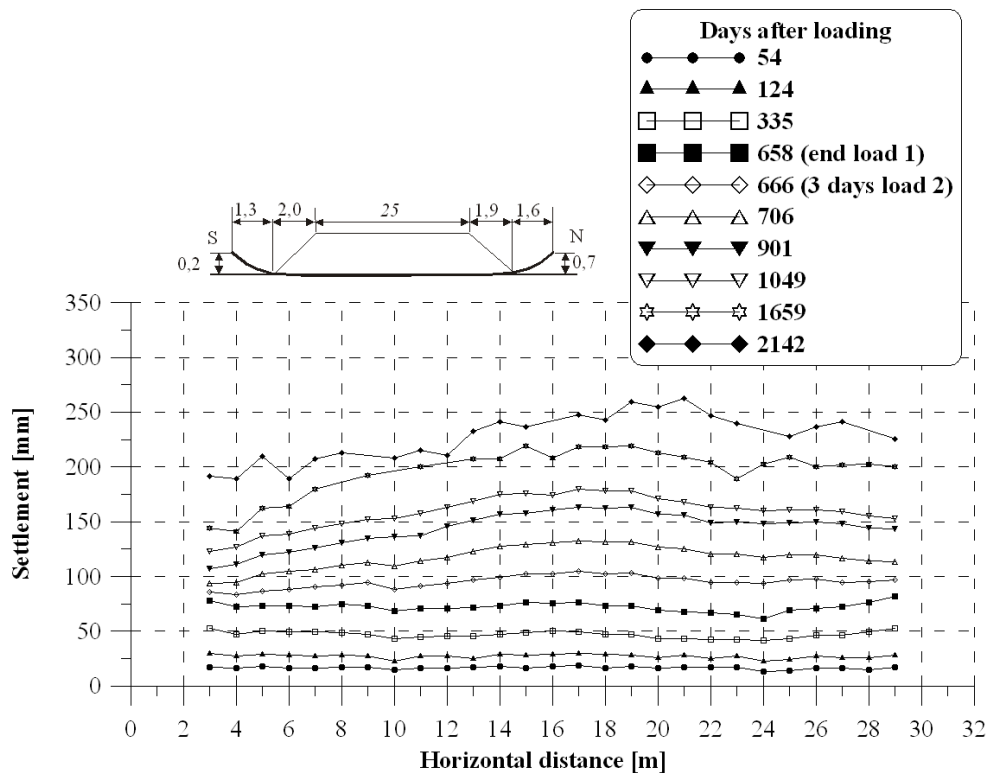


Figure 5.10 Measurements from the settlement hose along the embankment at the ground surface.

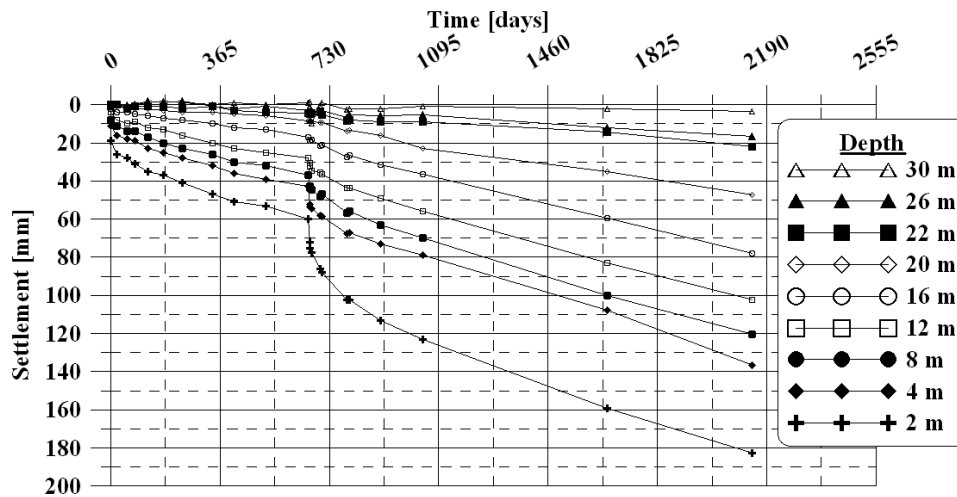


Figure 5.11 Settlement over time for different depths from the bellow hose in the clay in the centre of the embankment.

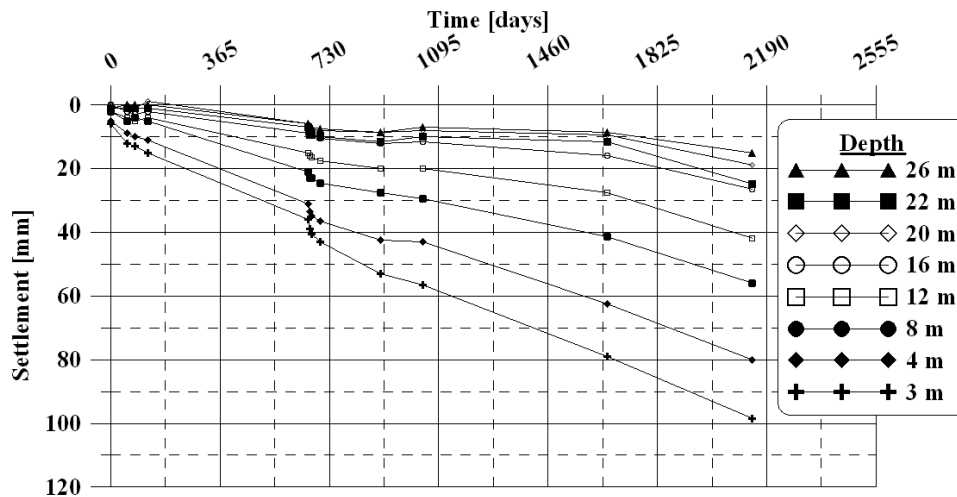


Figure 5.12 Settlement over time for different depths from the bellow hose in the clay in the area just outside the embankment.

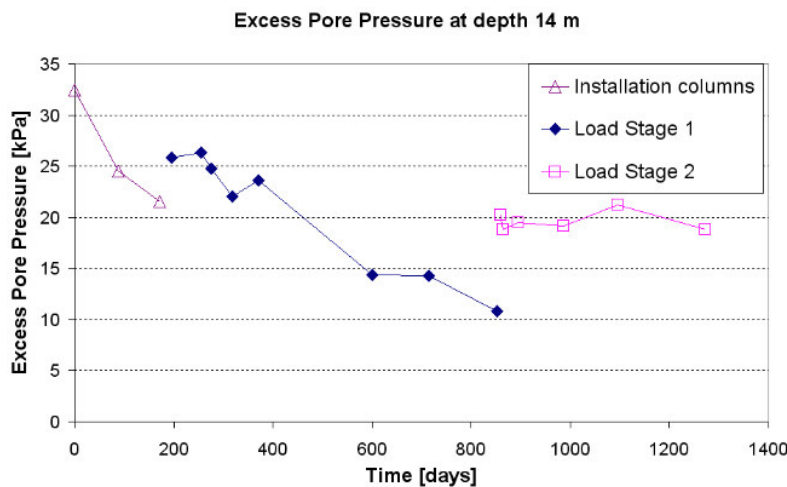


Figure 5.13 Excess pore pressure over time at a depth of 14 m in the centre of the embankment.

5.3 Kaserntorget - Groundwater lowering

Kaserntorget is an area in central Gothenburg, see Figure 5.14. This area has a long history of construction in varying forms, starting from the early 17th century. It started with the fortification (Carolus Dux) of Gothenburg in the 17th century and in the middle and late 19th century it was transformed into a more modern city environment, see SBK (2000).



Figure 5.14 View of the area studied in central Gothenburg, picture from www.enero.se.

The buildings that were constructed during the transformation in the middle of the 19th century are mainly still there and are more or less unchanged, except for certain new construction in recent years. When the old fortification was demolished it is most likely that the area was filled with the demolition material. From about 1970 a groundwater lowering was temporarily occurring in this area, as can be seen in Figure 5.20.

5.3.1 Ground conditions

The ground conditions for the area studied consist of a few metres of fill with underlying soft clay to a depth of 30-45 m. Underneath the clay there is a non-cohesive material a few metres in thickness on rock. The ground surface slopes slightly southwards from about level +17 to +14.

The ground water table is about 1.5-2.0 m below the ground surface. The hydraulic conductivity is in the range $5-10 \cdot 10^{-10}$ m/s.

The unit weight for the clay varies between 15 and about 18 kN/m³, see Figure 5.15a. The shear strength is about 15-25 kPa down to a depth of about 10 m and then with an increase of about 1 kPa/m, see Figure 5.15b. The scatter shown in Figure 5.15b is probably due to the differences in the thickness of the filling for the area.

The water content is about 80% in the top part of the clay, decreasing to around 50% at a depth of about 35 m. The liquid limit is of the same order, as can be seen in Figure 5.16a. The OCR in the area is about 1.2-1.3 as can be seen in Figure 5.16b, with a higher OCR in the top 5 - 10 m of the clay layer. The evaluated oedometer modulus, M_0 , from the CRS tests for the overconsolidated stress region starts at around 3 MPa at the top of the clay layer, increasing to about 10 MPa at a depth of 35 m, see Figure 5.17a. From experience the oedometer modulus, M_0 , evaluated from CRS tests in this stress region, is far too low. For the normally consolidated stress range the oedometer modulus, M_L , varies between 500 and 1500 kPa for the soil profile, see Figure 5.17b.

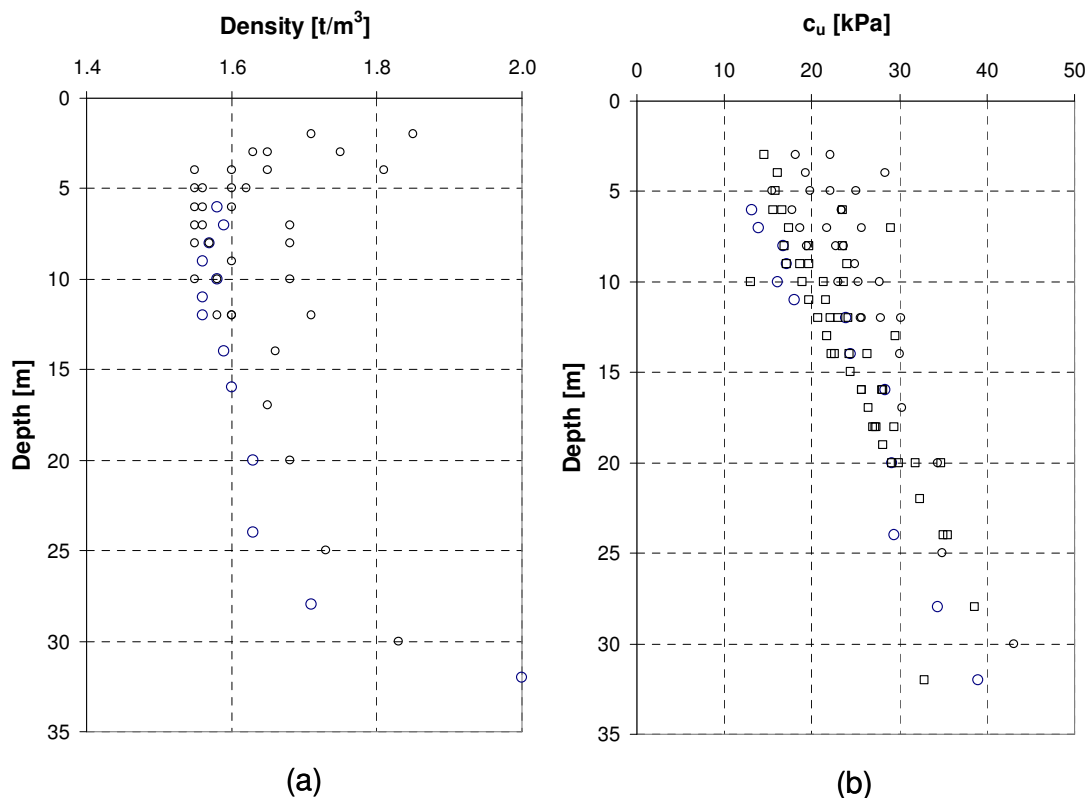


Figure 5.15 (a) Density in relation to depth and (b) shear strength in relation to depth at Kaserntorget evaluated from field vane tests and fall cone tests.

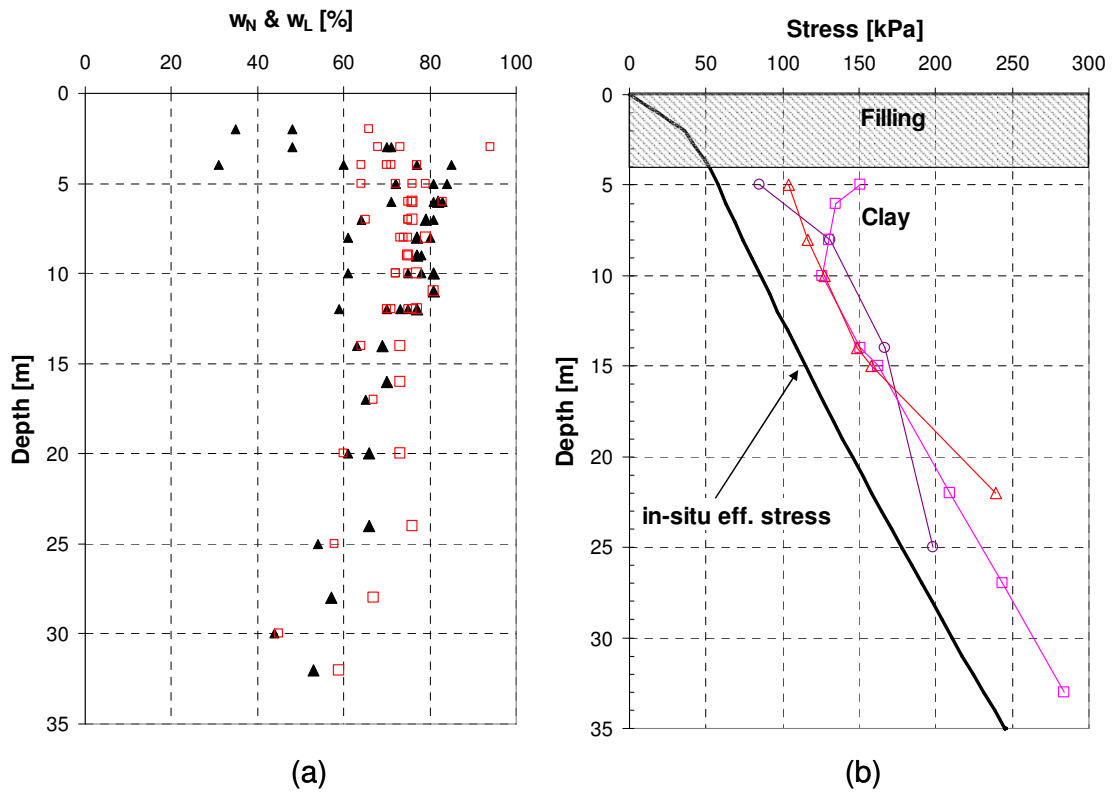


Figure 5.16 (a) water content (\blacktriangle) and liquid limit (\square) in relation to depth and (b) evaluated preconsolidation stress from CRS oedometer tests performed according to the Swedish practice.

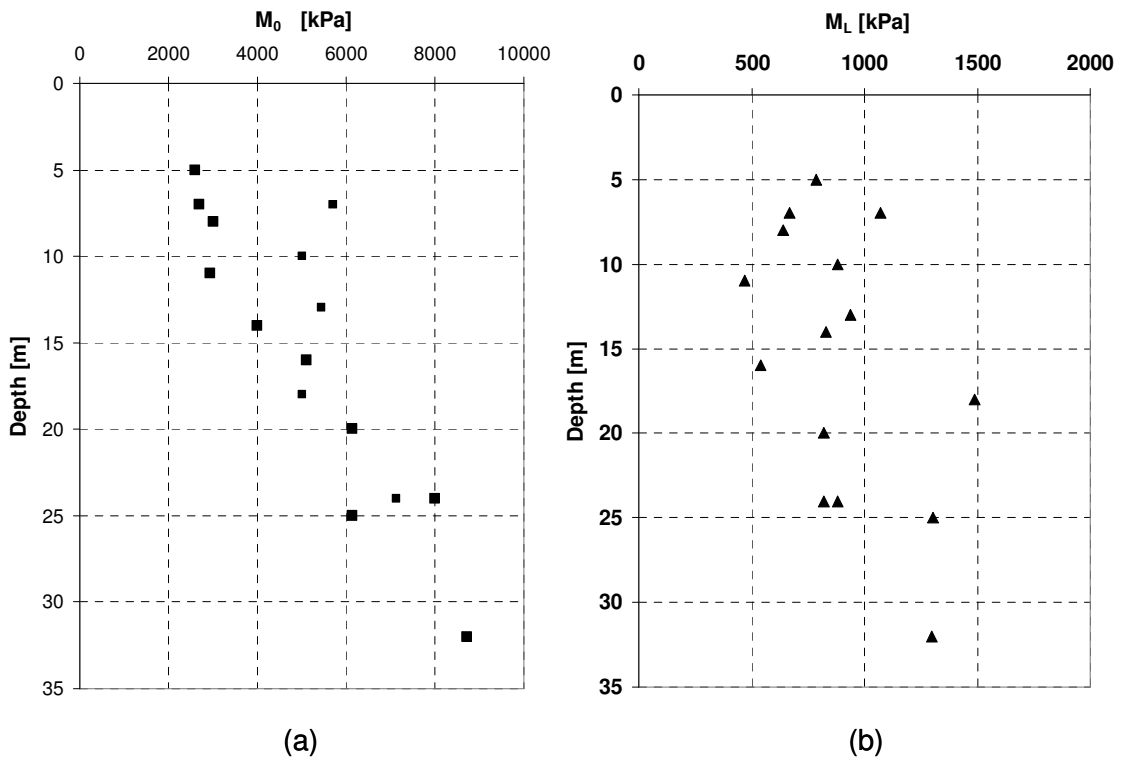


Figure 5.17 Oedometer modulus in relation to depth (a) in the overconsolidated stress region and (b) in the normal consolidated stress region.

5.3.2 Measurements

In the area studied the groundwater level and pore water pressure have been studied from about 1968 up the present day. Figure 5.18 shows an overview of some of the groundwater and pore pressure gauges. In Figure 5.19 the estimated clay thickness is shown as well as the location of settlement gauge CS 4.

Figure 5.20 shows some of the measured groundwater levels in the bottom of the non-cohesive material underneath the clay layer. Figure 5.21 shows the measurement of the settlement for the CS 4 gauge.

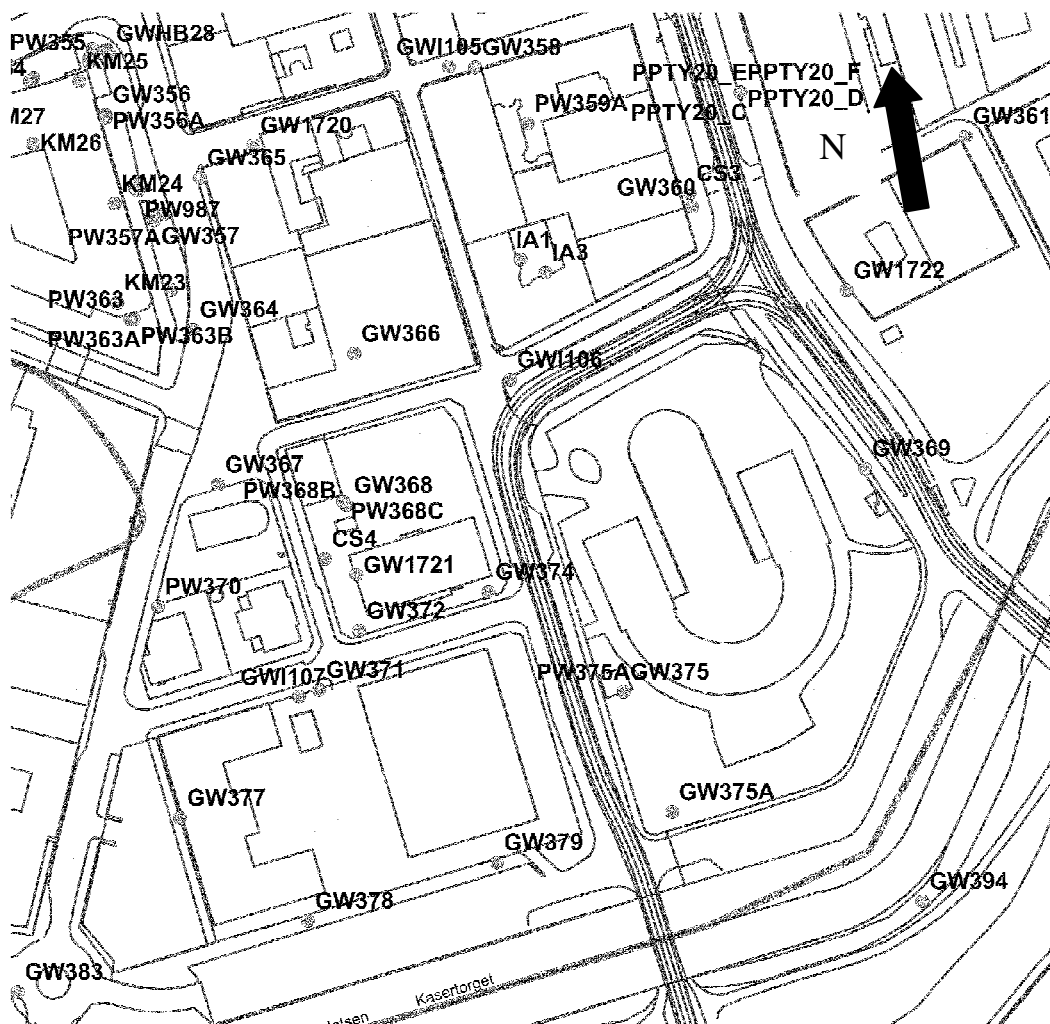


Figure 5.18 Location of peizometers and groundwater gauges at Kaserntorget.

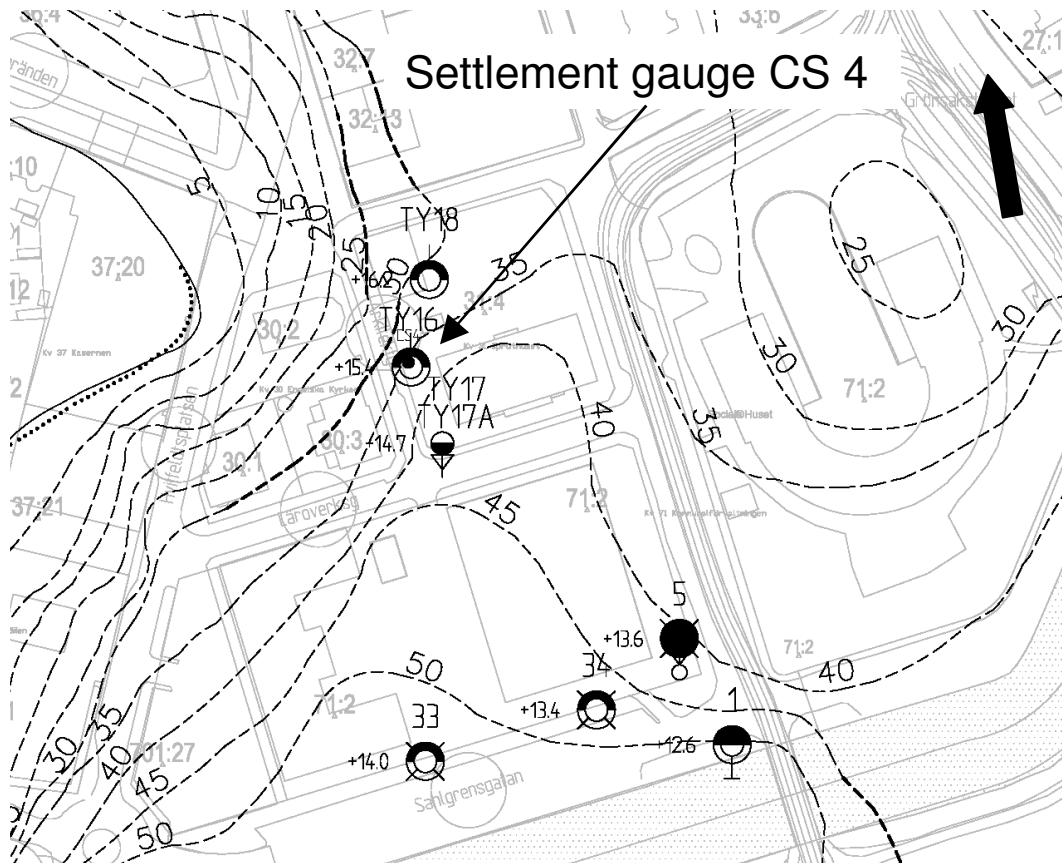


Figure 5.19 Estimated clay thickness for the area studied and the location of settlement gauge CS 4.

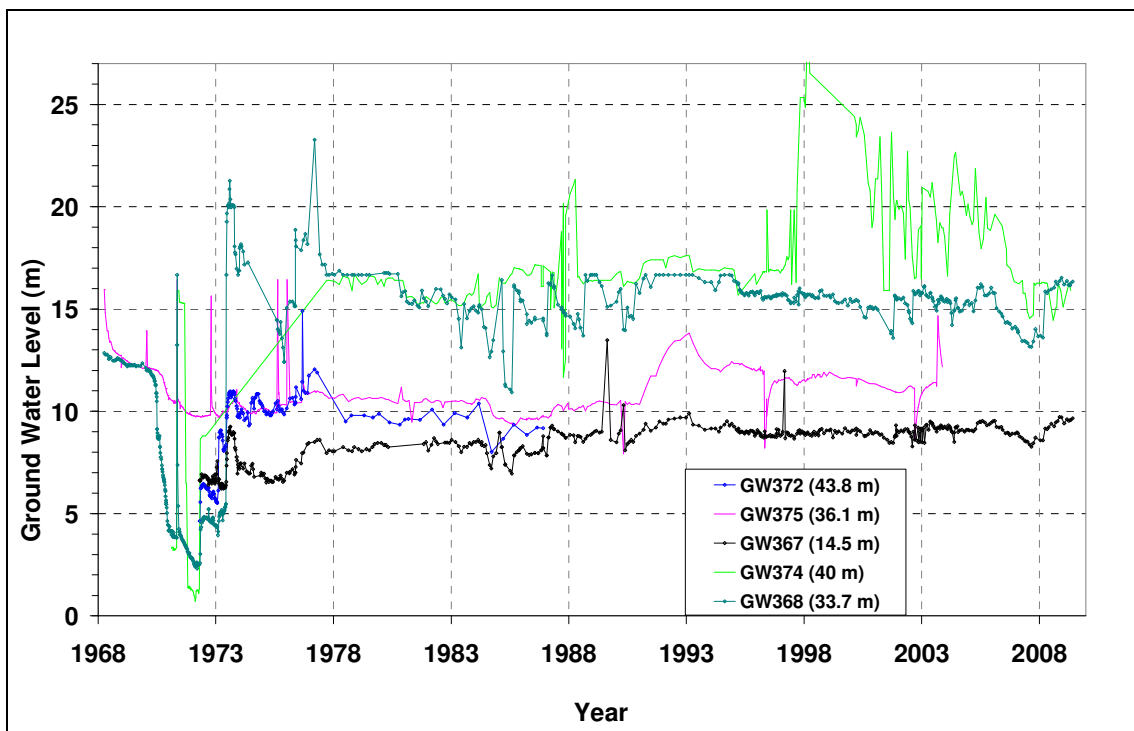


Figure 5.20 Measured ground water level (above sea level) for the area studied.

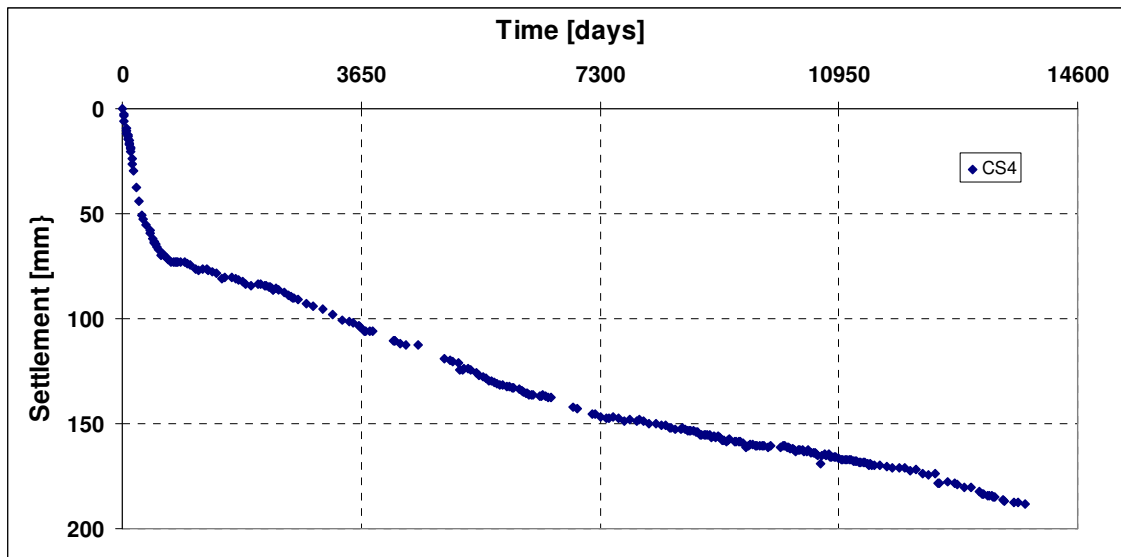


Figure 5.21 Measured settlement at the ground surface for point CS 4, starting from July 1, 1971.

6. CALCULATIONS AND COMPARISONS

In this chapter the calculated results from the three test sites will be presented and for two of them compared to the measured values. The test sites are described in detail in chapter 5. Only for the hypothetical test site all three programs will be used. This is due to usability of the programs.

In the end of each test site there is a discussion to conclude the comparisons and highlight some of the important aspects when modelling.

6.1 Hypothetical test site

The hypothetical case is an embankment on soft soil with the soil condition described in chapter 5.1. The calculations are performed for a time of 50 years after construction and a selection of results are presented below and are compared.

6.1.1 Input parameters

The input parameters used for the hypothetical test site for the different programs are presented below. For the sake of simplicity the creep number, r , is used here for the description of the creep properties. For the correlation between the creep parameters see Table 3.3.

The embankment is assumed to be constructed within 60 days.

For the programs Embankco and GS settlement the assumed input parameters are presented below and in Table 6.1.

For the dry crust, the upper 1.5 m, no creep has been assumed to occur.

Table 6.1 Input parameters for Embankco and GS Settlement.

Depth (m)	Unit weight (kN/m ³)	M_0 (MPa)	M_L (kPa)	M' (-)	σ'_c (kPa)	σ'_L (kPa)	r_0 (-)	r_1 (-)	k_{init} (m/s)
0	17	5	500	15	60	70	-	-	1.0E-8
1.5	17	5	500	15	60	70	-	-	1.0E-8
1.5	15	3	200	11	40	50	1100	95	1.0E-9
5	15.2	3.75	280	11	57	67	1100	105	9.0E-10
11	15.5	6.2	490	12	105	115	1100	110	7.7E-10
40	17	18	1670	14	346	356	4000	230	1.0E-10

Note. r_0 is only used in the GS Settlement program.

For the GS Settlement program the oedometer modulus factors a_0 and a_1 were set at 0.8 and 1.0 respectively. The factors b_0 and b_1 that control the transition between r_0 to r_1 were set at $1/OCR$ and 1 respectively. The reference time, t_r , were set to one day.

The factor, β_ϵ , that control the rate of change of the hydraulic conductivity with strain were set at 3 for the whole soil profile for both of the programs.

For the SSC model the assumed input parameters are presented below and in Table 6.2, Table 6.3 and in Figure 6.1.

The embankment is modelled as a linear elastic material with a Youngs modulus of $E = 100$ MPa and the Poisson's ratio $\nu = 0.3$.

Table 6.2 Input parameters for the dry crust (Mohr-Coulomb model)

Depth (m)	E (MPa)	E_{oed} (MPa)	ϕ' (deg)	c' (kPa)	ν (-)	K_0 (-)
0-1.5	4	5	30°	5	0.3	0.8

Table 6.3 Input parameters for the clay layer (SSC model).

Depth (m)	κ^* (-)	λ^* (-)	ϕ' (deg)	c' (kPa)	OCR (-)	POP (kPa)	ν_{ur} (-)	K_0^{nc} (-)
1.5 - 5	0.015	0.22	30°	1	-	16	0.15	0.50
5 - 40	0.015	0.22	30°	1	1.3	-	0.15	0.50

In the calculation it is assumed that the horizontal hydraulic conductivity is the same as the vertical. Due to the input possibilities in the Plaxis software some of the parameters are simplified by stepwise changes as seen in Figure 6.1.

In Figure 6.2a the in-situ effective stress is plotted together with the preconsolidation stress and the calculated final effective stress. In Figure 6.2b the vertical stress increase from the embankment is plotted.

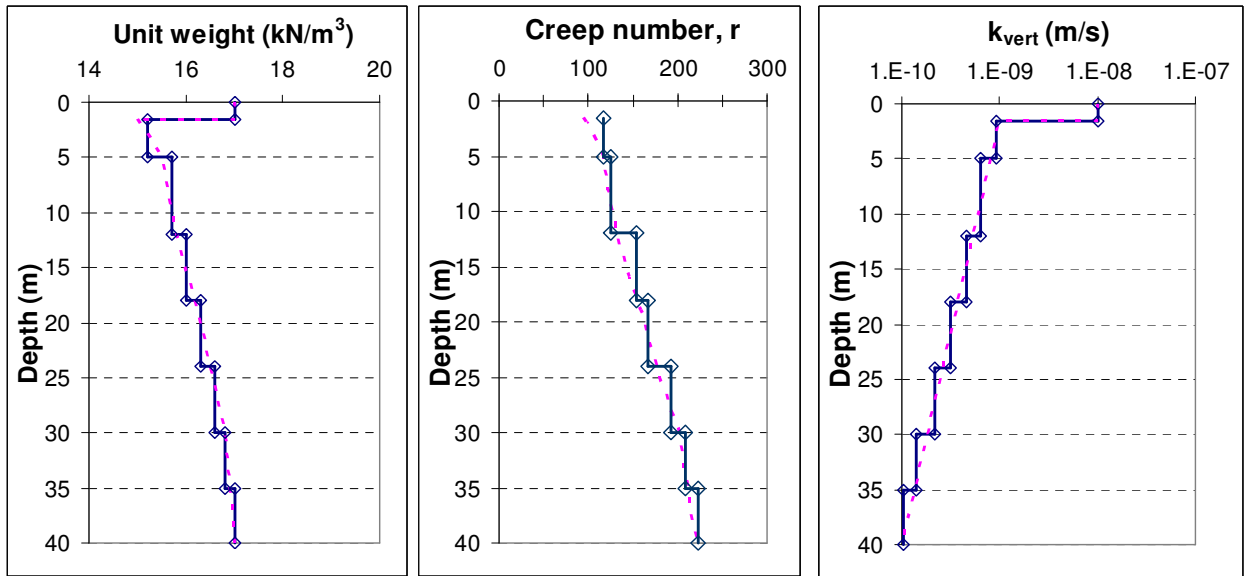


Figure 6.1 Input parameters for Plaxis (unbroken line with squares) compared to Embankco and GS Settlement (broken line) for the unit weight, creep number and the vertical hydraulic conductivity.

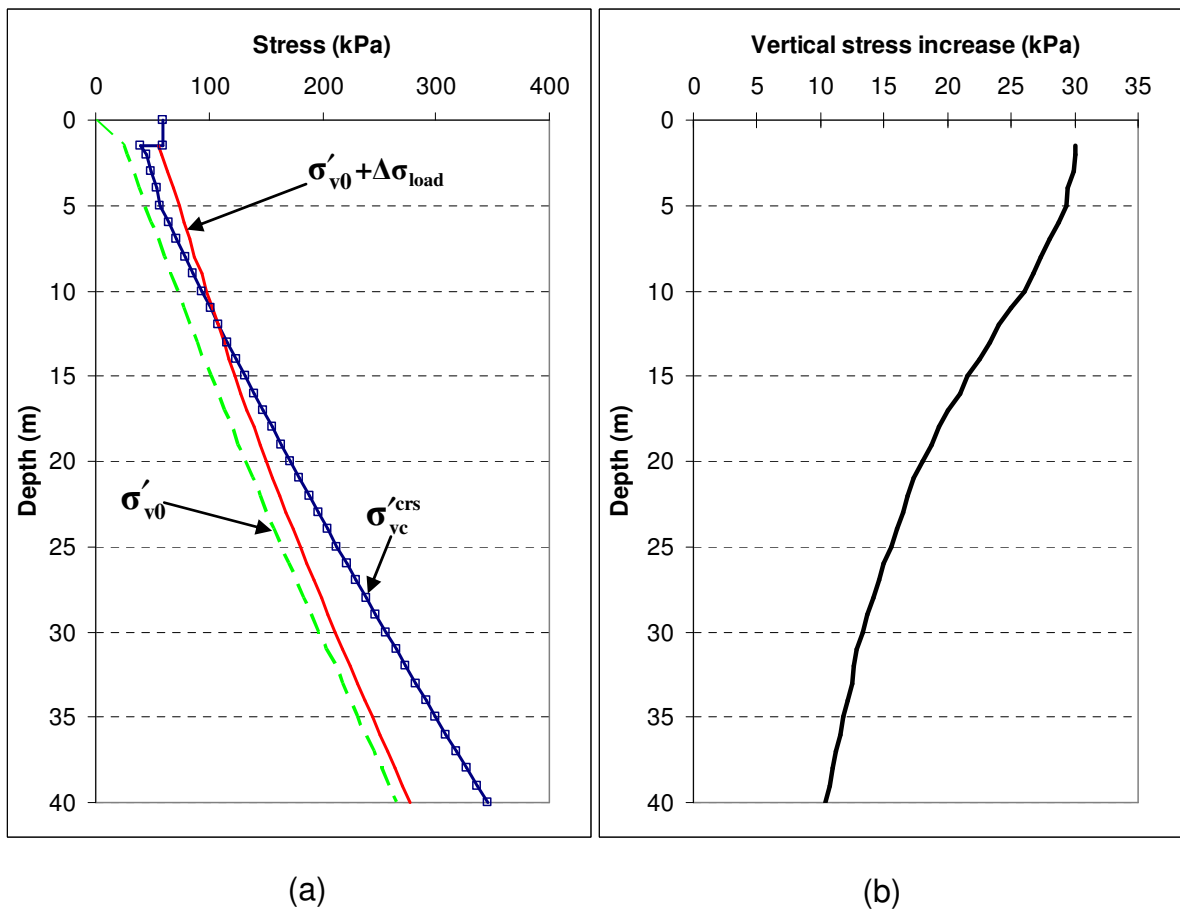


Figure 6.2 (a) In-situ effective stress (σ'_{v0}), preconsolidation stress ($\sigma'_c{}^{crs}$) and the calculated effective stress due to the load increase ($\sigma'_{v0} + \Delta\sigma_{load}$) according to elastic solution. (b) The load increase towards depth calculated according to elastic solution.

As could be seen in Figure 6.2 the calculated final effective stress, $\sigma'_{v0} + \Delta\sigma$, is greater than the preconsolidation stress above 12 m depth. This implies that most of the displacements will be within the depth 1.5 m to about 12 m.

For the Embankco program there is an option of reduction of the surface load due to submersion below the groundwater level. This has been set to no reduction during this calculation, due to that GS Settlement program does not have this option and a better correlation between these two programs is of interest.

6.1.2 Results and comparison between programs

A selection of results is presented below. In Figure 6.3 the time – settlement curve is shown and in Figure 6.4 the vertical displacement against depth for two times, 10 years and 50 years.

In Figure 6.5 the excess pore pressure is shown for three times, 60 days, 10 years and 50 years.

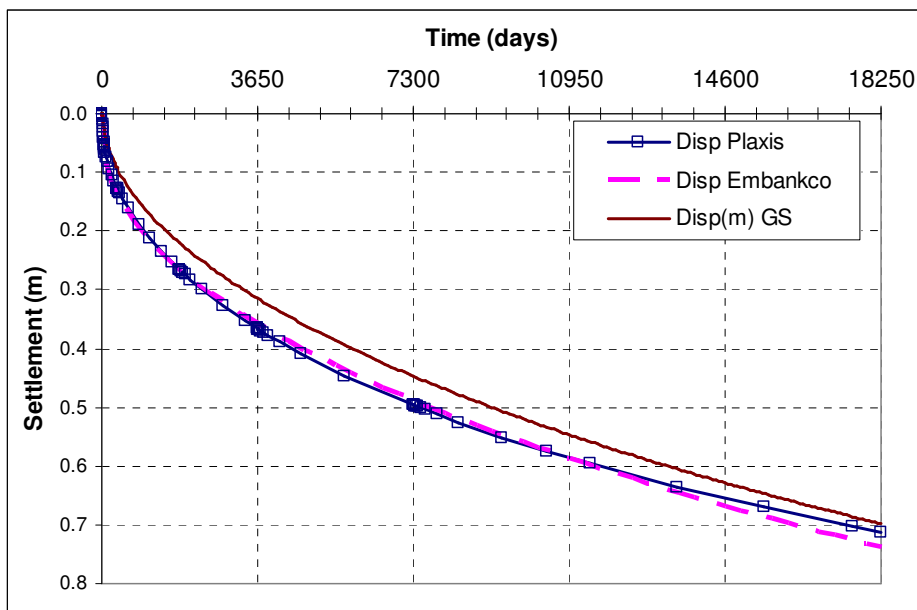


Figure 6.3 Calculated vertical displacement in relation to time for all three programs.

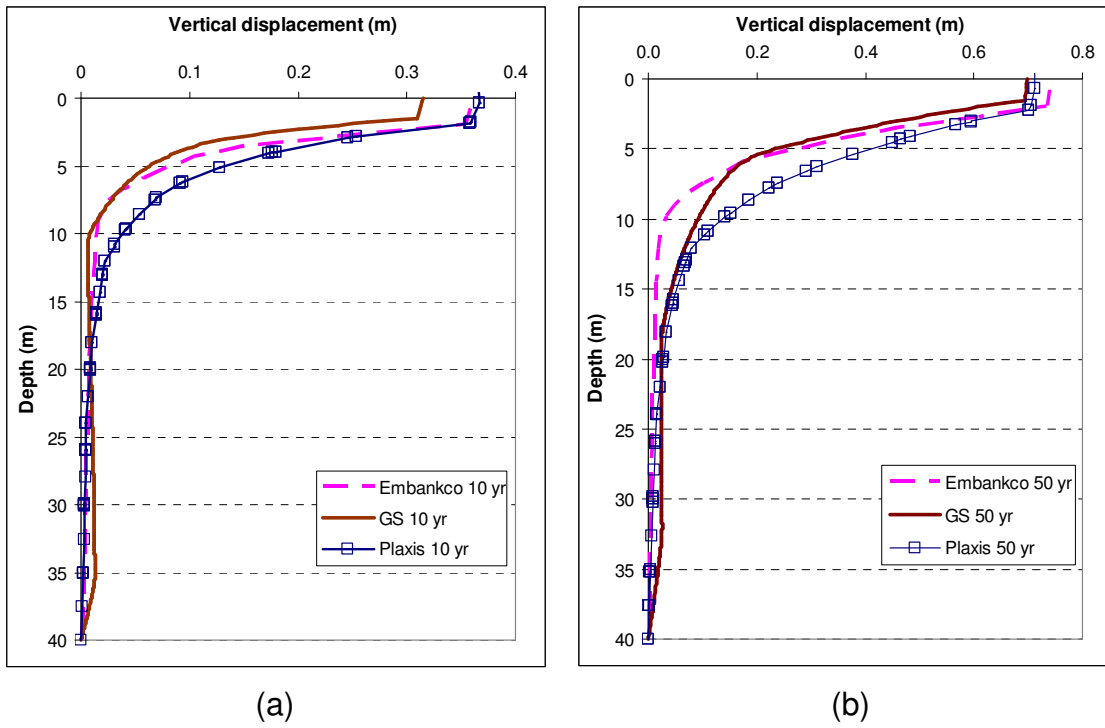
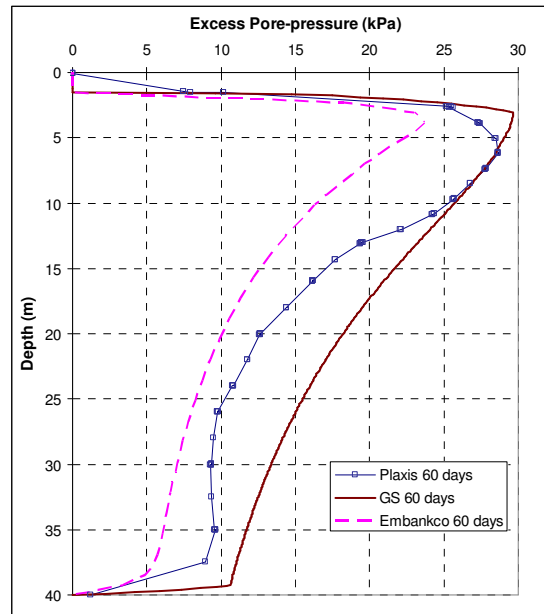
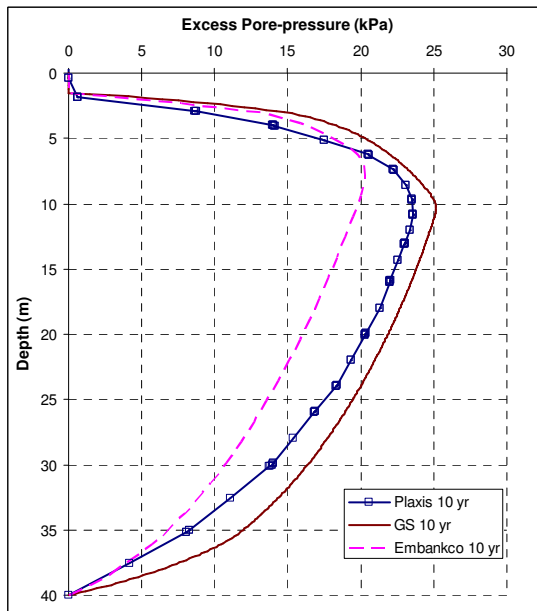


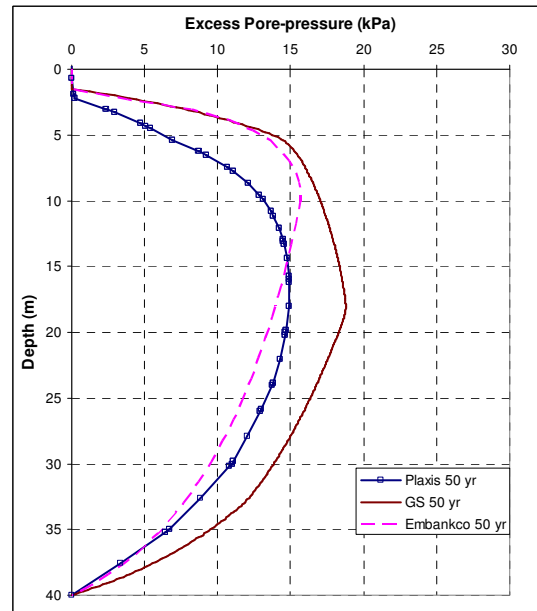
Figure 6.4 Calculated vertical displacement in relation to depth after (a) 10 years and (b) 50 years for all three programs.



(a)



(b)



(c)

Figure 6.5 Calculated excess pore pressure after (a) 60 days (b) 10 years and (c) 50 years for all three programs.

6.1.3 Discussion

As could be seen in Figure 6.3 the time–settlement curves for all three programs correspond very well and the settlement after 50 years is about 0.7 m. It can be seen in Figure 6.3 that the settlement rate from Plaxis starts to decrease a little more than Embankco and GS Settlement. This is probably due to the reduction of the load as the dry crust is being pushed down under the ground water table.

Figure 6.4 gives a clear view of where the displacements occur in the soil profile. All three programs produce very similar results, but for Plaxis the displacement is greater to a depth of about 12 m. This corresponds to the results in Figure 6.5 where one could see that the dissipation of excess pore pressure is faster for Plaxis than the other two, apart from the initial phase for Embankco.

As can be seen in Figure 6.5 the excess pore pressure after 60 days are quite different for all three models. This is due to the way they calculate the stress increase from a load that has been applied. The way Embankco handles with the increase of excess pore pressure is described in chapter 3.1. For the GS Settlement program the calculated load is assumed to produce the same excess pore pressure and for Plaxis the excess pore pressure depends, among other things, the total stress change in all directions and on the defined soil stiffness, both for the embankment and the soil layers.

6.2 Nödinge test embankment

The Nödinge test embankment is described in chapter 5.2. Here a selection of calculation results will be presented and compared to measured values. There will also be a prediction of the settlement after 40 years. As mentioned earlier, only the GS Settlement and Plaxis programs will be used for this test site.

6.2.1 Input parameters

The input parameters used to describe the soil profile are presented below.

The oedometer modulus, M_0 , is set to $75 \cdot \sigma'_c$ for the undisturbed soil since no unload/reload test has been conducted. The limit stress, σ'_L , is set at $\sigma'_c + 20$ kPa for the undisturbed soil beneath the LCCs. This implies that since the effective stress doesn't exceed the defined limit stress the M' value has no influence on the results of the calculation for the undisturbed soil in the GS Settlement calculations. The evaluated preconsolidation stress and oedometer modulus, M_L , used for the GS Settlement calculation are shown in Figure 6.6.

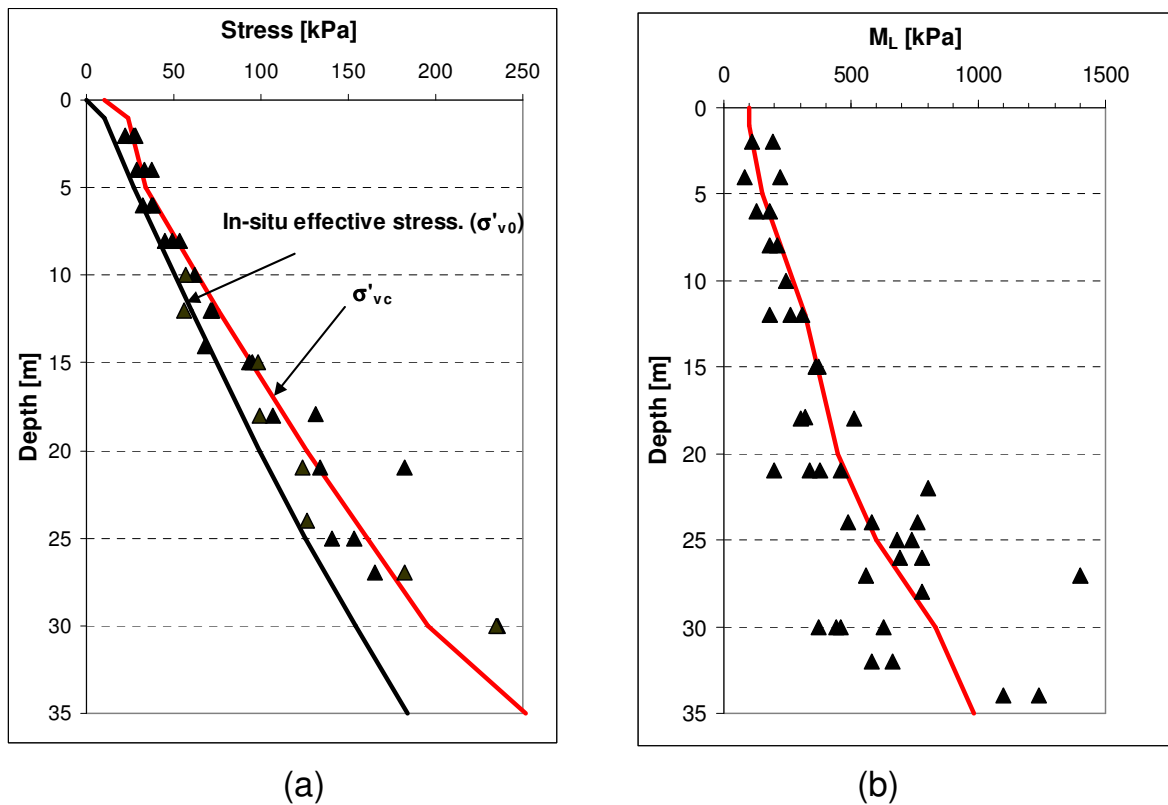


Figure 6.6 (a) Evaluated in-situ effective stress, preconsolidation stress and results from CRS oedometer test evaluated according to Sällfors method.
 (b) Oedometer modulus in the normal consolidated region, M_L .

The preconsolidation stress corresponds to an OCR of 1.2, except for the top and bottom where the OCR increases towards the boundaries. The creep number is evaluated from the water content according to eq. (4.1). The input parameters that have been used for the unstabilised soil for the GS Settlement program are presented in Table 6.4 and Figure 6.7.

Table 6.4 Parameters for the unstabilised soil for the GS Settlement program.

Depth (m)	M_0 (MPa)	M_L (kPa)	M' (-)	σ'_c (kPa)	r_0 (-)	r_1 (-)	k_i (m/s)
0-1	0.75-1.8	100	10	10-24	1000	200-90	1E-9
5	2.6	150	10	34	1000	90	1E-9
12	5.6	320	12	75	1000	95	8E-10
20	9.5	450	12	126	1000	133	7E-10
25	12	600	13	161	1000	143	6E-10
30	14.7	830	14	196	2250	154	5E-10
35	18.9	980	14	252	3000	200	5E-10

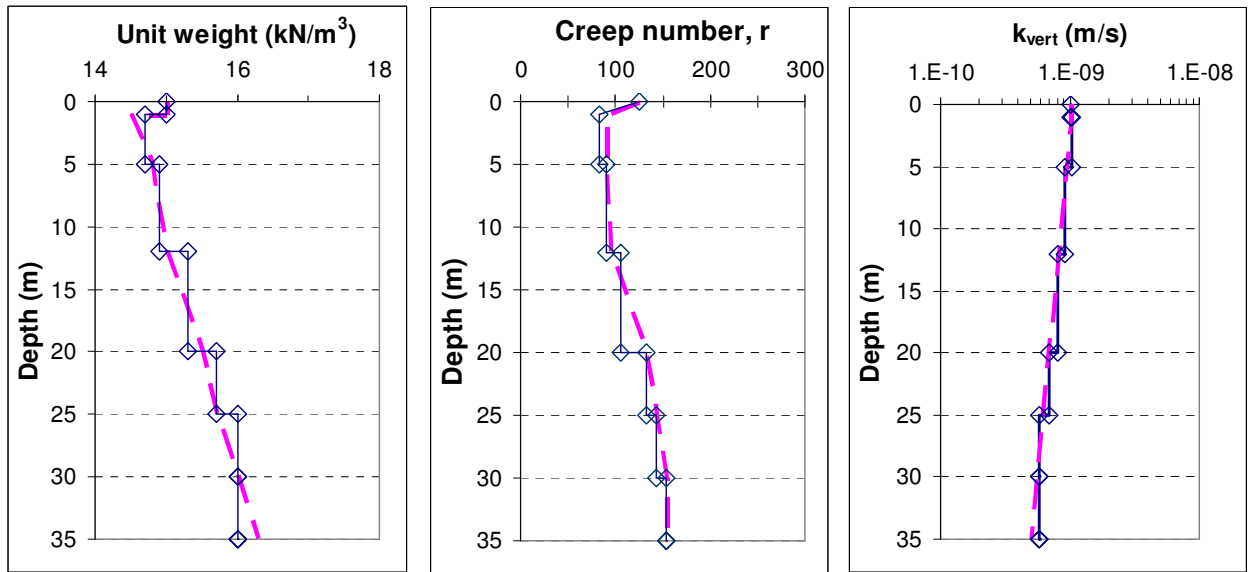


Figure 6.7 Input parameters for Plaxis (full line with squares) compared to GS Settlement (dotted line) for the unit weight, creep number and the vertical hydraulic conductivity.

For the GS Settlement program the LCCs and the soil need to be modelled as a composite material. This is conducted according to a suggested method by Alén et al. (2006). Alén et al. (2006) proposed a method to determine the stress distribution with depth for a floating block of LCC. This method has been used and calibrated so the input of the stress increase due to the external load in GS Settlement program corresponds to the stress increase given by FE analysis from Plaxis.

The parameter that has been calibrated in the above mention method is the factor for the load distribution, η_{LC} . This factor is defined as

$$\eta_{LC} = \left(\frac{d}{h}\right)^{\beta} \quad \text{with} \quad \beta = \frac{1}{(M_{block} / M_{soil})^a - (M_{soil} / M_{block})^a} \quad (6.1)$$

Where d is the depth of the reinforcement (LCC) and h the total depth of the compressible soil.

After calibration against the FE analysis the exponent, a , is set to 0.25 and the relation between M_{block}/M_{soil} is set to 5. This combination produced an acceptable agreement of the stress distribution for the unstabilised soil underneath the block of LCCs, see Figure 6.8.

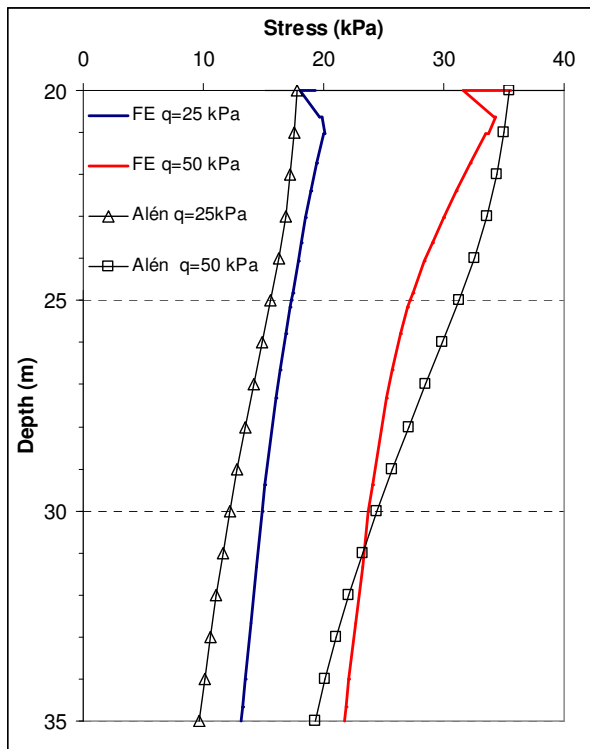


Figure 6.8 Compared stress distribution underneath the stabilised soil in the centre of the embankment between FE analysis and method suggested by Alén et al. (2006) after calibration for the two loads.

Focus is on the stress distribution beneath the stabilized soil for the GS Settlement program since this program is one-dimensional and the stabilised zone is modelled as a block.

For a detailed explanation of the method the reader is referred to Alén et al. (2006).

The oedometer modulus factors a_0 and a_1 were set to 1.0 for the composite material and 0.8 and 1.0 respectively for the soil beneath the LCC block. The factor b_0 is set equal to $1/OCR$ and b_1 are set to 1.1. The reference time, t_r , were set to one day.

The composite material have be calculated without creep effects except for the top 5 m as seen in Table 6.5. The top 5 m is modelled with creep due to an assumption of a transition zone and that the stiffness of the LCCs in the top part is low as discussed by Alén et al. (2005).

As described in chapter 5.2.2 the columns where 12 m and 20 m long and placed in a quadratic pattern. This results to different coverage areas, a_s , in relation to depth for the columns. The columns coverage area for the top part (0-12m) is $a_{s1} = 0.126$ and for the lower part (12-20) is $a_{s2} = 0.063$.

The LCCs are assumed to behave elastically. It is known that the quality of the LCCs in the top part is low. Hence the elastic stiffness is assumed to be 6 MPa the top metre, increasing to 10 MPa at depth of 3 m. Between the depths 3 m and 5 m the Youngs modulus for the LCCs, E_{col} , increase from 10 MPa to 100 MPa and are then assumed constant. For the composite material a weighted modulus is used since the GS Settlement program is one-dimensional. The modulus used in the block are calculated as

$$M_{block}(z) = a_s \cdot E_{col}(z) + (1 - a_s) \cdot M(z) \quad (6.2)$$

The same procedure is done for the hydraulic conductivity where the hydraulic conductivity for the LCCs are set to $1 \cdot 10^{-8}$ m/s. The hydraulic conductivity used in the block are calculated as

$$k_{block}(z) = a_s \cdot k_{col}(z) + (1 - a_s) \cdot k(z) \quad (6.3)$$

The input parameter for the composite material that represents the soil and the LCCs is presented in Table 6.5.

Table 6.5 Input parameters for the composite material that represent the soil and LCCs.

Depth (m)	Unit weight (kN/m ³)	M ₀ (MPa)	M _L (MPa)	σ' _c (kPa)	r ₀ =r ₁ (-)	k _{init} (m/s)
0 – 1	15	1.4	0.85	10 – 19	1500	3E-9
1 – 3	14.7	1.4 – 2.1	0.85 – 1.6	19 – 27	1500	2E-9
3 – 5	14.7	2.1 – 14	1.6 – 12	27 – 34	1500	2E-9
5 – 12	14.9	14 – 16	12 – 12.9	34 – 75	-	2E-9
12 – 20	15.3	7.4 – 9.6	3.5 – 3.75	75 – 126	-	1.5E-9

The input parameters for the SSC model are determined from back-calculations of some of the CRS oedometer tests conducted on samples of soft clay in the area of the test embankment. In Figure 6.9 and Figure 6.10 show four back-calculated results from the FE analysis compared with measured values from CRS oedometer tests. The calibrated soft clay parameters for the SSC model are presented in Table 6.6 and Figure 6.7. The parameter used for the back-calculations in Figure 6.9 and Figure 6.10 are the same as given for the correspondingly layer in Table 6.6 and Figure 6.7.

The horizontal hydraulic conductivity is set equal to the vertical hydraulic conductivity for the Plaxis program.

The back-calculation is performed using the same procedure that was described in chapter 4.2.4.

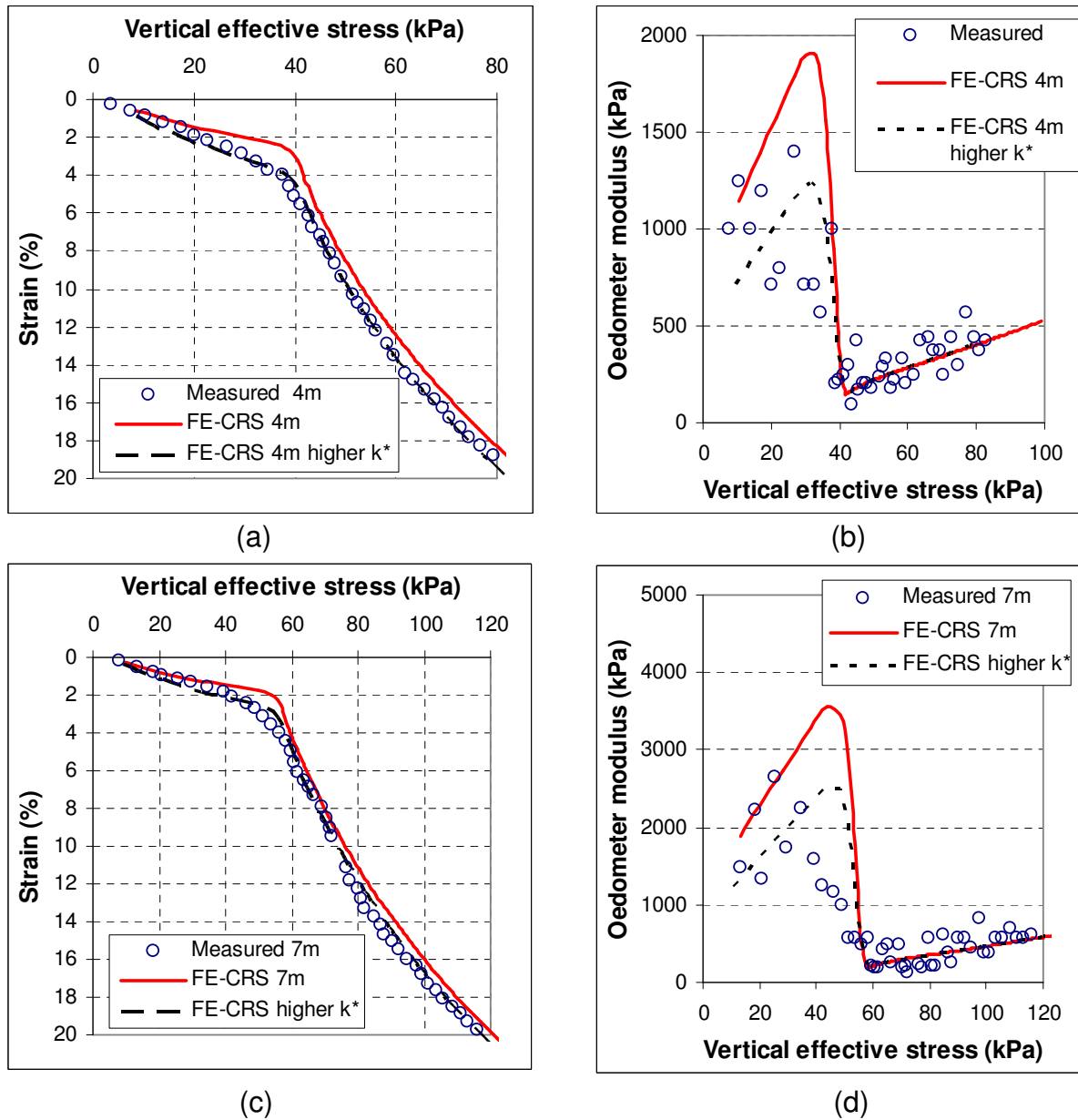


Figure 6.9 Back-calculated CRS curves for calibration compared with measured values for the depths 4 m and 7 m. In (a) and (c) the stress-strain curves and in (b) and (d) the oedometer modulus curve.

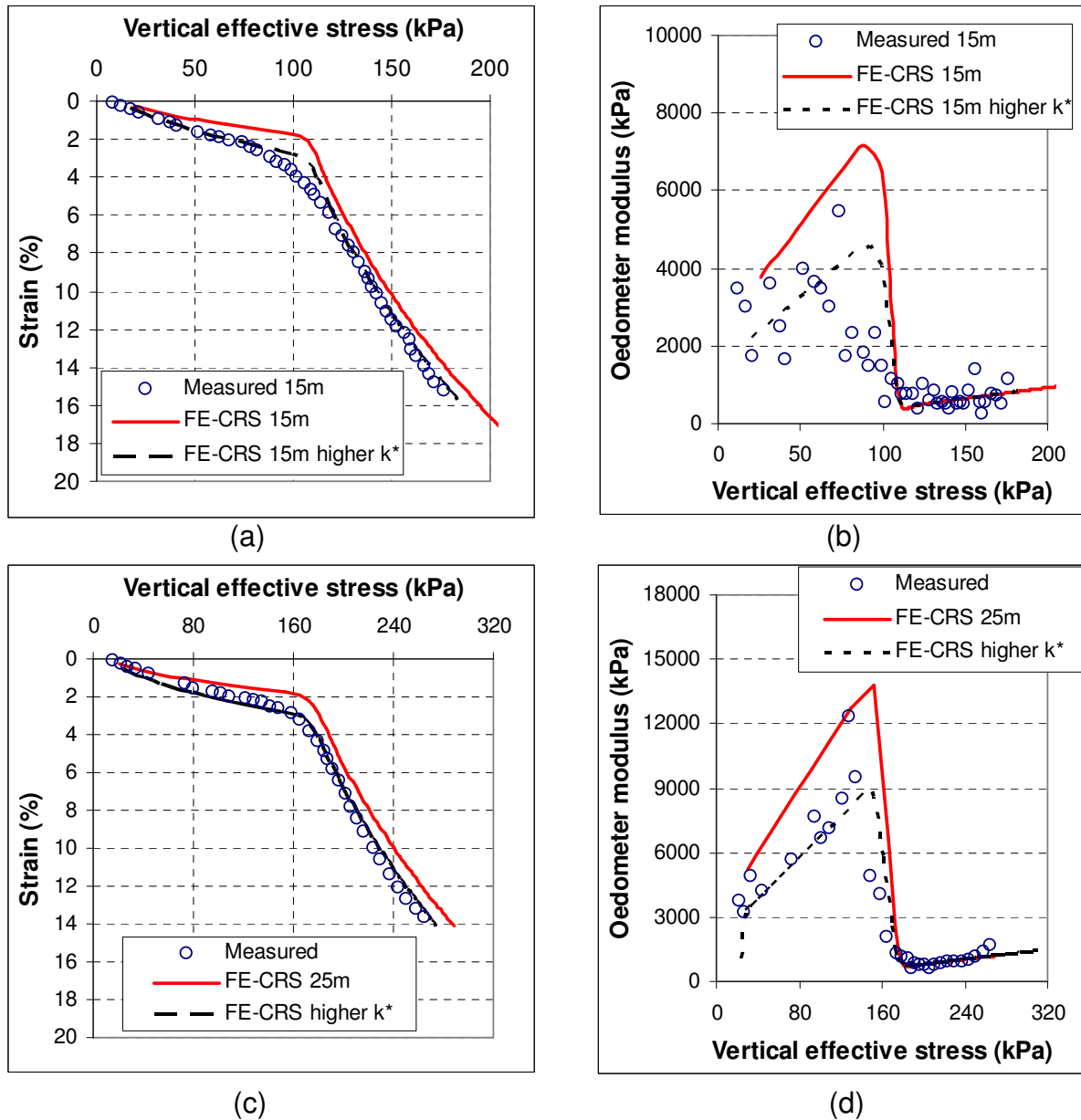


Figure 6.10 Back-calculated CRS curves for calibration compared with measured values for depths 15 m and 25 m. In (a) and (c) the stress-strain curves and in (b) and (d) the oedometer modulus curve.

As can be seen in Figure 6.9 and Figure 6.10 there are two curves from the FE analysis. The modelled curve with the higher κ^* -value is chosen so that a best fit of the CRS curve is achieved by simply changing the κ^* -value. The other modelled curve represents a more likely behaviour in the overconsolidated region. As discussed earlier, the evaluated oedometer modulus in the overconsolidated region is normally too low. Consequently, the κ^* -value that produces the slightly higher oedometer modulus is used in the calculations.

The material properties used in SSC model are listed in Table 6.6 and in Figure 6.7.

As can be seen in Table 6.6, the top layer down to a depth of 1 m has a higher effective cohesion. This is assumed due to vegetation and fluctuation of the groundwater table that would probably give a dry crust.

Table 6.6 Clay parameters used for the SSC-model.

Depth (m)	κ^* (-)	λ^* (-)	μ^* (-)	ϕ' (deg)	c' (kPa)	OCR (-)	POP (kPa)	v_{ur} (-)
0 - 1	0.028	0.28	0.008	30°	6	-	10	0.15
1 - 5	0.025	0.25	0.012	30°	1	-	10	0.15
5 - 12	0.017	0.26	0.011	30°	1	1.25	-	0.15
12 - 20	0.017	0.26	0.0095	30°	1	1.25	-	0.15
20 - 25	0.012	0.26	0.0075	30°	1	1.25	-	0.15
25 - 30	0.012	0.26	0.0070	30°	1	1.3	-	0.15
30 - 35	0.012	0.26	0.0065	30°	1	1.35	-	0.15

The embankment is modelled with a linear elastic model with Youngs modulus of 50 MPa and a unit weight of 17 kN/m³.

Because the Plaxis 2D is used the LCCs are simplified into solid elements with a corresponding thickness. The thickness of the solid elements is set to 0.2 m, which represents about the same volume for the LCC as for the field case. The stiffness of the LCCs is described above. See Figure 6.11 for a FE mesh used to model the Nödinge test embankment.

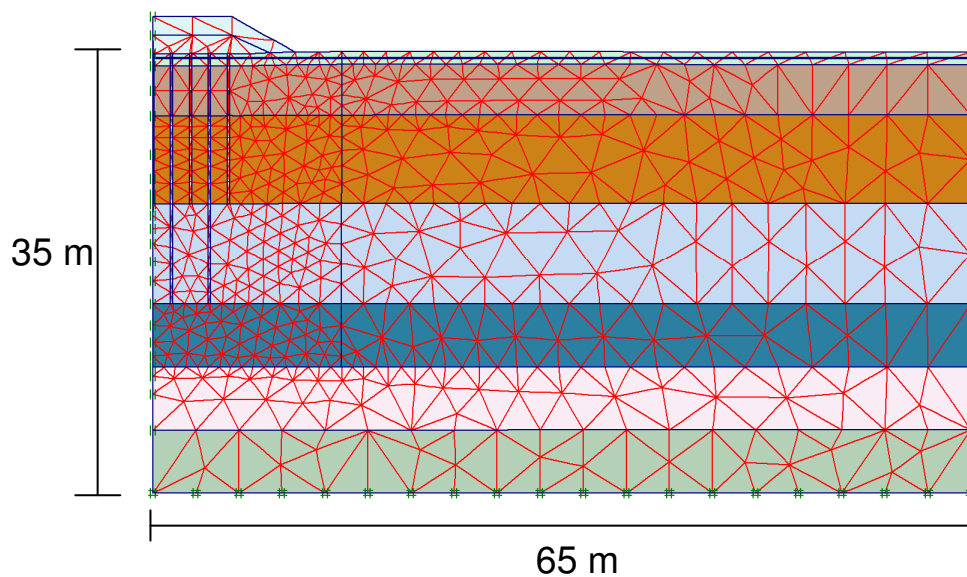


Figure 6.11 FE-mesh used in Plaxis for the Nödinge test embankment.

The initial conditions are generated by using the K_0 procedure and the K_0 value is set according to eq. (4.6) and eq. (4.7). The hydrostatic water pressure is also generated from a groundwater level 0.5 m below the ground surface.

The boundary conditions of the model are as follows

- Horizontal displacement is prevented at the sides of the model.
- Both horizontal and vertical displacement is prevented at the bottom of the model.
- Closed consolidation boundaries are set at the sides of the mesh and open at the top and bottom boundaries of the model.

The calculation stages follow the actual construction stages of the embankment. In the calculation the LCCs is “wished in placed”, which means that they give no disturbance to the surrounding soil. This is a rough simplification since it is known that the installation of LCCs in soft clays creates excess pore pressures and displacements in the surrounding soil.

6.2.2 Results and comparison with measurements

A selection of results is presented below. A comparison between measured and calculated settlement is presented for both programs in the centre of the embankment. In Figure 6.12 the settlement in relation to depth is presented and in Figure 6.13 time-settlement curve for the test embankment’s lifetime. In Figure 6.14 a time-settlement curve is presented with a prediction of the settlement to 40 years.

The calculated excess pore pressure in relation to depth for two different times is shown in Figure 6.15 and in Figure 6.16 excess pore pressure with time at a depth of 14 m is shown.

It should be mentioned that the measurement of the excess pore pressure during the project was difficult and care should be taken when comparing with calculated values.

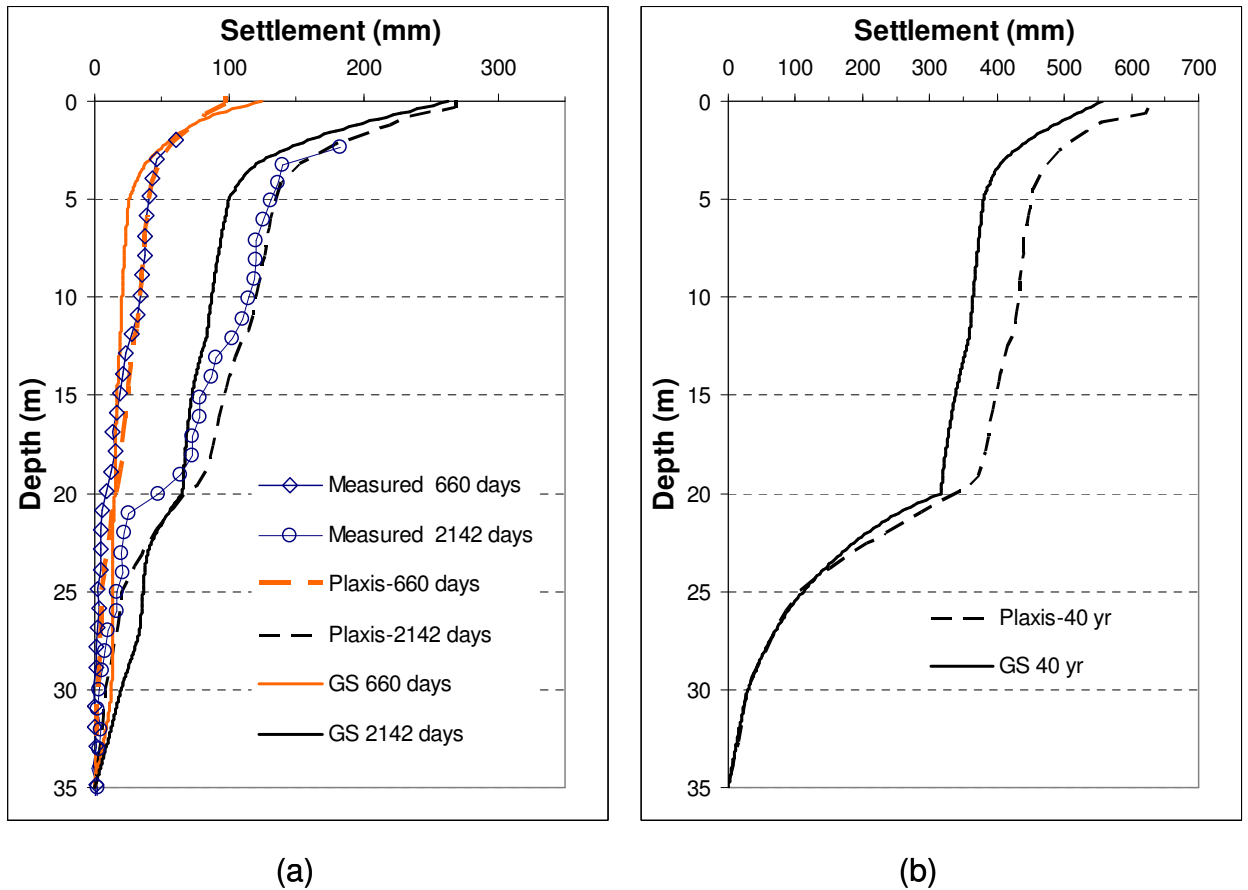


Figure 6.12 In (a) calculated and measured settlement in relation to depth and in (b) prediction of the settlement in relation to depth after 40 years in the centre of the embankment in the clay.

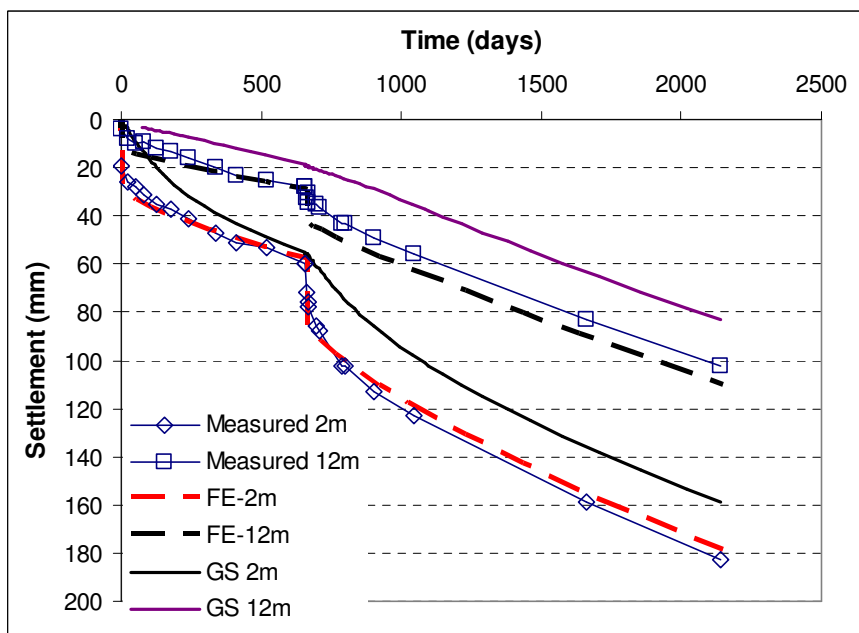


Figure 6.13 Time-settlement curve for different depths with measured and calculated values for both programs in the centre of the embankment.

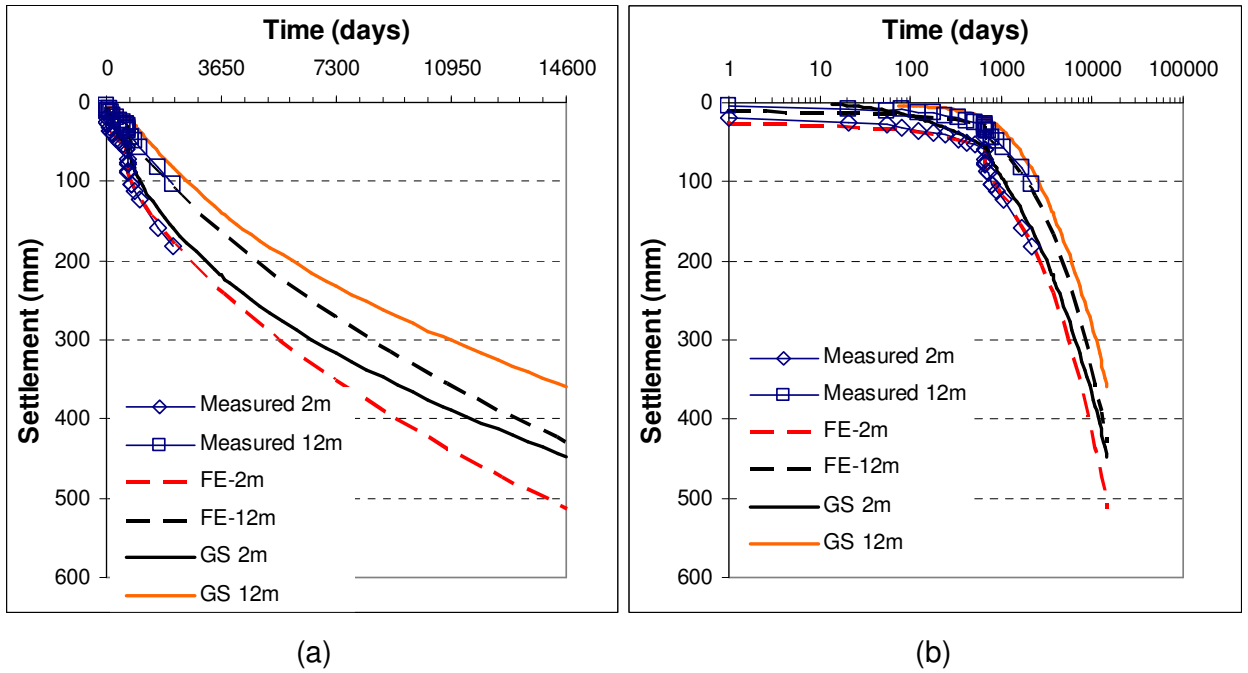


Figure 6.14 Time-settlement curve for different depths with measured and calculated values and a calculated prediction to 40 years for both programs in the centre of the embankment. (a) time in linear scale and (b) time in log scale.

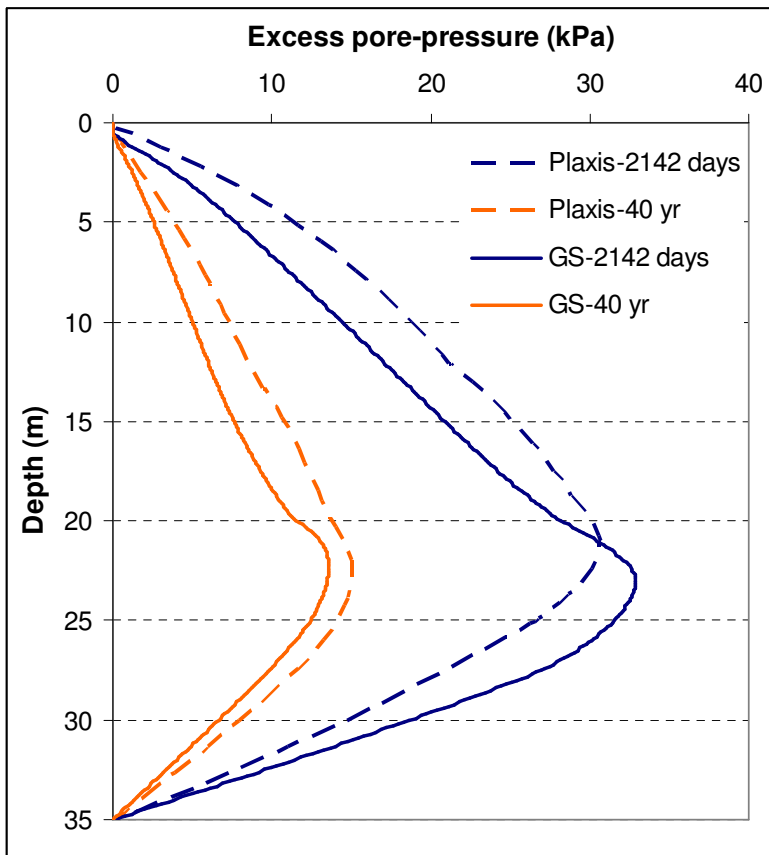


Figure 6.15 Calculated excess pore pressure for both programs at two different times in the centre of the embankment in the clay.

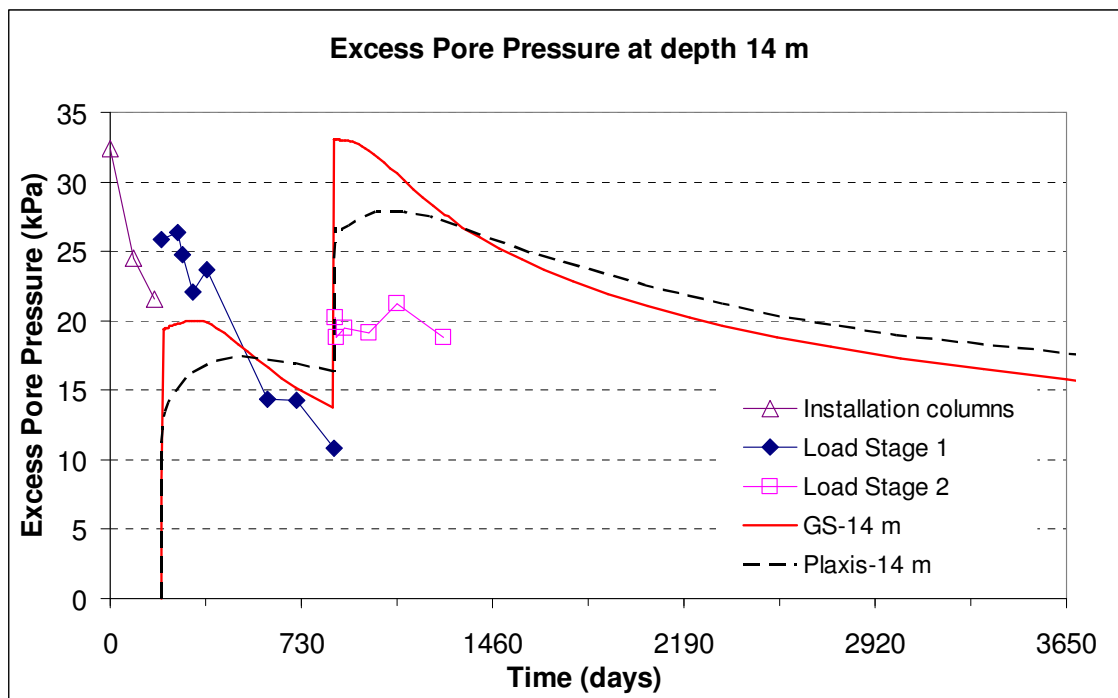


Figure 6.16 Calculated and measured excess pore pressure with time at a depth of 14 m in the centre of the embankment in the clay between the LCCs.

6.2.3 Discussion

As can be seen in Figure 6.12 both programs capture the overall behaviour very well. However, both programs have tendency to overpredict the settlement at the transition zone at a depth of 20 m compared to the measured values. It can also be seen in Figure 6.12 that the GS Settlement program shows a very distinct break at the transition zone at a depth of 20 m, i.e. because the soil and LCCs are modelled as a composite material and behave as a block, whereas Plaxis produces a slightly smoother transition zone. Neither of these programs is expected to produce a perfect match since the problem is complex and very much a three-dimensional problem.

Figure 6.12b shows a prediction of the settlement at 40 years and the total calculated settlement is about 0.6 m at the ground surface. The programs produces very similar settlement in relation to depth after 40 years in Figure 6.12b and the difference is in the area of the transition zone between 18 m 21 m. Just underneath the LCCs the settlement are calculated to become about 0.31 m for the GS Settlement and 0.34 m for the Plaxis program.

In Figure 6.13 the calculated settlement from Plaxis correspond very well with the time-settlement curve for the measured period, while the calculation from the GS Settlement program underpredicts the settlements for the studied depths. As can be seen in Figure 6.12a the GS Settlement

calculation underpredicts the settlement above 18 m and overpredicts the settlement below 18 m depth compared with the measurements at 2,142 days.

In Figure 6.14 it can be seen that the settlement rate, after about 12 years, for GS settlement declines faster than the calculated settlement from Plaxis. This is probably due to that the LCC block in the GS Settlement program has a higher hydraulic conductivity than the corresponding soil volume in Plaxis and therefore consolidate faster in these layers.

The excess pore pressure in relation to depth in Figure 6.15 shows that the differences in the results between the programs are relatively small. The calculated excess pore pressure from GS Settlement tends to consolidate faster in the clay beneath the block, probably due to that drainage through the block is greater than when modelling the LCCs as solid elements as in Plaxis. The comparison between the measured and the calculated excess pore pressure for a depth of 14 m, as shown in Figure 6.16, reveals that the GS Settlement program starts with a higher excess pore pressure than Plaxis. This is due to the fact that the entire calculated external load in GS Settlement program becomes excess pore pressure. The measured excess pore pressure is affected considerably from the installation of the LCCs. As seen in the beginning of the measurements in Figure 6.16 the excess pore pressure is about 33 kPa in the start of the measurements and about 22 kPa just before the first load was applied.

The comparison between the calculated and measured values for the excess pore pressure is difficult since the calculations do not consider any installation effects, and consequently zero excess pore pressure starts at the start of the first load stage. For the second load stage the increase in excess pore pressure is roughly twice as much for GS Settlement than for the Plaxis program that also has about the same increase as the measured one.

It can be said that the overall behaviour seems to be satisfactory for both programs but a question mark remains regarding the effects from the installation of the LCC.

As mentioned previously, the calculation programs used in this project are one- and two- dimensional respectively. This implies that neither of the programs is capable of modelling these types of problems without making simplifications regarding geometry, stiffness parameters etc.

6.3 Kaserntorget

The soil profile and pore pressure history of the test site Kaserntorget are described in chapter 5.3. At the Kaserntorget test site settlement calculation were made for one section that corresponds to where the settlement gauge CS 4 is placed, see Figure 5.19.

Since this test site has a very complex loading and groundwater history two different approaches are adopted to calculate the settlement. The first one starts from when the groundwater lowering starts, in 1968, and the second one starts from when the filling were applied, set at 1830 in the calculations. The calculations are referred to as the short and the long model and starts in 1968 and 1830 respectively.

Below input parameters and a selection of results are presented and compared with the measured settlement.

6.3.1 Input parameters

The input parameters used to describe the soil profile are presented below.

If nothing else is stated the same parameters were used for both the short and the long model for both of the programs.

For GS Settlement program the oedometer modulus factors a_0 and a_1 were set at 0.8 and 1.0 for the clay. The factor b_0 is set equal at $1/OCR$ and b_1 are set at 1.1. The reference time, t_r , were set at one day. The creep parameter r_0 is set equal to 1,000 for the entire clay layer for both models. This is done on the basis of that the groundwater recovery would not take place and therefore this would give a low starting creep number, r_0 , according to Olsson & Alén (2009).

Since no unload/reload test has been conducted the oedometer modulus for the overconsolidated region is set to $75 \cdot \sigma'_c$. The limit stress, σ'_L , is set as $\sigma'_c + 20$ kPa for the clay layers. The modulus number is set according to Larsson (1981) as $M' = 4.5 + 6/w_N$.

The top four metres of fill are modelled as a material with no creep effects and an oedometer modulus of 20 MPa.

The evaluated in-situ effective stress and preconsolidation stress for both the short and the long model are shown in Figure 6.17. For the long model

the groundwater table is assumed to be one metre below the ground level and a hydrostatic pore pressure profile is assumed.

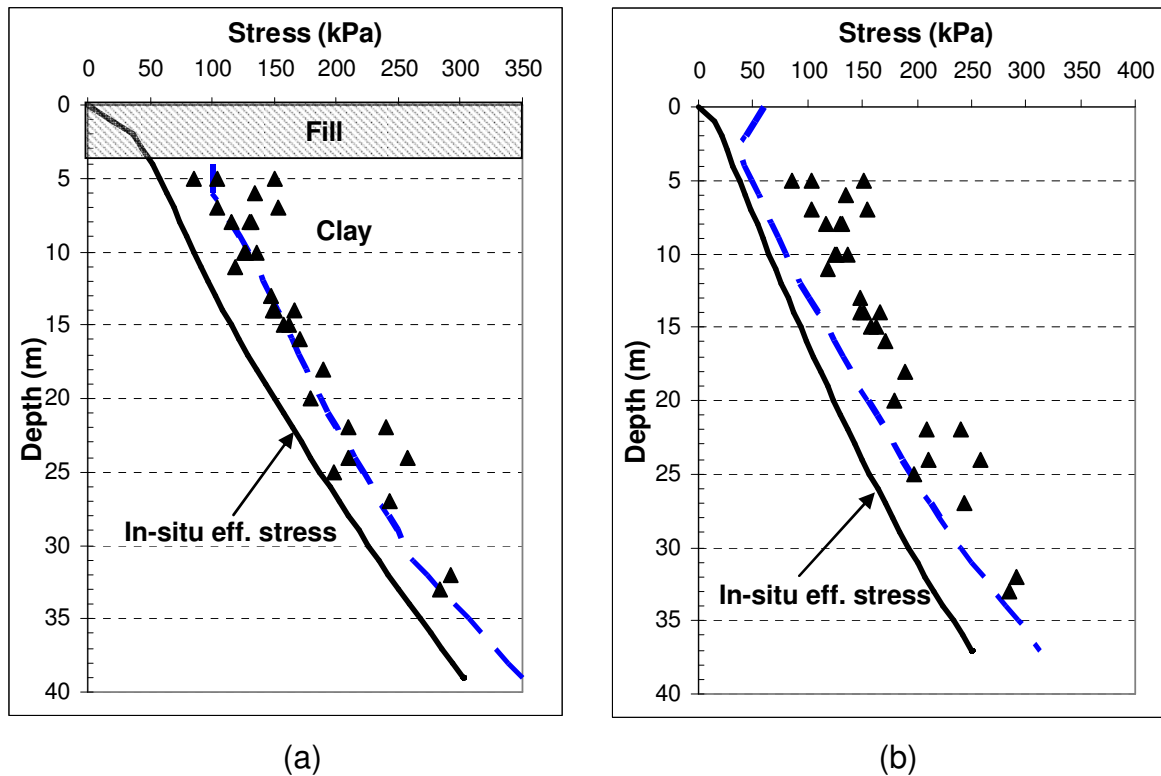


Figure 6.17 Evaluated in-situ effective stress and preconsolidation stress (\blacktriangle) for (a) the short model (start 1968) and (b) the long model (start 1830). The used preconsolidation stress in the GS Settlement program is represented by the broken line.

The evaluated preconsolidation stress presented in Figure 6.17 is from CRS oedometer tests conducted in the studied area and all the tests were conducted after 1990. The preconsolidation stress used for the short model is evaluated from these tests and for the long model it is assumed that the preconsolidation stress corresponds to an OCR of about 1.25, except for the top part of the soil profile where the preconsolidation stress increases to 60 kPa as shown in Figure 6.17b.

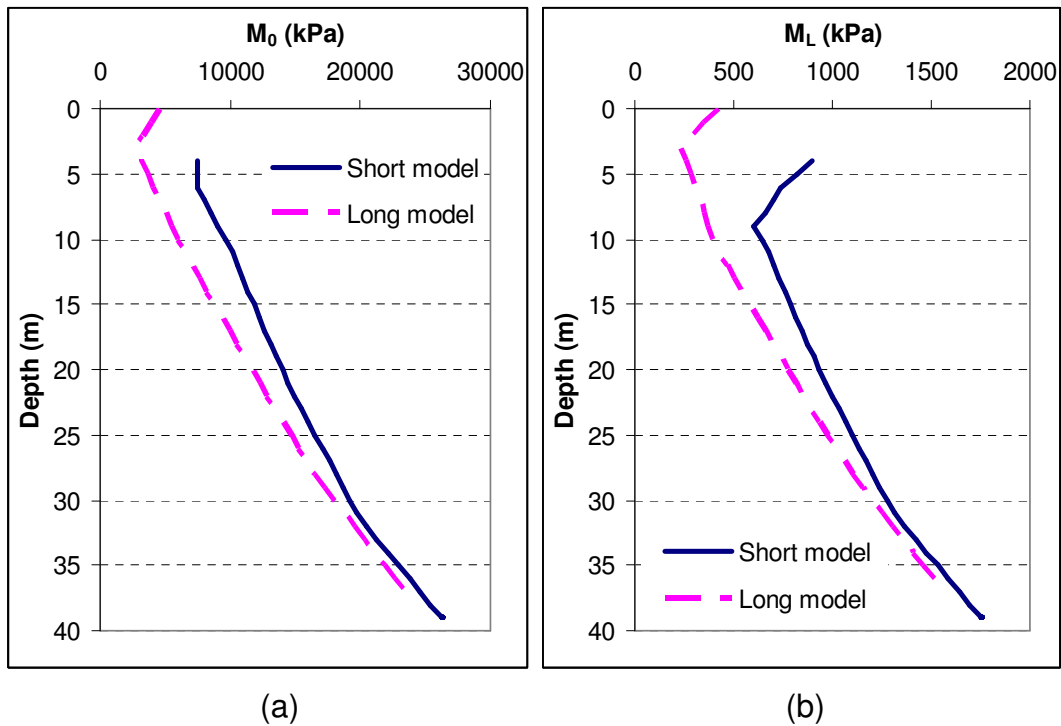


Figure 6.18 Used oedometer modulus in the long and short model. (a) the overconsolidated oedometer modulus, M_0 , and (b) the oedometer modulus in the normal consolidated region, M_L .

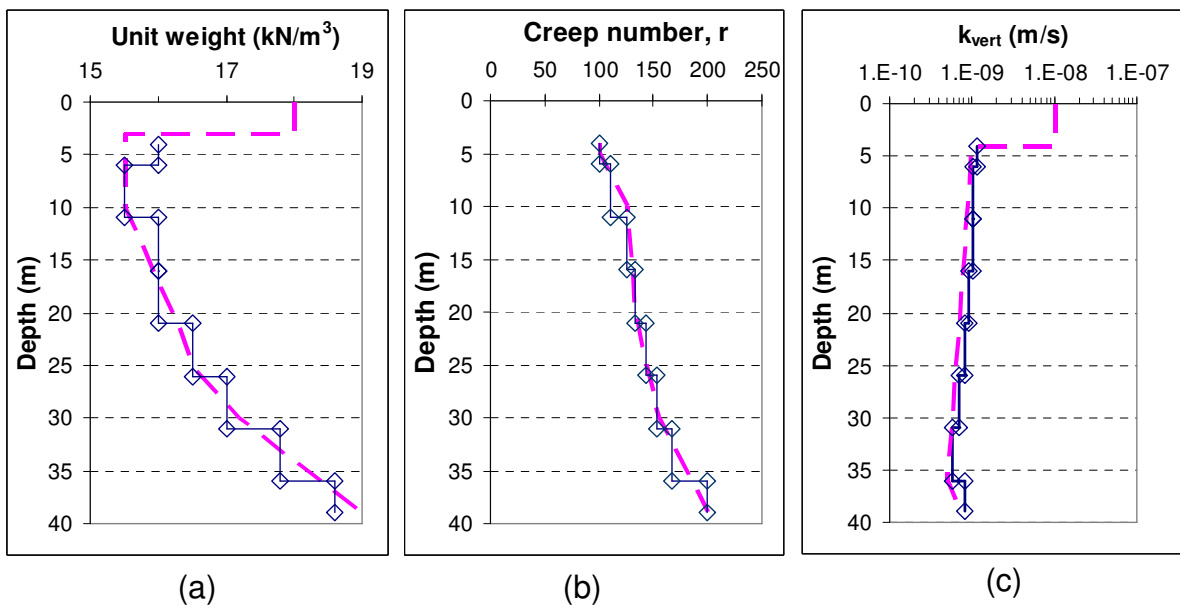


Figure 6.19 Input parameters for Plaxis (unbroken line with squares) compared to GS Settlement (broken line) for the unit weight, creep number and the vertical hydraulic conductivity.

The horizontal hydraulic conductivity is set equal to the vertical hydraulic conductivity for the Plaxis program.

The input parameters for the SSC model are determined from back-calculations of some of the CRS oedometer tests that have been conducted on samples of soft clay in the area. The CRS oedometer test results that have been used here are from a borehole approximately 100 m from the settlement gauge CS 4. The in-situ effective stress has been corrected for that specific location although the difference is small. The OCR is assumed to be the same for these two locations.

In Figure 6.20 and Figure 6.21 show two back-calculated results from FE analysis compared to values measured in CRS oedometer tests. The calibrated soft clay parameters for the SSC model are presented in Table 6.7.

The back-calculation is performed using the same procedure as described in chapter 4.2.4.

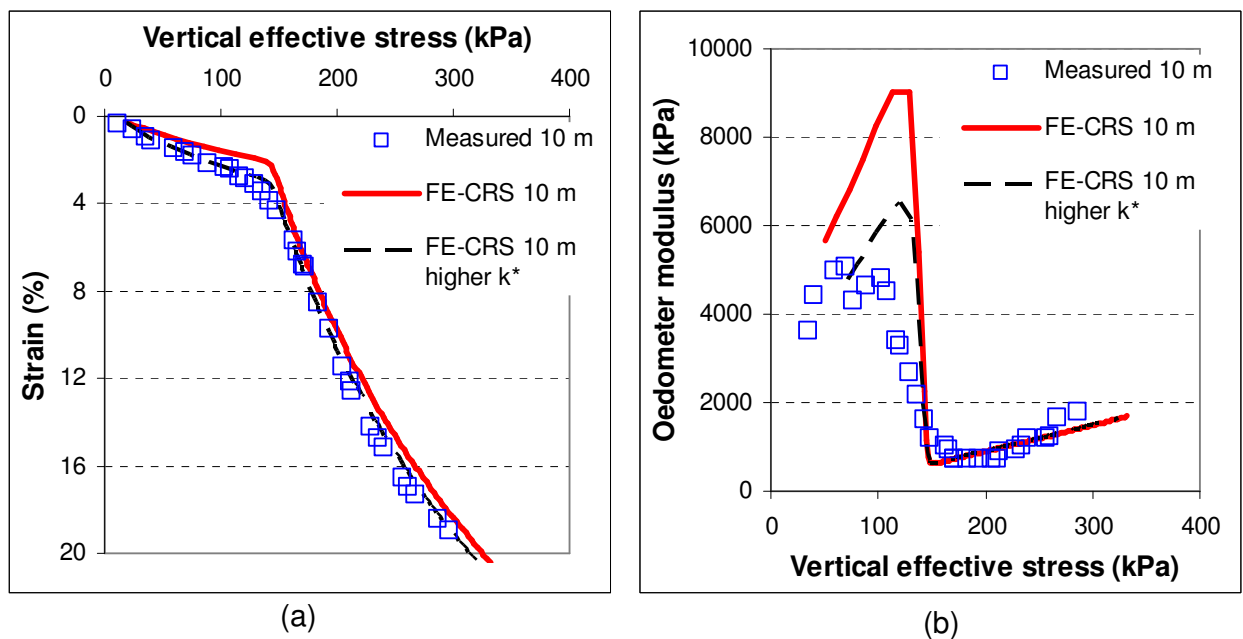


Figure 6.20 Back-calculated CRS curve for calibration compared with measured values for the depth 10 m. (a) the stress-strain curve and (b) the oedometer modulus curve.

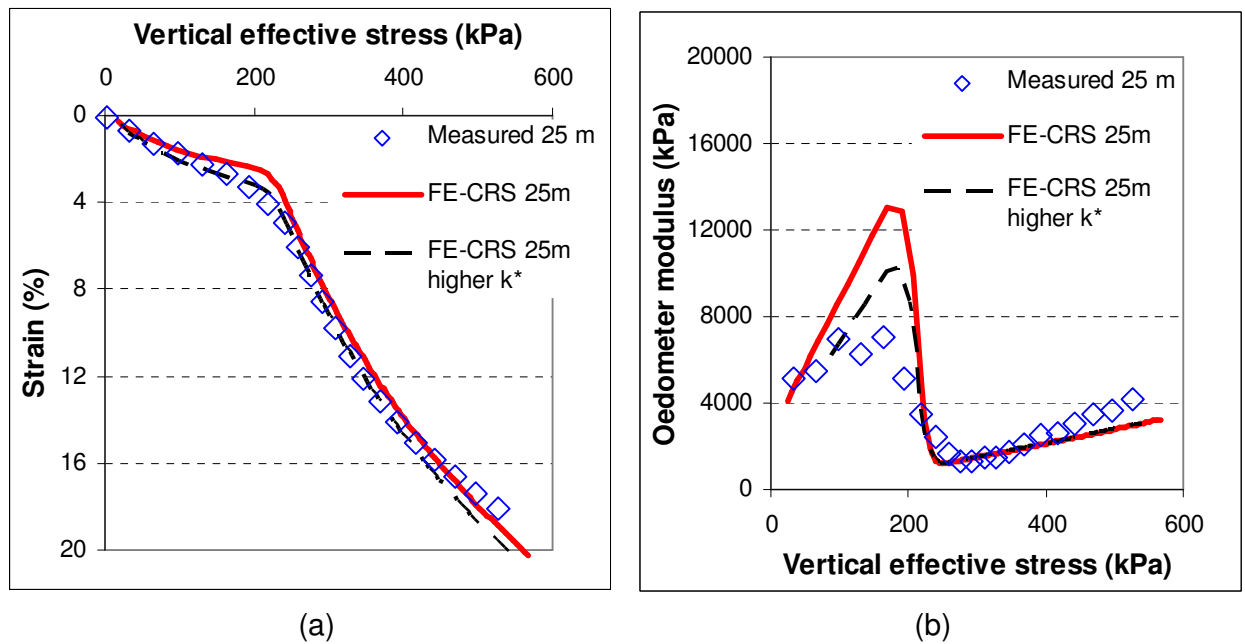


Figure 6.21 Back-calculated CRS curve for calibration compared with measured values for the depth 25 m. (a) the stress-strain curve and (b) the oedometer modulus curve.

As can be seen in Figure 6.20 and Figure 6.21 there are two curves from the FE analysis. The curve modelled with the higher κ^* -value is chosen so that a best fit of the CRS curve is achieved by simply changing the κ^* -value. The other modelled curve represent a more likely behaviour in the overconsolidated region, as discussed earlier, the evaluated oedometer modulus in the overconsolidated region is normally too low. Consequently, the κ^* -value that produces the slightly higher oedometer modulus is used in the calculations.

Table 6.7 Clay parameters used for the SSC model for the short model.

Depth (m)	κ^* (-)	λ^* (-)	μ^* (-)	ϕ' (deg)	c' (kPa)	OCR (-)	POP (kPa)	K_0^{nc} (-)
4 - 6	0.017	0.25	0.01	30°	1	-	45	0.5
6 - 11	0.017	0.25	0.009	30°	1	-	40	0.5
11 - 16	0.017	0.25	0.008	30°	1	1.35	-	0.5
16 - 21	0.017	0.25	0.0075	30°	1	1.30	-	0.5
21 - 26	0.015	0.22	0.0070	30°	1	1.30	-	0.5
26 - 31	0.015	0.22	0.0065	30°	1	1.30	-	0.5
31 - 36	0.015	0.22	0.0060	30°	1	1.35	-	0.5
36 - 39	0.012	0.22	0.0050	30°	1	1.35	-	0.5

The geometry used in Plaxis is simplified to horizontal layers for the entire soil profile and Figure 6.22 shows the FE mesh used to model the Kaserntorget test site.

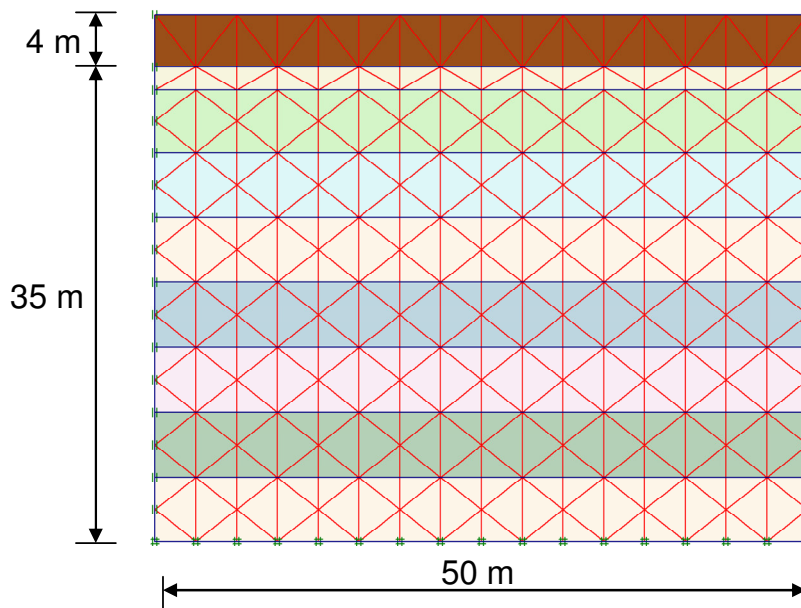


Figure 6.22 FE mesh used in Plaxis for the Kaserntorget test site (short model).

The initial conditions are generated by using the K_0 procedure and the K_0 value is set according to eq. (4.6) and eq. (4.7). The groundwater pressure is also generated.

The boundary conditions for the model are as follows

- Horizontal displacement is prevented at the sides of the model.
- Both horizontal and vertical displacement is prevented at the bottom of the model.
- Closed consolidation boundaries are set at the sides of the mesh and open at the top and bottom boundaries.

The calculation stages for the short model starts at 1968 and follow the evaluated pore pressure changes according to Figure 6.23. This is simulated by changing the pore pressure at the bottom of the clay layers accordingly.

The differences for the long model are that it starts at 1830 with application of the fill and is then let to consolidate until 1968. The clay layer is also said to be about 2-3 m thicker than it is today due to the settlement that is calculated for this time.

The calculation stages are the same for both of the programs.

6.3.2 Groundwater level over time

The lowering of the groundwater level in the layer underneath the clay that has occurred in the studied area can be seen in Figure 6.23 together with the evaluated groundwater level used in the calculation.

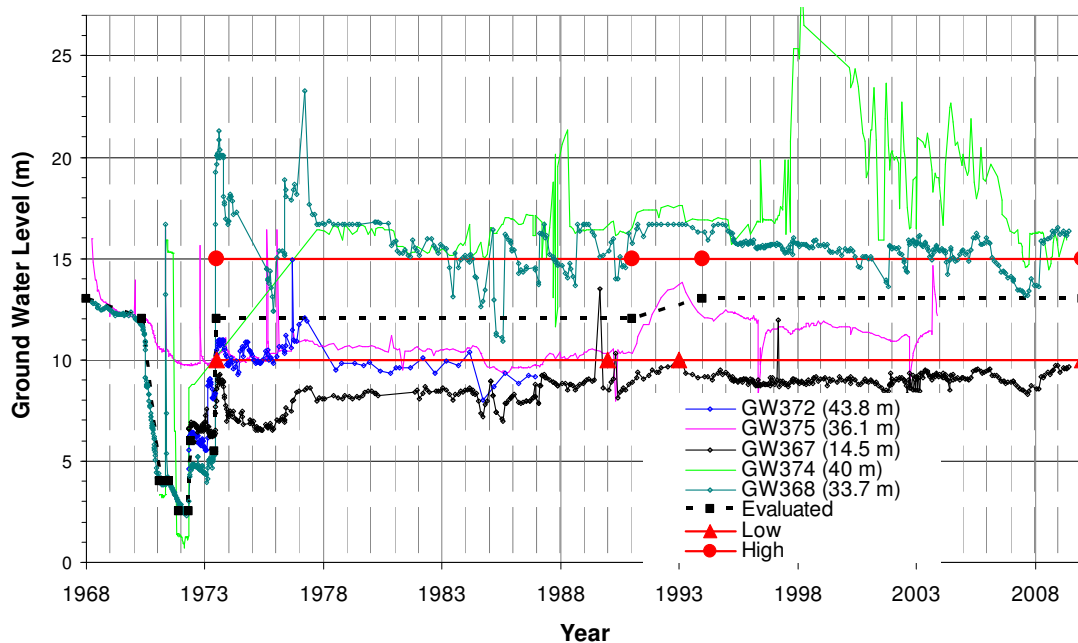


Figure 6.23 Measurements and evaluated groundwater level change over time underneath the clay layer.

As can be seen in Figure 6.23 a high and low line for the groundwater level is plotted and they are used in a sensitivity calculation to show the influence of the input values of the groundwater level.

6.3.3 Results and comparison with measurements

A selection of results is presented below. Comparison between measured and calculated settlement are presented for both programs. In Figure 6.24 to Figure 6.26 shows the time–settlement curve for the short and the long model for the evaluated groundwater level shown in Figure 6.23. In Figure 6.27 to Figure 6.30 the excess pore pressure is shown, both over time for a certain depth and in relation to depth for two different times. In Figure 6.31 and Figure 6.32 the time–settlement curve for the short and the long model respectively are shown for the evaluated and the two extreme groundwater levels, high and low, as shown in Figure 6.23. Observe that the settlement reference is 1971-07-01. That is the time for the start of the measurements of the settlement.

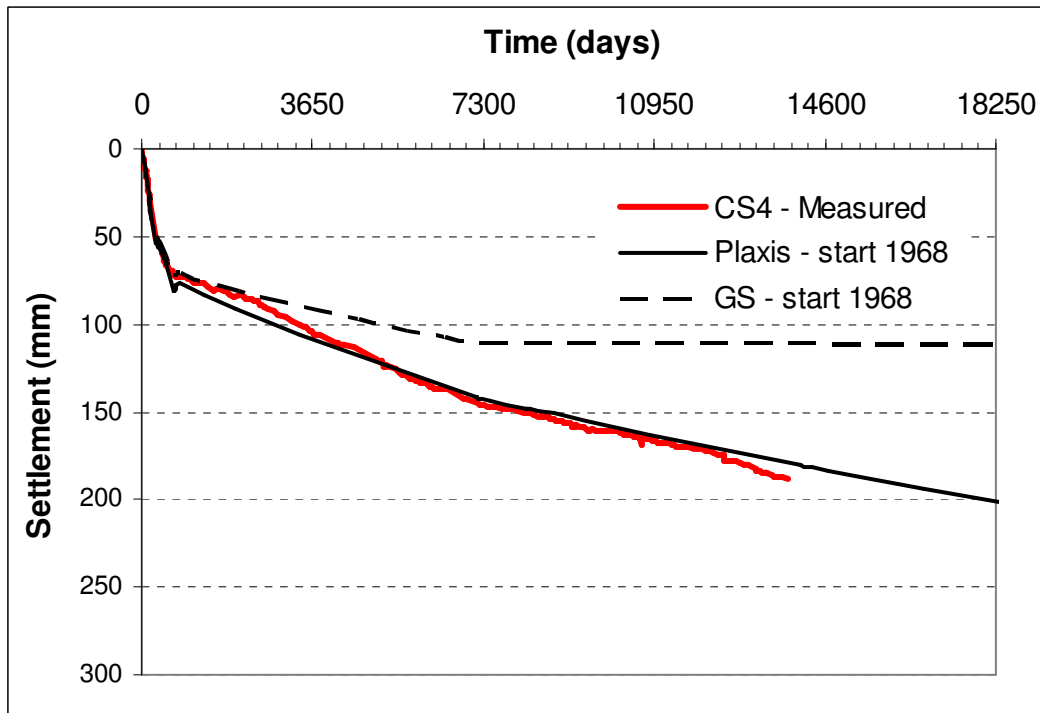


Figure 6.24 Time- settlement curve with measured and calculated values for the short model for both programs with the evaluated groundwater level. The starting date for the settlement curves is 1971-07-01.

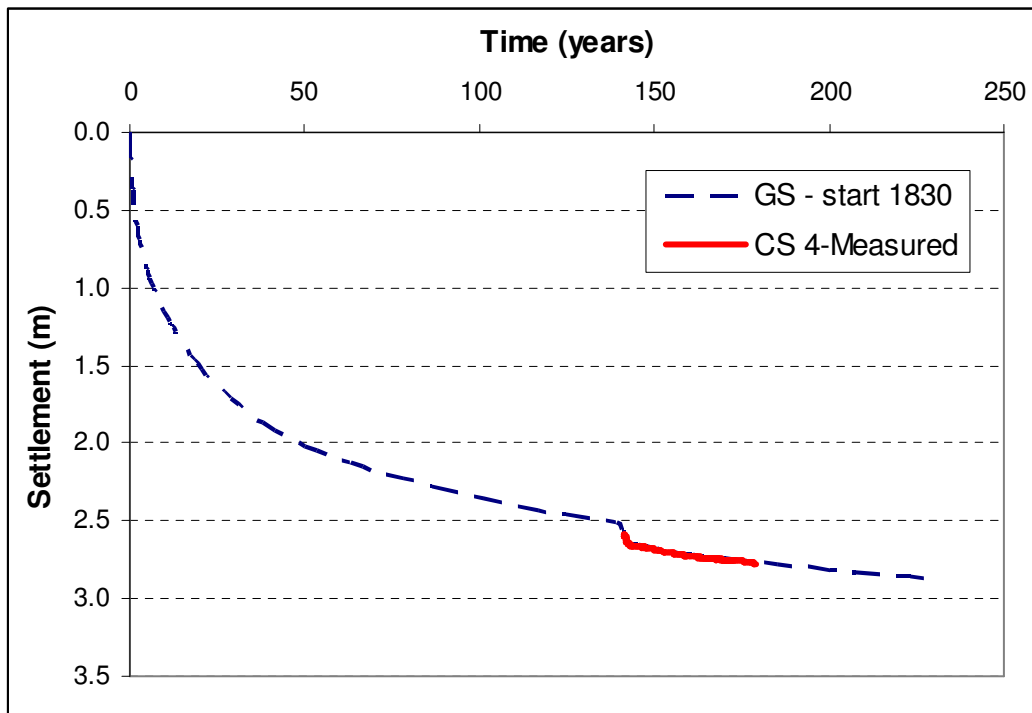


Figure 6.25 Time-settlement curve with measured and calculated values for the long model for the GS Settlement program with the evaluated groundwater level. The starting date for the calculated and measured settlement curve is 1830-01-01 and 1971-07-01 respectively.

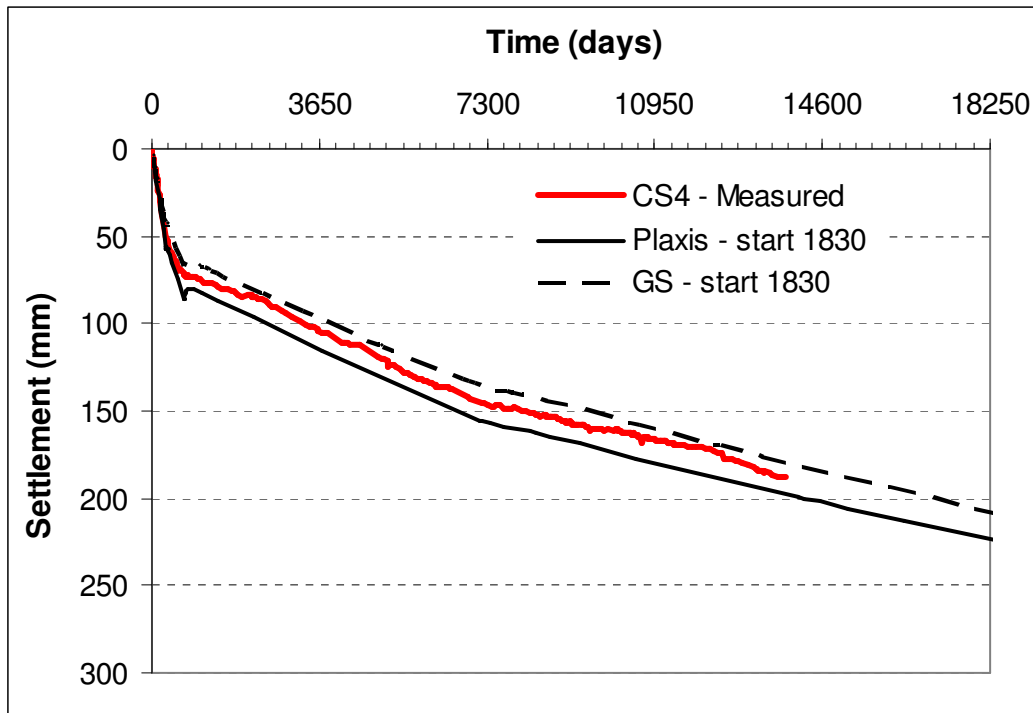


Figure 6.26 Time–settlement curve with measured and calculated values for the long model for both programs with the evaluated groundwater level. The starting date for the settlement curves is 1971-07-01.

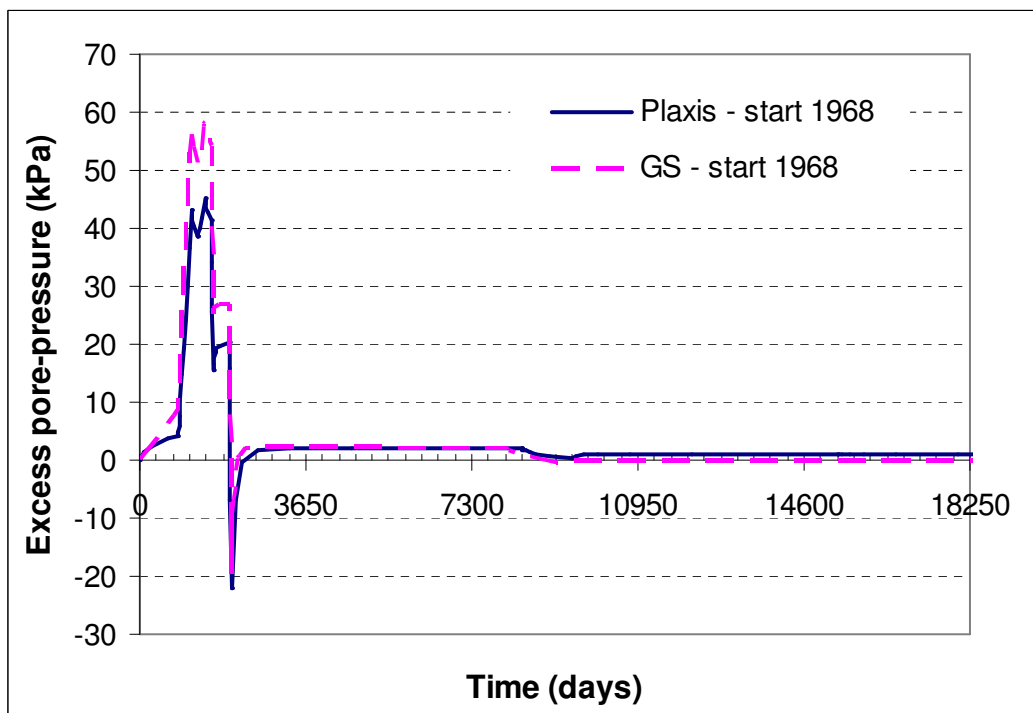


Figure 6.27 Excess pore pressure over time at about 3 m above bottom for the short model.

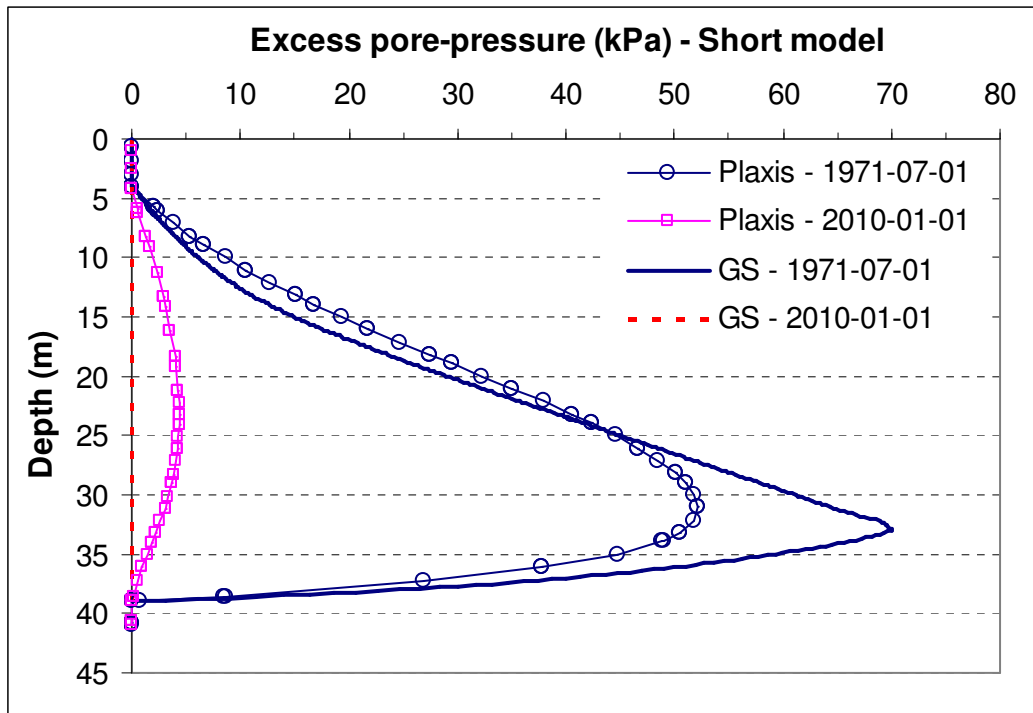


Figure 6.28 Excess pore pressure with depth for both programs at two different times for the short model.

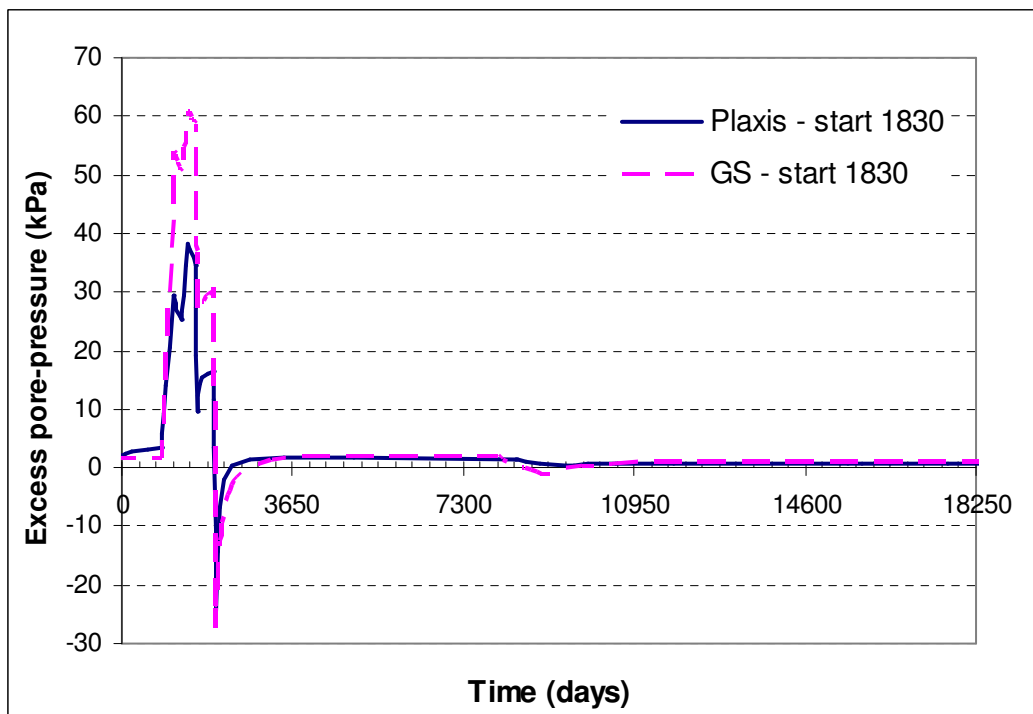


Figure 6.29 Excess pore pressure over time at about 3 m above bottom for the long model.

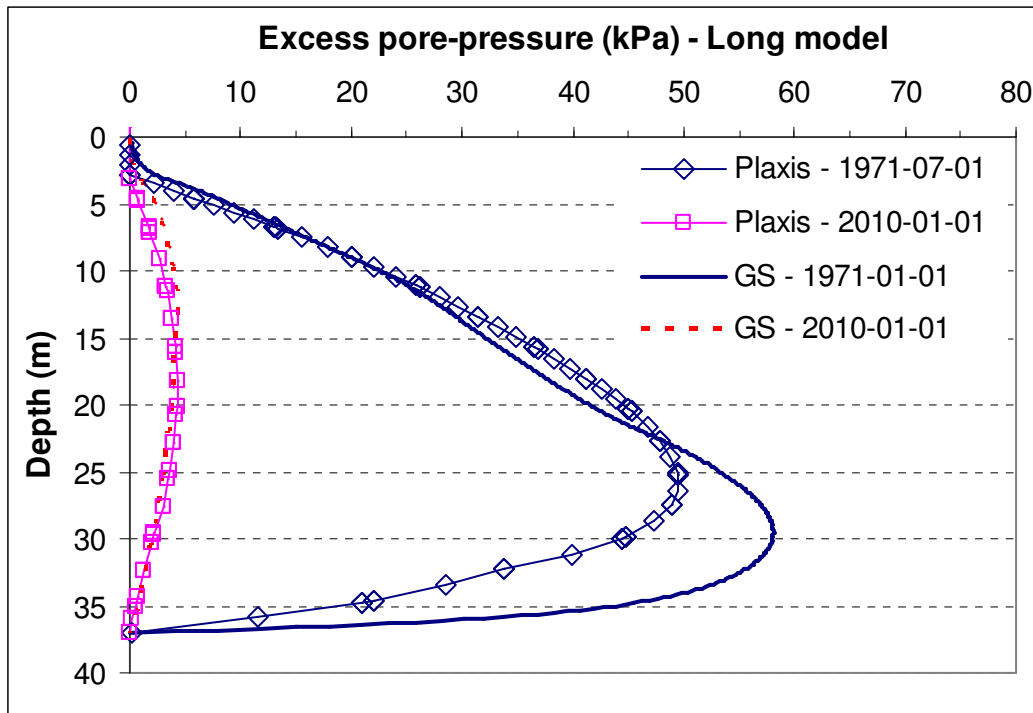


Figure 6.30 Excess pore pressure with depth for both programs at two different times for the long model.

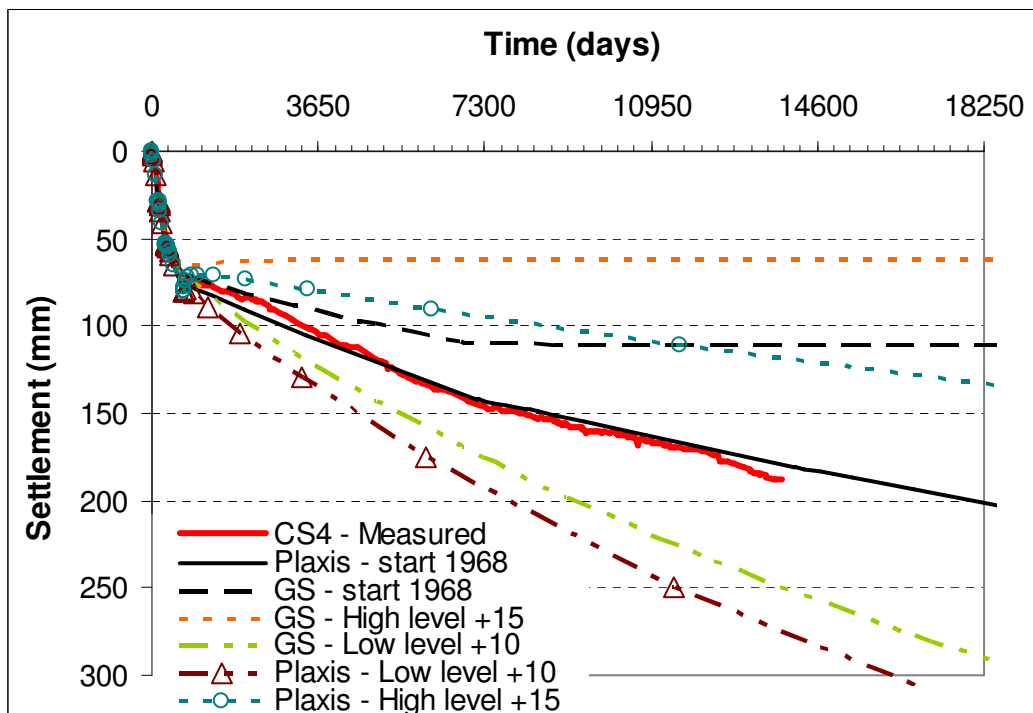


Figure 6.31 Time-settlement curve with measured and calculated values for the short model for both programs. With the evaluated levels, the low and the high groundwater level. The starting date for the settlement curves is 1971-07-01.

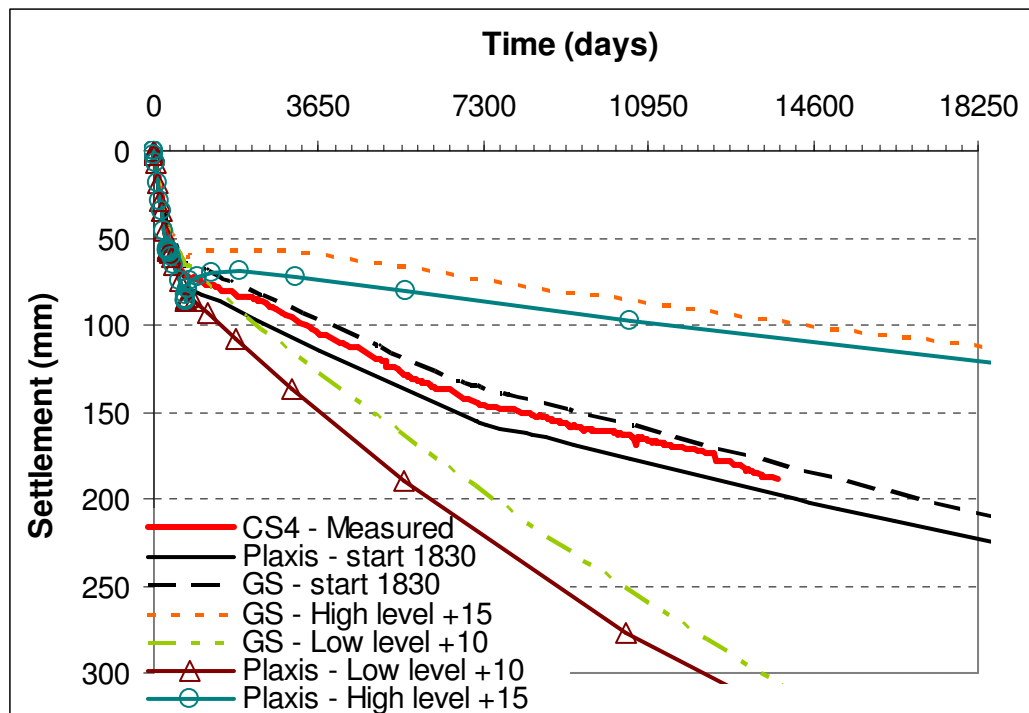


Figure 6.32 Time-settlement curve with measured and calculated values for the long model for both programs. With the evaluated values, the low and the high groundwater level. The starting date for the settlement curves is 1971-07-01.

6.3.4 Discussion

The calculation for this test site has been conducted in two ways. One that starts when the first groundwater measurements were conducted, called short model, and one that starts at an estimated time for when the fill was applied, called long model. These two models were conducted to highlight some possibilities as well as difficulties of the two programs used.

In Figure 6.24 it can be seen that the initial calculated settlement during the first two years corresponds very well to the measured settlement for both of the programs. After the initial settlement the GS Settlement program underpredicts the measured settlement and after about 20 years (7,300 days) the settlement more or less stops. This is probably because the evaluated groundwater level is back to the same level as it was when the calculation started in 1968 and all excess pore pressure has dissipated, as can be seen in Figure 6.27 and Figure 6.28.

For the SSC model the settlement curve, Figure 6.24, has a very good match with the measurements for the entire time period with the chosen groundwater level. It can also be seen in Figure 6.27 and Figure 6.28 that a small excess pore pressure exists after the groundwater level has returned to its starting level. This excess pore pressure is created by creep and is an

effect of the input parameters and OCR that has been chosen for this soil profile.

The probable reason for the difference between the calculated settlements in the programs is that the GS Settlement program does not capture what is likely to be ongoing settlement in the area when the groundwater level is back at the starting level for this case. This means that the GS Settlement program calculates the effect of the groundwater lowering but not the likely ongoing settlement. It also implies that since most of the soil profile, when the groundwater level rises back to the starting level, is back at the starting effective stress the creep effects are more or less negligible. This is not due to the theoretical model itself but probably its implementation.

When modelling the long model, i.e. starting time in 1830, the calculated settlement from 1830-01-01 is shown in Figure 6.25 together with the measurements. The magnitude of the settlement until 1968, i.e. when the groundwater lowering began, is of minor importance and only the result from the GS Settlement program is presented. However, the settlement from SSC model is in the same range. The calculated and measured values correspond very well for both programs during the entire time period to the evaluated groundwater level, see Figure 6.26. The results using the SSC model are more or less the same for both cases. For the GS Settlement program, however, there is a significant difference. In this case the GS Settlement program captures the likely ongoing settlement in the area and therefore much better agreement of the measured settlement is achieved. The excess pore pressure for the long model in 1968 is about 2 kPa about 3 metres above the bottom, as can be seen in Figure 6.29. The maximum excess pore pressure in the soil profile is less than 5 kPa for both programs in 1968. This corresponds to about the same excess pore pressure in 2010 as can be seen in Figure 6.29 and Figure 6.30.

The behaviour of the excess pore pressure is very similar for both programs for the long model and this is expected since the simplified geometry for this case is very much one-dimensional.

The results of the sensitivity analysis are presented in Figure 6.31 and Figure 6.32. The sensitivity analysis only considers the effect of an increase to a stationary level of the groundwater in the bottom aquifer. That is from the time period just after 1973 when the apparent increase in the groundwater level occurs, see Figure 6.23. The purpose is simply to show what the settlement would be according to the programs with these two 'extreme' groundwater levels.

For both the short and the long model it can be seen that the outcome of the size of the settlement depends to a large extent on the final groundwater level that has been chosen.

For the short model it can be seen that for the high groundwater level the ground heaves a few millimetres. After the small heave the settlement stops in effect for the GS Settlement program whilst the SSC model continues to creep at more or less the same rate as the evaluated groundwater level. The settlement difference compared to the measured is about 70% (0.140 m) for the GS Settlement program and 35% (0.065 m) for the Plaxis program after 40 years.

For the low groundwater level both programs produces similar results and overpredict the measured settlement by about 40% (0.050 m) after 40 years for the short model.

The sensitivity analysis for the long model produces similar results for both programs, see Figure 6.32. This is in agreement with what has been discussed above. For the low and high groundwater levels the programs under- and over- predict the settlement by about 45% (0.050 m) and about 75% (0.150 m) respectively after 40 years.

Both programs are capable of capturing the measured settlement curve even though the GS Settlement program did not do so for the short model. However, it most likely captures the effect of the lowering of the groundwater level. Since the groundwater level rises back to the starting level the effect should diminish and return to the settlement rate, if any, before the groundwater change.

7. DISCUSSION

This chapter provides a discussion of the contents of this thesis. It also summarises the main conclusions of the thesis.

7.1 Introduction

In this thesis the main purpose has been to calculate long-term settlement under real and realistic conditions and using available numerical tools. There is also a discussion about determination of soil parameters for settlement calculations and the inherent difficulties.

Burland (1987) clearly illustrated the link between different areas in geotechnical engineering in his Nash lecture entitled “The teaching of soil mechanics - A personal view”. In his lecture he presented the view that geotechnical engineering practice comprises four parts.

1. The ground profile
2. Soil behaviour
3. Modelling
4. Empiricism

Burland formulated that the three first parts could form the apexes of a triangle with empiricism occupying the centre including all three together, as shown in Figure 7.1.

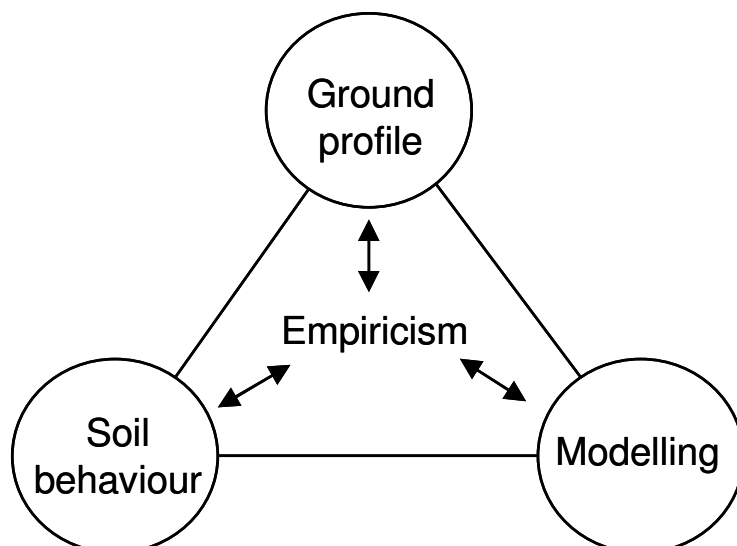


Figure 7.1 Modified Burland triangle from Burland (1987).

This triangle has come to be known as the Burland triangle. This triangle clearly illustrates the interaction between all parts of what the engineer needs to take into consideration when building on soil. It shows in

particular that empiricism should be used for all the major elements, represented in each of the circles.

There are numerous numerical programs for calculating deformation, such as settlement. When using a numerical program for calculating settlement the engineer must be aware of the strength, weaknesses and limitations of the different programs and the constitutive models otherwise the results could be misleading.

Normally, when using numerical tools for calculating settlement in Sweden input parameters are evaluated from a CRS oedometer tests without any unloading and reloading cycles. Although these types of tests are relatively quick and easy to run, they do not give us the important parameters, such as the oedometer modulus in the overconsolidated stress region or the creep parameter. These parameters are normally obtained by the engineer from empiricism.

Determining parameters to be used for settlement analysis is not a straightforward task. Different models sometimes give us different sets of parameters, even if they correspond more or less to the same thing. The models used in this thesis all incorporate creep and do so in different ways, e.g. the Chalmers model in the GS Settlement program defines the creep number by a straight line dependent on the effective stress, see Figure 4.2, and for the SSC model the OCR and the κ^* , λ^* and μ^* values as seen in eq. (3.20) determine the creep rate. However, the underlying theory is very similar, as can be seen in Chapter 3.

7.2 Soil parameters

When a geotechnical engineer makes a prediction of, for example, deformation of a structure or settlement of an embankment, it is in most cases based on results from thin laboratory samples. These samples have been extruded from the ground and delivered to a laboratory for testing.

When a sample is extruded from the ground it will experience an unloading and this unloading creates a negative pore pressure and keeps the sample intact. Whether or not this negative pore pressure remains, or how much of it, when the testing starts is difficult to know. However, this is normally assumed for an oedometer test as shown in Figure 2.3. If no negative pore pressure remains, the starting point for the laboratory test in Figure 2.3 would be in the origin ($s' = t = 0$ kPa). This would most likely lead to greater strains and lower stiffness in the overconsolidated region. A

detailed study regarding sampling effects in soft clays can be found in, for example, Hight (2001).

As mentioned in Chapter 4 the CRS oedometer test is the commonly used test in Sweden and the test results are naturally very much dependent on the quality and handling of the soil sample. For this test there is a method proposed by Lunne et al. (1997) and Larsson et al. (2007) to indicate the disturbance of the tested soil sample.

When using the CRS oedometer test for evaluating the soil parameters when calculating settlement it is important that the strain rate for the test is clearly defined. Since the evaluated preconsolidation stress is strain rate dependent it is only defined if the strain rate is stated together with the evaluated preconsolidation stress.

An obvious question that arises is how the parameters are affected by the sample disturbance and the testing procedure. Many researchers have studied this effect, such as Tavenas & Leroueil (1987) and Hight (2001) to name but a few. For the sake of simplicity, it could be concluded that the bounding surface, the preconsolidation stress, shrinks and that the small strain stiffness, e.g. the oedometer modulus in the overconsolidated region, decreases as the disturbances increase.

As mentioned earlier in this thesis, the oedometer modulus in the overconsolidated region from a CRS oedometer test should not be evaluated directly from the test result if no unload/reload procedure has been conducted. However, empiricism could be used for an estimation of the in situ oedometer modulus.

Claesson (2003) put forward a model, described in Chapter 4.2.3, to describe the oedometer modulus curve better. In this thesis a method for evaluating the transition zone is suggested, based on the CRS oedometer test performed and evaluated accordingly to Swedish practice. Using this method of evaluating the transition zone or using the suggested values would in most cases produce very small differences in the settlement result. However, the suggested evaluation method seems to correspond better to the evaluation of the transition zone of the creep number, i.e. for parameters a_1 and r_1 , as suggested by Claesson (2003). It would seem logical that for the stresses where the creep contributes most would also be where the oedometer modulus has its lowest value, i.e. in the normally consolidated region.

When calculating long-term settlement of soft clays, the creep contribution could be substantial. Evaluation of the creep parameter is normally done from a thin clay sample in an IL oedometer test with an increase in load every 24 hour. As discussed in Chapter 4.2.1 this could sometimes be misleading for soft clays from the studied region since the excess pore pressure takes a long time to dissipate and 'pure' creep is not evaluated. This could be solved by allowing load step of interest in an IL oedometer test to act long enough.

Often the creep parameter is only determined from empirical relationships and in Sweden the correlation with the water content is used most often. This empirical relationship is most cases evaluated from a 24-hour IL oedometer test and, as mentioned above, the creep parameter is sometimes misinterpreted for this short time period. This makes it more important to validate that the creep parameter used is appropriate for the case being studied, especially when creep effects are of great importance.

In the Chalmers model, presented by Claesson (2003), the creep parameter is defined as shown in Figure 4.2. However, the creep number, r_0 , in the overconsolidated stress region is very difficult to determine. In the method proposed by Olsson & Alén (2009) the creep number, for the Chalmers model, is evaluated from the final effective stress as described in Chapter 4.2.3. Since this method will produce a starting creep number, r_0 , that is dependent on the final effective stress the difference compared to the suggested values by Claesson (2003) will be minor for final effective stress around the preconsolidation stress. However, for small final effective stress changes, i.e. a small increase in vertical load, the creep number, r_0 , will be higher and for extremely small effective stress changes the creep number, r_0 , will approach infinity. Very high values for the creep number (e.g. $> 5,000$) should be used with caution and the meaning of using a model that includes creep in this way could perhaps be questioned.

7.3 Modelling

As can be seen in Figure 7.1 modelling is just one of the four elements and all are needed in order to make a reliable prediction. Modelling could be conceptual, analytical or physical. However, modelling today is often referred to as numerical modelling. This is too narrow a definition, and it could divert us from a deeper understanding of modelling as an essential engineering problem-solving methodology.

Modelling is not just using a numerical tool and using input parameters to obtain a result and from this result trying to decide its meaning. If a

numerical tool is used with consideration of its possibilities and limitations it is a very powerful tool that could help the engineer to understand and predict the behaviour of the construction.

In Sweden, the evaluation of the preconsolidation stress is normally done using the Sällfors method for soft clays, see Figure 2.5. Using this method implies that a reduction in the preconsolidation stress is made due to strain rate effects from a laboratory test. This reduction is done in such a way that the evaluated preconsolidation stress would correspond better to the field case, where the strain rate is lower than in the laboratory test. This procedure was constructed in a time when manual calculation was the normal way of estimating the settlement and creep effects were either added on later in some way, e.g. primary and secondary consolidation as two separate processes, or included by setting the OCR equal to one. This refers to soft clays with a normally consolidated condition corresponding to an OCR of about 1.3.

Using this method in more recent and more advanced models, where strain rate effects (viscous behaviour) are included, would imply that the Sällfors method of evaluating the preconsolidation stress would be conservative since the strain rate effects should be taken care of within the constitutive model and not in the evaluation method of a laboratory test. When using such a model, with viscous behaviour, it would probably be more appropriate to back-calculate the laboratory test to achieve more appropriate soil parameters for use in the constitutive model. At the same time, there is the opportunity to study the behaviour of the constitutive model to see if it behaves as anticipated.

This does not imply that the empiricism should not be used for the soil studied. On the contrary, the choice of soil parameter used for the constitutive model should be compared to and evaluated with empiricism as suggested in Figure 7.1.

For the programs that are used in this thesis, only one is capable of back-calculating the type of laboratory test that was available for the respective test site, namely the Plaxis program. For the test sites, the Nödinge test embankment and Kaserntorget, back-calculation was conducted to establish proper soil parameters. There was a special focus on the preconsolidation stress and the oedometer modulus in the overconsolidated region since the normal parameters i.e. M_L , M' and r , could be evaluated either from the CRS oedometer test or by empirical relationship. No IL oedometer test was conducted for either of the test sites.

To back-calculate a CRS oedometer test a procedure for establishing more appropriate input parameters is suggested. In this procedure certain assumptions are made to calculate the earth pressure coefficient in the normally consolidated stress region using Jaky's formula, see eq. (4.6). For the overconsolidated stress region eq. (4.7) by Schmidt (1966) is used and this corresponds to the suggested equation by Larsson et al. (2007). These equations are used in this thesis because they are relatively accurate and fairly simple. However, they do not consider all aspects of the soil behaviour, e.g. anisotropy. In Sivakumar et al. (2009) a more detailed assessment of the earth pressure coefficient is presented.

7.4 Conclusions

The overall conclusion from this thesis is that all three programs, Embankco, GS Settlement and SSC model, could predict the settlement for the cases studied with relatively good agreement compared to the measured values. As mentioned previously, the Embankco program was only used for the hypothetical case.

The hypothetical test site was constructed to demonstrate from an empirical point of view how the programs correspond regarding the vertical settlement prediction. As can be seen in Chapter 6.1 all three programs correspond quite well for this case and time period.

The main conclusions from the two test sites based on the results are as follows:

- The two programs, GS Settlement and SSC model, were able to predict the overall behaviour of vertical settlement very well.
- Both programs have problems capturing the measured transition zone in the clay directly underneath the lime cement columns for the Nödinge test embankment.
- The SSC model in Plaxis is able to capture the behaviour from a CRS oedometer test results very well for effective stresses not too far above the preconsolidation stress.
- The λ^* value in the SSC model should correspond to the M_L value if the final effective stress is not too far above the preconsolidation stress.

- The κ^* value in the SSC model should be chosen low enough so that it represents a more realistic M_0 value and does not fit the CRS curve exactly, which is probably not appropriate if no unload/reload cycle is made.
- The SSC model in Plaxis is able to capture the ongoing settlement in a soil profile, either by including the entire stress history and basing the input parameters on empiricism or by back-calculating laboratory tests from the present time.
- The GS Settlement program is able to capture the ongoing settlement in a soil profile, if the entire stress history is included.

7.4.1 Recommendations

When using numerical tools, such as those described in this thesis, it is very important that the user have a sound understanding of the theories used in the constitutive model.

Some of the main recommendations after conducting this thesis are

- Study the geological history and use empiricism of the site to establish a first engineering description of the soil.
- Conduct sufficient and appropriate field and laboratory investigations to establish the ground profile.
- When possible, a back-calculation of laboratory test results is strongly recommended, both for obtaining a better understanding of the constitutive model and how accurately the constitutive model is able to reproduce the laboratory test results.
- Conduct sufficient and appropriate laboratory tests so that the soil behaviour can be established.
- Make a prediction of, for example, the settlement with an appropriate model.

7.4.2 Concluding remarks

The Embankco and GS Settlement programs are one-dimensional and are therefore only capable of calculating the vertical settlement. This gives a

number of different limitations, such as horizontal deformation can not be predicted, the interaction between the soil and reinforcement or other constructions can not be studied, possible failure zones can not be identified etc.

However, in the GS Settlement program the engineer can make use of analytical expressions that simplify a three-dimensional problem to a one-dimensional problem and implement the vertical stress increase. This was used for the Nödinge test embankment. However, in the GS Settlement program the increase in excess pore pressure corresponds to the vertical stress increase and this is most likely not the case in reality.

One-dimensional programs are often sufficient to use when calculating long-term settlement, as long as no complex problems need to be solved, as mentioned above. They are normally easy to use and the underlying theory is relatively easy to understand. This implies that the results should be relatively easy to interpret and examine.

One of the benefits of using two- and three-dimensional programs when calculating settlement or deformations is that it gives a much broader view of the entire problem, e.g. the interaction between soil and structure or reinforcement or detection of possible failure zones.

However, the result is no better than what the model could reproduce from the input parameters and one should bear in mind that the model is not reality but simply a mathematical description of it.

To establish a better prediction of the long-term settlement of, for example, embankments or buildings, measurements in situ are extremely important. Normally, measurements are made on the ground surface of the structure and this gives us the total settlement. However, this does not provide any information about where the settlement takes place in relation to depth. Consequently, if long-term settlement is or could be a problem, the recommendation is to measure the settlement in relation to depth together with the pore pressure at certain appropriate depths.

8. FURTHER RESEARCH

This chapter presents some of the identified future research work.

8.1 Laboratory testing

Creep behaviour in soft clays has been studied for many years and most of the research is based on one-dimensional conditions, the oedometer test. Normally, the evaluation of the creep parameter is from a conventional IL oedometer test.

The following points have been identified as future research work

- Study the time-dependent effects in a CRS oedometer test and trying to establish an evaluation method for estimating the creep parameter.
- Procedure for an IL oedometer test for typical Gothenburg clay.
- Establish the anisotropy and destructuration of soft clay.
- Creep at small effective stress changes.
- Study the K_0^{nc} for soft clays and the effects of how the K_0 value changes due to creep.
- Determination of the hydraulic conductivity and the validity of Darcy's law for small gradients in soft clay.

8.2 Field test and monitoring

A major research area would be to establish a test site to study the creep behaviour in deep deposits of soft clay, with a special focus on stress increase around the preconsolidation stress. This could be studied both with and without reinforcement of the soft clay, e.g. with LCCs or piles.

This would give a better understanding of the effect a surcharge would have on the soft clay. Both vertical and horizontal displacements should be monitored together with the excess pore pressure in relation to depth.

8.3 Numerical modelling

In the future the numerical tools will become more available and will be used in the geotechnical design process. The use of these numerical tools could be a

future research area to perhaps establish certain guidelines or recommendations for different types of engineering problems.

8.4 Constitutive modelling

There are a number of constitutive models on the market but very few that incorporate strain rate behaviour or creep. Development or adaption of a three-dimensional constitutive model for Swedish soft clays, with Swedish empiricism, which incorporates strain rate behaviour could be a research area.

REFERENCES

- Alén, C., Baker, S., Ekström, J., Hallingberg, A., Svahn, V., & Sällfors, G., 2005. Test Embankments on Lime/Cement Stabilized Clay, Proc. Deep Mixing '05, Stockholm, p.213-219.
- Alén, C., Sällfors, G., Bengtsson, P.-E., & Baker, S., 2006. Test embankments Rv 45/Nordlänken, Embankments on lime/cement stabilized soil, The Swedish Deep stabilization Research Centre, Report 15, Linköping. In Swedish.
- Alte, B., Olsson, T., Sällfors, G., & Bergsten, H., 1989. "Study of the Gothenburg clay" Geological - geotechnical study of clay from great depths in kv. Guldet, Gothenburg. (In Swedish).
- Augustesen, A., Liingaard, M., & Lade, P. V., 2004. Evaluation of Time-Dependent Behavior of Soils: International Journal of Geomechanics, Vol. 4, p. 137-156.
- Baker, S., Sällfors, G., & Alén, C., 2005. Deformation properties of lime/cement columns. Evaluation from in-situ full scale tests of stabilized clay, Proc. Deep Mixing '05, Stockholm, p. 29-33.
- Berre, T., 1995. Methods for triaxial compression tests on water-saturated soils, 11th European Conference on Soil Mechanics and Foundation Engineering: Copenhagen.
- Bjerrum, L., 1967. Engineering geology of Norwegian normally-consolidated marine clays as related to settlements of buildings (Seventh Rankine Lecture) Geotechnique Vol. 17, p. 83-118.
- Boudali, M., Leroueil, S., & Murthy, B. R. S., 1994. Viscous behaviour of natural clays, Proc. 13th International Conference on Soil Mechanics and Foundation Engineering, New Delhi, India, 1, p. 411-416.
- Brinkgreve, R. B. J., Broere, W., & Waterman, D., 2006. PLAXIS Manual 2D - Version 8, Netherlands.
- Buisman, K., 1936. Results from long duration settlement tests., Proc. 1st International Conference on Soil Mechanics and Foundation Engineering, Cambridge, Vol. 1, p. 103-107.

- Burland, J. B., 1987. Nash lecture: The teaching of soil mechanics - A personal view, Proceedings, 9th ECSMFE, Dublin, vol. 3, p. 1427-1447.
- Burland, J. B., 1989. Ninth Laurits Bjerrum Memorial Lecture: "Small is beautiful" - the stiffness of soils at small strains: Canadian Geotechnical Journal, Vol. 26, p. 499-516.
- Campanella, R. G., & Mitchell, J. K., 1968. Influence of temperature variations on soil behaviour, ASCE, vol.94, p.709-734.
- Christensen, S., 1995. Long-term Processes in Geomaterials. Creep Parameters from Oedometer Tests on Illitic Clays., SINTEF Geotechnical Engineering, Trondheim.
- Claesson, P., 2003. Long term settlements in soft clays, PhD Thesis, Department of Geotechnical Engineering, Chalmers University of Technology, Gothenburg
- Crawford, C. B., 1964. Interpretation of the consolidation test.: Journal of the Soil Mechanics and Foundations Division, Vol. Vol. 90, p. 87-102.
- DeGroot, D. J., 2001. Laboratory measurement and interpretation of soft clay mechanical behavior: American Society of Civil Engineers, Geotechnical special publication No.119, p. 167-200.
- Emdal, A., & Svanö, G., 1988. Krykon Ver.02. A FEM Program for One-Dimensional Analysis including creep effects, Report No. STF69 F88009,
- Eriksson, L. G., 1989. Temperature effects on consolidation properties of sulphide clays, Proc. 12th International Conference on Soil Mechanics and Foundation Engineering, Rio de Janeiro, Vol. 3, p. 2087-2090.
- Garlanger, J. E., 1972. The consolidation of soils exhibiting creep under constant effective stress: Geotechnique, Vol. 22, p. 71-78.

- Graham, J., 2006. The 2003 R.M. Hardy Lecture: Soil parameters for numerical analysis in clay: *Canadian Geotechnical Journal*, Vol. 43, p. 187-209.
- Hight, D. W., 2001. Sampling Effects in Soft Clays: An update on Ladd and Lambe (1963), *Soil behavior and soft ground construction*, Cambridge, Massachusetts, Geotechnical special publication no. 119, p.86-121.
- Jaky, J., 1944. The coefficient of earth pressure at rest: *J. Soc. Hung. Eng. Arch.*, p. 355-358.
- Janbu, N., 1969. The resistance concept applied to deformations of soils, *Proc. of the 7th International Conference on Soil Mechanics and Foundation Engineering*, Mexico, p. 193-196.
- Janbu, N., 1970. *Grunnlag i geoteknikk*: Tapir, Trondheim.
- Jardine, R. J., Fourie, A., Maswoswe, J., & Burland, J. B., 1985. Field and laboratory measurements of soil stiffness, *Proceedings of the 11th International Conference on Soil Mechanics and Foundation Engineering*, San Francisco, Vol. 2, p. 223-228.
- Jostad, H. P., 1993. *Bifurcation analysis of frictional materials*, Norwegian university of science and technology, Trondheim.
- Jumikis, A. R., 1967. *Introduction to soil mechanics*: Van Nostrand Co., Princeton.
- Kullingsjö, A., 2007. *Effects of deep excavations in soft clay on the immediate surroundings*, PhD Thesis, Department of Civil and Environmental Engineering, Division of GeoEngineering Chalmers University of Technology, Gothenburg
- La Rochelle, P., Sarraith, J., Tavenas, F., Roy, M., & Leroueil, S., 1981. Causes of sampling disturbance and design of new sampler for sensitive soils: *Canadian Geotechnical Journal*, Vol. 18, p. 52-66.
- Ladd, C. C., & Foott, R., 1974. New Design procedure for stability of soft clays: *Journal of the Geotechnical Engineering Division*, Vol. 100, p. 763-786.

- Larsson, R., 1977. Basic behaviour of Scandinavian soft clays, Swedish Geotechnical Institute, Report No. 4, Linköping.
- Larsson, R., 1981. Drained behaviour of Swedish clays, Swedish Geotechnical Institute, Report No. 12, Linköping.
- Larsson, R., 1986. Consolidation of soft soils, Swedish Geotechnical Institute, Report No. 29, Linköping.
- Larsson, R., Bengtsson, P.-E., & Eriksson, L., 1997. Prediction of settlements of embankments on soft, fine-grained soils, Swedish Geotechnical Institute, Information 13E, Linköping.
- Larsson, R., Sällfors, G., Bengtsson, P.-E., Alén, C., Bergdahl, U., & Eriksson, L., 2007. Shear strength - evaluation of cohesion soil, Swedish Geotechnical Institute, Information 3, Linköping. (In Swedish).
- Leonards, G. A., & Altschaeffl, A. G., 1964. Compressibility of clay: J. Soil Mech. Found. Div., ASCE, 90(5), p. 133-155.
- Leroueil, S., 2006. The isostache approach. Where are we 50 years after its development by professor Suklje?, Proc. 13th Danube Eur. conf. on Geotechnical Engineering, Ljubljana,
- Leroueil, S., Kabbaj, M., Tavenas, F., & Bouchard, R., 1985. Stress-strain-strain rate relation for the compressibility of sensitive natural clays: Géotechnique, Vol. 35(2), p. 159-180.
- Lunne, T., Berre, T., & Strandvik, S., 1997. Sample disturbance effects in soft low plastic Norwegian clays, Proc. International Symposium on Recent Developments in Soil Mechanics, Rio de Janeiro, p. 81-102.
- Magnan, J. P., Baghery, S., Brucy, M., & Tavenas, F., 1979. Etude numérique de la consolidation unidimensionnelle en tenant compte des variations de la perméabilité et de la compressibilité du sol, du fluage et de la non-saturation.: Bulletin de Liaison, Vol. 103, p. 83-94.
- Marques, M. E. S., Leroueil, S., & de Almeida, M. d. S. S., 2004. Viscous behaviour of St-Roch-de-l'Achigan clay, Quebec: Canadian Geotechnical Journal, Vol. 41, p. 25-38.

- Mesri, G., & Castro, A., 1987. The C_a/C_c Concept and K_0 During Secondary Compression: Journal of the Geotechnical Engineering Division, ASCE, Vol. 112, p. 230-247.
- Mesri, G., & Godlewski, P. M., 1977. Time and stress-compressibility interrelationship: American Society of Civil Engineers, Journal of the Geotechnical Engineering Division, Vol. 103, p. 417-430.
- Olsson, M., & Alén, C., 2009. Choice of creep number for high plastic clays, Division of Geoengineering, Chalmers University of Technology, Gothenburg. (In Swedish).
- Olsson, M., Edstam, T., & Alén, C., 2008. Some experiences from full-scale test embankments on floating lime-cement columns, Proc. of the second international workshop on Geotechnics of Soft Soils, Glasgow, Scotland, p. 77-85.
- Parry, R. H. G., 1970. Overconsolidation in soft clay deposits: Geotechnique, Vol. 20, p. 442-446.
- Satibi, S., 2009. Numerical Analysis and Design Criteria of Embankments on Floating Piles, PhD Thesis, Department of Civil- and Environmental Engineering, Institute of Geotechnical Engineering, University of Stuttgart, Stuttgart
- SBK, 2000. Program - Detaljplan för området 28 kv Jungfrustigen/socialhuset och 29 kv Gamla Latin m.fl, Stadsbyggnadskontoret/Kulturfastigheter i Göteborg AB, Dnr 714/99, Göteborg. (In Swedish).
- Schmidt, B., 1966. Earth pressures at rest related to stress history. Discussion: Can. Geotech. J., Vol. 3, p. 239-242.
- Sivakumar, V., Navaneethan, T., Hughes, D., & Gallagher, G., 2009. An assessment of the earth pressure coefficient in overconsolidated clays: Geotechnique, Vol. 59, p. 825-838.
- Stolle, D. F. E., Bonnier, P. G., & Vermeer, P. A., 1997. A soft soil model and experiences with two integration schemes, Proc. NUMGO VI, Montreal, p.123-128.

- Suklje, L., 1957. The analysis of consolidation process by the isotaches method., 4th International Conference on Soil Mechanics and Foundation Engineering., London, Vol. 1, p.200-206.
- Suklje, L., 1978. Stresses and strains in non-linear viscous soils: International Journal for Numerical and Analytical Methods in Geomechanics, Vol. 2, p. 129-58.
- Svanö, G., 1986. One-dimensional strain as a function of effective stress and time, SINTEF, Trondheim. (In Norwegian).
- Svanö, G., Christensen, S., & Nordahl, S., 1991. A soil model for consolidation and creep, Proc. of the 10th European Conference on Soil Mechanics and Foundation Engineering, Florence, p. 269-272.
- Sällfors, G., 1975. Preconsolidation pressure of soft, high-plastic clays, PhD Thesis, Geotechnical Department, Chalmers University of Technology, Göteborg
- Sällfors, G., & Andréasson, L., 1986. Compression properties - Geotechnical laboratory directive, part 10 Bygghögningsrådet, Stockholm. (In Swedish).
- Tavenas, F., & Leroueil, S., 1987. "Laboratory and in situ stress-strain-time behaviour of soft clays: a state-of-the-art", International Symposium on Geotechnical Engineering of Soft Soils, Mexico City, vol. 2, p.1-46.
- Taylor, D. W., 1942. Research on consolidation of clays: Massachusetts Institute of Technology - Department of Civil and Sanitary Engineering - Serial, 147 p.
- Taylor, D. W., & Merchant, W., 1940. Theory of clay consolidation accounting for secondary compression: Journal of Mathematics and Physics, Vol. 19, p. 167-185.
- Terzaghi, K., 1923. Die Berechnung der Durchlässigkeitsziffer des Tones aus dem Verlauf der hydrodynamischen Spannungserscheinungen.: Akademie der Wissenschaften in Wien. Mathematisch-Naturwissenschaftliche Klasse. Sitzungsberichte. Abteilung II a., Vol. Vol. 132, p. 125-138.

- Terzaghi, K., 1943. Theoretical soil mechanics: Theoretical Soil Mechanics.
- Tidfors, M., 1987. Temperature effects on deformations properties on clay - A laboratory study, Chalmers University of Technology, Gothenburg. (In Swedish).
- Tidfors, M., & Sällfors, G., 1989. Temperature effect on preconsolidation pressure: Geotechnical Testing Journal, Vol. 12, p. 93-97.
- Vermeer, P. A., & Neher, H. P., 1999. A soft soil model that accounts for creep, Proceedings of the international symposium 'Beyond 2000 in Computational Geotechnics', Amsterdam, p.249–261.
- Vermeer, P. A., Stolle, D. F. E., & Bonnier, P. G., 1998. From the classical theory of secondary compression to modern creep analysis, Proc. Computer Methods and advances in Geomechanics, Wuhan, China, p.2469-2478.
- Wood, D. M., 1990. Soil behaviour and critical state soil mechanics: Cambridge University Press, Cambridge.



Statens geotekniska institut
Swedish Geotechnical Institute

SE-581 93 Linköping, Sweden

Tel: 013-20 18 00, Int + 46 13 201800

Fax: 013-20 19 14, Int + 46 13 201914

E-mail: sgi@swedgeo.se Internet: www.swedgeo.se